1-1-2017

Human Kinome In Skeletal Muscle Insulin Resistance

Yue Qi
Wayne State University,

HUMAN KINOME IN SKELETAL MUSCLE INSULIN RESISTANCE

by

YUE QI

DISSERTATION

Submitted to the Graduate School

of Wayne State University,

Detroit, Michigan

in partial fulfillment of the requirements

for the degree of

DOCTOR OF PHILOSOPHY

2017

MAJOR: PHARMACEUTICAL SCIENCES

Approved By:

_____

Advisor Date

_____

_____

_____

_____

DEDICATION

To my supportive and lovely wife who has been there for me all the time,

Shilian Duan

To the people who gave me life, who taught me how to be a man, my loving parents,

Yongli Qi and Ping Hou

To my children who are always my deepest motivations,

Timothy D. Qi and Joyce D. Qi

To LORD my God, I dedicate all my heart and all my soul and all my mind and all my strength to glorify His name alone.

ACKNOWLEDGEMENTS

First of all, I would like to deeply thank my PhD advisor Dr. Zhengping Yi who has been continuously supporting me for the past five years. I do appreciate and feel very fortunate to join his lab, and I can still recall the first talk with Dr. Yi that his research topics were so attractive to me. I can't achieve this milestone without his continuous supports and advices. For me, he is a kind and generous teacher, mentor and friend.

Second, I would like to thank Dr. Xiangmin Zhang who taught me molecular biology techniques and helped me with literature search when I just joined the lab. Also, I want to acknowledge my project supervisor, Dr. Danjun Ma. His inspirations for proteomics deeply influenced my career goals, and he is the person who brought me to the proteomics field, I can't thank Dr. Danjun Ma enough for his teaching and training during my graduate study. What's more, I need to thank my lifetime teacher and friend, Dr. Michael Caruso who assisted me with lab techniques, literature search, presentation skills and writing. Furthermore, I want to extend my sincere thanks to Mr. Griffin Calme who helped me with data analysis and bioinformatics.

Third, I would particularly like to thank my PhD committee members, Dr. Assia Shisheva, Dr. Anjaneyulu Kowluru, Dr. Fei Chen and Dr. Kyle Burghardt, for their continuous supports and availability. I am very grateful for their comments and suggestions which guide the future direction of my research projects.

Meanwhile, I want to acknowledge all the physicians, nurses, and students who work in the clinical research center. I want to mention Dr. Berhane Seyoum, Dr. Abdullah Mallisho and Roy Collins, RN who have been working with us for more than 6 years. I need to thank all the current and former graduate students who assisted my experiments: Mr. Zhao Yang, Ms. Divyasri Damacharla, Miss. Shukurat Sulaiman, Mr. Majed Alharbi and Mr. Nishit Shah.

Last but not least, I would specially acknowledge my previous mentor, Dr. Hongquan Duan, for his generous support during my Master's degree study in Tianjin Medical University. He was the person who led me to understand how the scientific field works, and taught me how to be a graduate student. I also want to mention my previous teachers and coworkers who inspired me to take the journey in academia. Dr. Kongde Xin, Dr. Shenan Tang, Dr. Chen Tang, Dr. Nan Qin and Dr. Meina Jin

TABLE OF CONTENTS

LIST OF TABLES

LIST OF FIGURES

LIST OF ABBREVIATIONS

ACTG1: Actin, cytoplasmic 2

AGC: Containing PKA, PKG, PKC families

AK1: Adenosine kinase 1

AKT: RAC-alpha serine/threonine-protein kinase

AMP: adenosine monophosphate

AMPK: AMP-activated protein kinase

APC: Adenomatosis polyposis coli

aPK: Atypical protein kinase

AS160: AKT substrate of 160 kDa

BMI: Body fat index

Braf: Serine/threonine-protein kinase B-raf

CACNB1: Voltage-dependent L-type calcium channel subunit beta-1

CAMK: Calcium/calmodulin-dependent protein kinase

CAMK2G: Calcium/calmodulin-dependent protein kinase type II subunit gamma

CaMKII: Ca2+/calmodulin-dependent protein kinase II

CDK2: Cyclin-dependent kinase 2

CK1: Casein kinase 1

CMGC: Containing CDK, MAPK, GSK3, CLK families

CML: Chronic myelogenous leukemia

Co-IP: Co-immunoprecipitation

COPD: Chronic obstructive pulmonary disease

CSNK1A1: Casein kinase I isoform alpha

CSNK2A1: Casein kinase II subunit alpha

DFG: Asp–Phe–Gly

DMEM: Modification of Basal Medium Eagle

DTT: Dithiothreitol

EDTA: Ethylenediaminetetraacetic acid

EGFR: Epidermal growth factor receptor

EIF3A: Eukaryotic translation initiation factor 3 subunit A

ePK: Eukaryotic protein kinase

ESI: Electrospray ionization

FBS: Fetal Bovine Serum

FDR: False discovery rate

FN1: Fibronectin

FoxO1: Forkhead box O1

FYN: Tyrosine-protein kinase Fyn

GLUT4: Glucose transporter type 4

GO: Gene ontology

GRB2: Growth factor receptor-bound protein 2

GSK3: Glycogen synthase kinase-3

GSK3β: glycogen synthase kinase-3 beta

HbA1C: Hemoglobin A1c

HDL: High-density lipoprotein

HK: Hexokinases

HK1: Hexokinase-1

HPLC: High-performance liquid chromatography instruments

HPLC: High-performance liquid chromatography

HRD: His–Arg–Asp

HSPA2: Heat shock-related 70 kDa protein 2

IAA: Iodoacetamide

IFN-γ: Interferon gamma

IKK: IκB kinase

IL-1: Interleukin-1

IL-6: Interleukin-6

ILK: Integrin-linked protein kinase

IMAT: Intermyocellular and perimuscular adipose tissue

iNOS: Inducible nitric oxide synthase

IPA: Ingenuity Pathway Analysis

IR: Insulin receptor

IRS: Insulin receptor substrate

JNK: Mitogen-activated protein kinase 8

KEGG: Kyoto Encyclopedia of Genes and Genomes

KHK: Ketohexokinases

LC: Lean control

LCK: Tyrosine-protein kinase Lck

LDL: Low-density lipoprotein

LTQ: Linear iontrap

MAP2K1 /MEK1: Dual specificity mitogen-activated protein kinase kinase 1

MAP2K2 /MEK2: Dual specificity mitogen-activated protein kinase kinase 2

MAP2K6/MEK6: Dual specificity mitogen-activated protein kinase kinase 6

MAPK1/ERK: Mitogen-activated protein kinase 1

MAPK12/p38γ: Mitogen-activated protein kinase 12

MAPK13/p38δ: Mitogen-activated protein kinase 13

MAPT: Microtubule-associated protein tau

MAST2: Microtubule-associated serine/threonine-protein kinase 2

MS: Mass spectrometry

mTOR: mammalian target of rapamycin kinase

mTORC1: Mammalian target of rapamycin complex 1

MYH1: Myosin heavy chain 1

NANA: Nascent polypeptide-associated complex alpha subunit

NEAA: Non-essential Amino Acid

NEK6: Serine/threonine-protein kinase Nek6

NF-κB: Nuclear factor of kappa light polypeptide gene enhancer in B cells

NSCLC: Non-small cell lung cancer

OBi: Obese participants with insulin resistance

OGTT: Oral glucose tolerance test

PA: Peak area

PBS: Phosphate-buffered saline

PFK2: 6-phosphofructo-2-kinase

PIP2: Phosphorylates phosphatidylinositol-4,5-bisphosphate

PIP3: Phosphatidylinositol-3,4,5-trisphosphate

PKA: Protein Kinase A

PPM: Parts per million

PPP1CA: Serine/threonine-protein phosphatase PP1-alpha catalytic subunit

PPP1R12A: Protein phosphatase 1 regulatory subunit 12A

PPP2R2A: Serine/threonine-protein phosphatase 2A 55 kDa regulatory subunit B alpha isoform

PRKAB2: 5'-AMP-activated protein kinase subunit beta-2

PRKACA: cAMP-dependent protein kinase catalytic subunit alpha

PRKAR2A: cAMP-dependent protein kinase type II-alpha regulatory subunit

PRKG1: cGMP-dependent protein kinase 1

PSG: Penicillin-Streptomycin-Glutamine

PSMA1: Proteasome subunit alpha type-1

PSMC3: 26S proteasome regulatory subunit 6A

PSMD11: 26S proteasome non-ATPase regulatory subunit 11

PSMD14: 26S proteasome non-ATPase regulatory subunit 14

PSMD7: 26S proteasome non-ATPase regulatory subunit 7

PTM: Protein post-translational modifications

RAP1B: ras-related protein Rap-1b

ROS: Reactive oxygen species

RPS3: 40S ribosomal protein S3

RPS6: Ribosomal protein S

RPS6: 40S ribosomal protein S6

RPS6KA3/RSK2: Ribosomal protein S6 kinase alpha-3

RTK: Receptor tyrosine kinases

SDS-PAGE: Sodium dodecyl sulfate polyacrylamide gel electrophoresis

SHP2: SH2 domain-containing protein tyrosine phosphatase-2

SILAC: Stable isotope labeling with amino acids in cell culture

SRC: Tyrosine-protein kinase Src

STE: Homologs of yeast Sterile 7, Sterile 11, Sterile 20 kinases

STK11/LKB1: Serine/threonine-protein kinase STK11

T1D: Type 1 diabetes

T2D: Type 2 diabetes

TK: Tyrosine kinase

TKL: Tyrosine kinase–like

TNF-α: Tumour necrosis factor alpha-like

TP53RK: TP53-regulating kinase

VIM: Vimentin

YES1: Tyrosine-protein kinase Yes

CHAPTER 1. INTRODUCTION

1.1 Human kinome and protein kinase domain

1.1.1 Protein kinases

Protein kinases are the enzymes that catalyze protein phosphorylation, one of the most important protein post-translational modifications (PTMs), by transferring a phosphate group from the nucleotide molecules (e.g., Adenosine triphosphate (ATP)) to the substrate proteins (Fontana & Lovenberg, 1973; Guidotti, Kurosawa, Chuang, & Costa, 1975; Insel, Bourne, Coffino, & Tomkins, 1975). Protein phosphorylation is critical to activate or deactivate protein functions: by adding a phosphate group, the protein conformation is altered, subsequently, the protein switches to “on” or “off” states that may enhance or reduce downstream cell signaling (Burnett & Kennedy, 1954; Cohen, 1982; O'Connor, Gard, & Lazarides, 1981). Since protein phosphorylation is highly regulated by kinases, protein kinases play critical roles in mediating multiple biological processes and molecular functions, such as cell proliferation (Aithal, Toback, & Cryst, 1980; Cerda et al., 2006; Kuninaka et al., 2007; Pelaia et al., 2007), apoptosis (Gabai, Mabuchi, Mosser, & Sherman, 2002; Otani, Erdos, & Leonard, 1993) and protein degradation (Cazarin, Andrade, & Carvalho, 2014; Lu et al., 1998; Mizuguchi et al., 1988; Tai et al., 2017). Importantly, deregulation of protein kinases may induce impaired cellular pathways and signal transduction, such as Wnt pathway (Ehyai et al., 2015; Ohishi et al., 2015) and insulin signaling pathway (Numata et al., 2011; Ohta et al., 2015; Sawada, Yamashita, Zhang, Nakagawa, & Ashida, 2014;

Whelan, Dias, Thiruneelakantapillai, Lane, & Hart, 2010), which contributes to a variety of human diseases, such as cancer (ElMokh et al., 2017; M. Li et al., 2017), cardiovascular disease (Behr et al., 2003; Oudit et al., 2004) and type 2 diabetes (Kume et al., 2016; Russo, Russo, & Ungaro, 2013; Sidarala & Kowluru, 2016).

1.1.2 The human kinome

In 2002, Manning *et al* (Manning, Whyte, Martinez, Hunter, & Sudarsanam, 2002), revealed a comprehensive discovery of protein kinase genes in human genome, where they reported 518 protein kinases in total (516 protein kinase based on their 2007 updates). The human kinome constitutes 1.7% of the human genes. Among the 518 protein kinases, 478 kinases have a “typical” eukaryotic catalytic domain, also known as eukaryotic protein kinase (ePK), containing 12 common subdomains which construct a highly conserved kinase catalytic core (Hanks & Hunter, 1995); meanwhile, there are 40 “atypical” protein kinase (aPK) which have the kinase activity but lack of the common eukaryotic catalytic domain (also known as the kinase core) (Manning et al., 2002).

1.1.3 Importance of ePK and its classification

Numerous studies have implied that typical ePKs are essential for normal cell signaling and responsible for pathogenesis of many human diseases. For example, RAC-alpha serine/threonine-protein kinase (Protein kinase B or AKT) is one of the very first discovered and extensively studied ePKs because AKT is able to phosphorylate a range of substrates which are in charge of various critical biological processes, such as cell growth, death and angiogenesis. In 1995,

Burgering, B. M *et al*. (Burgering & Coffer, 1995) reported that AKT is directly involved in phosphatidylinositol-3-OH kinase (PI3K) signaling cascade. During the past few decades, PI3K/AKT signaling have been proven to participate in many molecular functions and diseases (e.g., insulin signaling, diabetes, cancer, etc.); For example: a) Farrar, C *et al*. (Farrar, Houser, & Clarke, 2005) revealed that activation of PI3K/AKT pathway increased protein expression of insulin receptor by 200% in protein repair deficient mice, which suggested that AKT is a key regulator in insulin signaling pathway. b) A genetic study (Yin et al., 2017) showed a significant associate of AKT gene level and type 2 diabetes in Chinese population (248 T2D cases and 101 controls). c) Zhang, Y., *et al.* (Y. Zhang et al., 2017) conducted a large proteogenomic study across more than 11,000 cancer samples assigned to 32 cancer types (Figure 1-2), and they reported that multiple oncogenic mutation in PI3K/AKT pathway which has been demonstrated to be abnormal in multiple types of cancer.

The 478 ePks have been classified into 8 groups:

1. PKA, PKG, PKC families (AGC) (e.g., AKT);
2. Calcium/calmodulin-dependent protein kinase (CAMK) (e.g., Mitogen-activated protein kinase 1);
3. Casein kinase 1 (CK1);
4. CDK, MAPK, GSK3, CLK families (CMGC) (e.g., Glycogen synthase kinase-3 alpha, Mitogen-activated protein kinase 8 or JNK1);

5. Homologs of yeast Sterile 7, Sterile 11, Sterile 20 kinases (STE) (e.g., Dual specificity mitogen-activated protein kinase kinase 1);

6. Tyrosine kinase (TK) (e.g., insulin receptor, Tyrosine-protein kinase Fyn);

7. Tyrosine kinase–like (TKL) (e.g., Serine/threonine-protein kinase B-raf);

8. Other kinase (Other) that contains eukaryotic catalytic domain but does not belong to any groups above.

The classification of typical ePKs was summarized in Table 1-1 (data source from (Manning et al., 2002), reformatted table). As can be seen from Table 1, the tyrosine kinase (TK) group comprised 90 kinases is the largest group; AGC, CAMK and CMGC groups contain moderate number of kinases (63, 74, and 61, respectively); STE, TKL and CK1 are in the lower end of the kinome (47, 43, and 12, respectively); Other group consists of relatively large number of kinases (83), which also play key roles in cellular functions and signal transduction, such as mitotic cell cycle progression regulated by serine/threonine-protein kinase Nek7 (Yissachar, Salem, Tennenbaum, & Motro, 2006).

1.1.4 aPKs also play critical roles

Forty atypical protein kinases have been categorized into 8 groups: PDHK, Alpha, RIO, ABC1, BRD, PIKK, Other, and A6 (A6 was excluded from the most up to date kinome database). The best well-studied aPK might be mammalian target of rapamycin kinase (mTOR), which directly or indirectly regulates numerous cell signaling pathways including PI3K/AKT pathway (Amin et al., 2008; Babchia, Calipel, Mouriaux, Faussat, & Mascarelli, 2010; H. Zhang et al., 2007), MAPK

signaling pathway (Aldonza et al., 2015; Dormond-Meuwly et al., 2011; Landau et al., 2009), JNK signaling pathway (A. Kim et al., 2017; March & Winton, 2011; Shanware et al., 2014). As an atypical protein kinase, mTOR does not contains a classic kinase core as ePKs; however, mTOR has two distinct complexes, mTORC1 (Raptor) and mTORC2 (Rictor), which exhibit different molecular functions (Lipton & Sahin, 2014). Nissim Hay *et al*.,(Hay & Sonenberg, 2004) reported that mTORC1 enhanced the protein synthesis by phosphorylating number of downstream transcription factors and ribosome kinases (e.g., Ribosomal protein S6 kinase beta-1), and AKT, a downstream effector of insulin receptor (IR)/insulin receptor (IRS)/PI3K pathway, was also a key mediator of mTORC1 (Figure 1-3); however, the mTORC2, as Sarbassov *et al*., (Sarbassov, Guertin, Ali, & Sabatini, 2005) described, could be an essential component to phosphorylate Akt on Ser^{473}, which demonstrated completely different cellular activity from mTORC1 (Figure 1-4). Hence, although the aPKs lack of a typical kinase core, they still exhibit strong regulatory impact on the cellular signal transduction.

1.1.5 Other kinases (non-protein kinases)

Beyond the 518 protein kinases in human, there are also many other non-protein kinases of which the three main classes (sugar kinase, nucleoside kinase and liquid kinase) are discussed in this chapter. Far less researchers focus on non-protein kinases (Maeda et al., 2006); however, some kinases in this category also play critical roles in cell signaling, such as PI3K.

1.1.5.1 Sugar kinases

Sugar kinases mainly control aerobic glycolysis which generates critical energy for tumor cells, so minimizing the catalytic activities of these kinases (e.g., 6-phosphofructo-2-kinase) could potentially inhibit the tumor growth (Chesney, Clark, Lanceta, Trent, & Telang, 2015). The sugar kinases can be categorized into 4 groups: Hexokinases (HK), Ketohexokinases (KHK), 6-phosphofructo-2-kinase (PFK2) and Galactokinase.

1.1.5.2 Nucleoside kinases

Nucleoside kinases catalyze the phosphorylation on 5'- hydroxyl group on ribonucleosides, and they have been widely recognized playing important roles in NAD salvage pathway (T. Zhang et al., 2009); however, their molecular functions have not been fully understood. One of the well-studied nucleoside kinases, adenosine kinase 1 (AK1), transfers the gamma-phosphate from a molecule of ATP to adenosine resulting in a molecule of adenosine monophosphate (AMP). AK1 is the key mediator to maintain the cellular energy homeostasis, and Amiri, M., *et al*. (Amiri, Conserva, Panayiotou, Karlsson, & Solaroli, 2013) discovered that AK9 also exhibits nucleoside diphosphate kinase activity.

1.1.5.3 Lipid kinases

Lipid kinases mainly phosphorylate lipids by adding a phosphate group, and serve as important switches to "turn on and off" cell signaling. One of the best known lipid kinases, PI3K, phosphorylates phosphatidylinositol-4,5-bisphosphate (PIP2), to form phosphatidylinositol-3,4,5-trisphosphate (PIP3), which is a critical

mediator in response to stimuli (i.e., growth factor, insulin), subsequently, activates an extremely important downstream protein kinase, AKT (Guerrero-Zotano, Mayer, & Arteaga, 2016). PI3Ks are heterodimeric enzymes including catalytic subunits (p110) and regulatory subunits (p85), named based on their molecular weight. The p85 subunit recruits by receptor tyrosine kinases (RTKs) directly, then the p110 subunit is activated by p85 resulting a fully functional PI3 kinase (Okkenhaug, 2013). Figure 1-5 (Martini, De Santis, Braccini, Gulluni, & Hirsch, 2014) showed that the pathway initiated by RTK and PI3K involves in numerous crucial substrates proteins (i.e., Phosphoinositide-dependent kinase-1, AKT, mTORC1, ERK1/2).

Hyper-activation and mutation of PI3K is very common in tumor cells and tissues where cell growth and proliferation are promoted whereas programmed cell death, apoptosis, is inactivated. Chen *et al*., (S. Chen et al., 2016) unveiled that inhibited PI3K activity reduced the colon cancer stem cell growth via decreased cell proliferation and increased cleaved caspase 3, which is a biomarker of cancer cell apoptosis.

Hypoactive PI3K in diabetic animal or human models has been demonstrated. Supplement nutrition D-chiro-inositol (DCI), an essential secondary messenger in insulin signaling, was reported to significantly increase PI3K protein abundance in liver and skeletal muscle of diabetic rats, and resulting in reduced fasting plasma glucose and increased glycogen synthesis through PI3K/AKT pathway (Gao et al., 2016).

1.1.6 Protein kinase catalytic core

Protein kinases, transferring a gamma-phosphate to substrate proteins and producing phosphorylated proteins, normally contain two types of domains, a highly conserved catalytic domain (kinase core) and a regulatory Src Homology 2 (SH2) or a Src Homology 3 (SH3) domain. Proto-oncogene tyrosine-protein kinase (Src), for example, has regulatory domains SH2 and SH3, and a tyrosine kinase catalytic domain. The regulatory domains, acted as adaptors, allow the upstream signaling protein binding, which activates the tyrosine domain; subsequently, the active kinase core changed its conformation to allow ATP and substrate binding (Thomas & Brugge, 1997). However, as Kornev *et al*., described (Kornev, Haste, Taylor, & Eyck, 2006): not all the protein kinases have regulatory domains. cAMP-dependent protein kinase (PKA), one of the first well characterized protein kinases, is a protein complex composed of catalytic subunits (i.e., PRKACA) and regulatory subunits. For example, PRKACA only contains a kinase core which includes an N-terminal lobe (N-lobe) and a C-terminal lobe (C-lobe), and a cleft or hinge region located between the N-lobe and C-lobe. The docking cleft is for ATP binding. In Figure 1-6, upon PKA regulatory/activated protein binding, the subdomains of kinase core change their orientation and form an active conformation of PKA, which allows one molecule of ATP to specifically dock into the binding cleft.

There are several highly conserved residues and motifs in the kinase core (C. Kim, Cheng, Saldanha, & Taylor, 2007). In the ATP binding cleft, N-lope forms a very hydrophobic pocket for ATP adenine ring, and glycine-rich loop (P-loop) forms a “lid” for three phosphate docking. One of the most important conserved

residues in the ATP binding pocket is the lysine in the N-lope (e.g., K^{72} in PKA), which stabilizes the alpha- and beta-phosphates in a low energy position in the binding domain. In the C-loop, there are two important motifs, Asp–Phe–Gly (DFG) motif and His–Arg–Asp (HRD) motif, which are highly conserved regions across all 478 ePKs. Another essential residue for exert catalytic activity is the aspartate (e.g., D^{184} in PKA) in the DFG motif, and D^{184} stabilizes the beta- and gamma-phosphate through metal atoms, such as magnesium. DFG motif together with the following two residues form a “magnesium-binding” loop that is also highly conserved in the kinase core. DFG motif has two conformations, “DFG-in” and “DFG-out”, where “DFG-in” is an active conformation that allows to form the magnesium-binding loop while “DFG-out” is inactive conformation that hides the conserved aspartate in the deep hydrophobic region prevents the three ATP phosphates from binding to the cleft between N-lope and C-lope (Vijayan et al., 2015). Therefore, inactive conformation of the kinase core (specifically DFG-out) might hinge ATP binding. One example of taking advantage of the conserved DFG motif: imatinib (Gleevec), one of most successful type II tyrosine kinase inhibitors treating chronic myelogenous leukemia, favors the DFG-out conformation to keep it from active (Figure 1-7) (Treiber & Shah, 2013). Another highly conserved motif in the kinase core is HRD motif which contains the aspartate (Asp^{166} in PKA) responsible for correcting orientation of substrate peptides. The 2nd residue which is apart from the aspartate in HRD motif to the C-terminal is another conserved lysine (Lys^{168} in PKA, Figure 1-6), which directly interacts with gamma-phosphate

in the ATP, and stabilizes the ATP binding. It plays a critical role in the gamma-phosphate transferring.

Mitogen-activated protein kinase 1 (MAPK1 or ERK2) is a key functional protein kinase in MAP kinase pathway, which has been known involving in numerous biological processes (e.g., cell growth (Husain et al., 2001) and apoptosis (Zhou et al., 2015)) and pathogenesis of human diseases (e.g., cancer (X. W. Li, Tuergan, & Abulizi, 2015) and diabetes (Kinoshita et al., 2011)). MAPK1 has very similar kinase core as PKA demonstrated above, and contains serval highly conserved residues: Lys^{54} in the N-lobe for ATP docking; Asp^{167} in DFG motif for activating MAPK1; Asp149 and Lys151 in the HRD catalytic motif for gamma-phosphate transferring (Figure 1-8).

In summary, a) N-lobe and C-lobe are forming the kinase core which presents in all eukaryotic protein kinases; b) The cleft or hinge for ATP binding contains multiple highly conserved domains: glycine-rich loop (ATP binding), DFG motif (active or inactive conformation) and HRD (catalytic activity); c) Two lysine residues (e.g., Lys^{72} in N-lobe and Lys^{168} in C-lobe, PKA) are highly conserved, and stabilize and correct orientation of ATP binding. d) Active protein kinases very likely form a perfect ATP binding microenvironment, conducting a successful gamma phosphate transfer from ATP to substrate proteins.

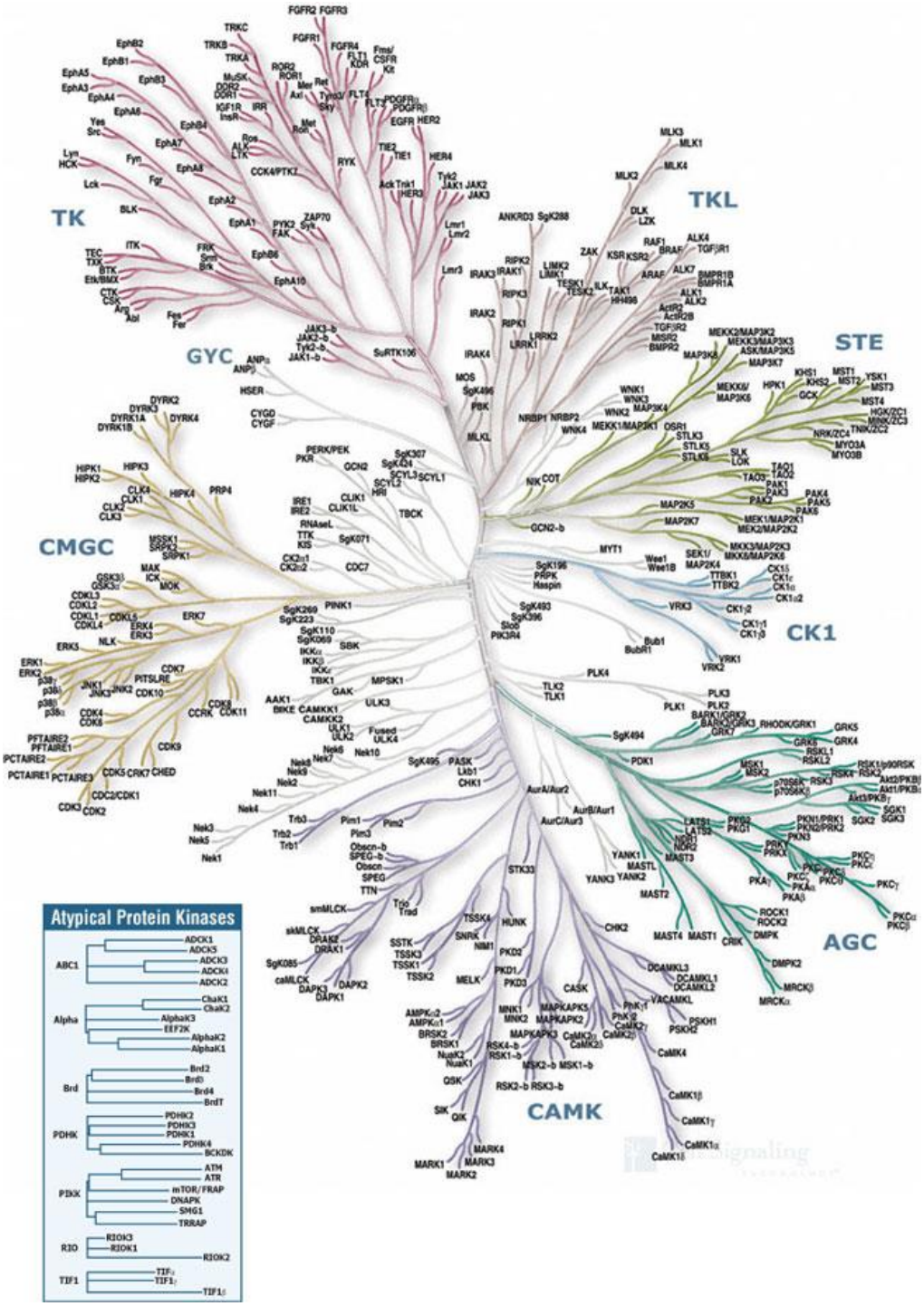

Figure 1-1. The Protein Kinase Complement of the Human Genome (Human Kinome). Figure adapted from G Manning *et al*., Science. 2002.

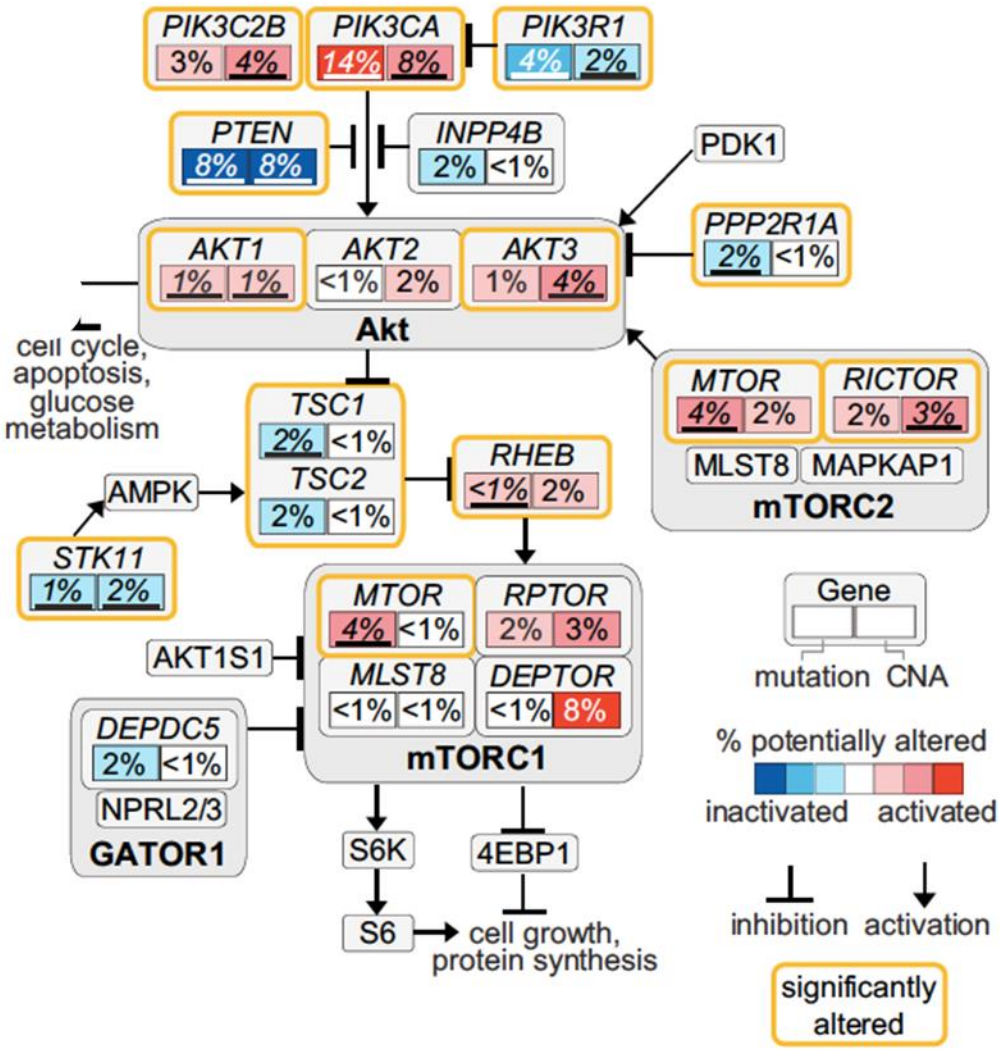

Figure 1-2. Diagram of somatic mutation and copy-number alteration (CNA) frequencies involving components of the PI3K/AKT/mTOR pathway. Figure adapted from Zhang *et al.*, Cancer Cell, 2017.

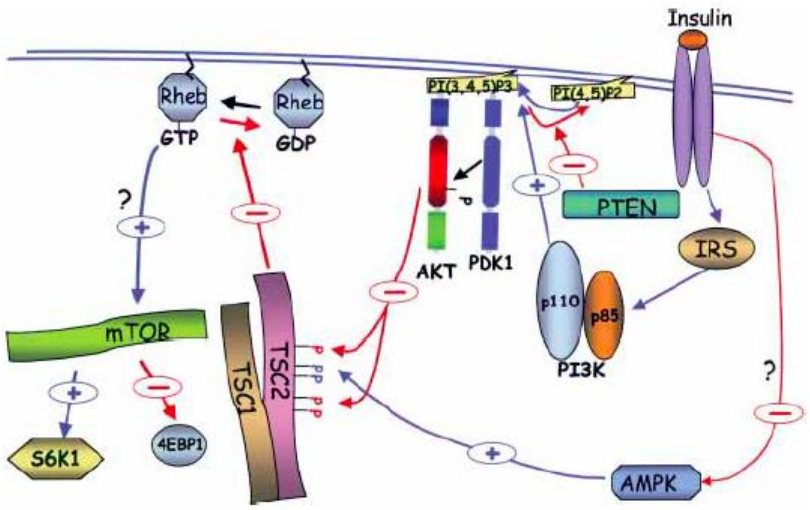

Figure 1-3. The regulation mTORC1 activity by insulin through PI3K/AKT/mTOR pathway. Figure adapted from Hay, N. and N. Sonenberg, Genes Dev, 2004.

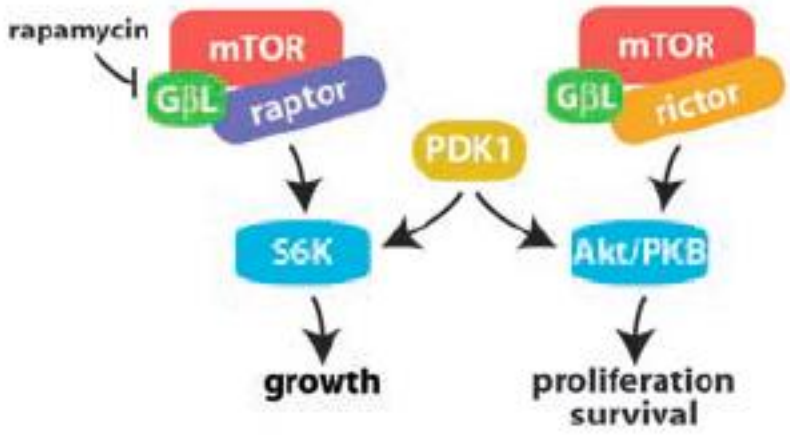

Figure 1-4. The critical role of rictor-mTOR (mTORC2) in Akt/PKB activation Figure adapted from Sarbassov *et al*., Science, 2005.

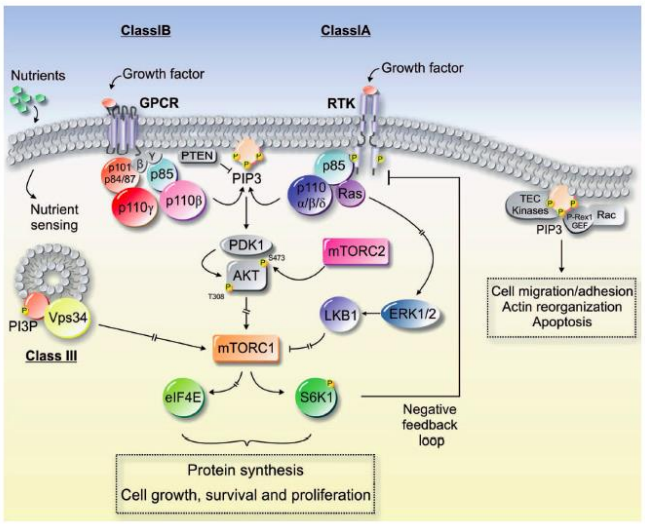

Figure 1-5. Overview of PI3 kinase and Akt signaling pathway. Figure adapted from Martini *et al*., Ann Med, 2014.

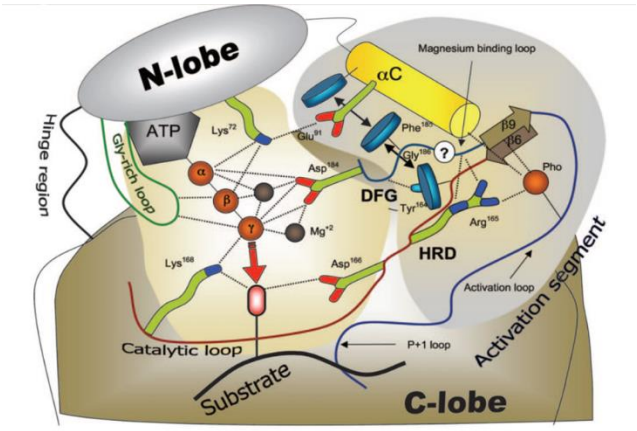

Figure 1-6. Diagram of known interactions between the protein kinase catalytic core, ATP and a substrate in PKA. Figure adapted from Kornev *et al*., PNAS, 2006.

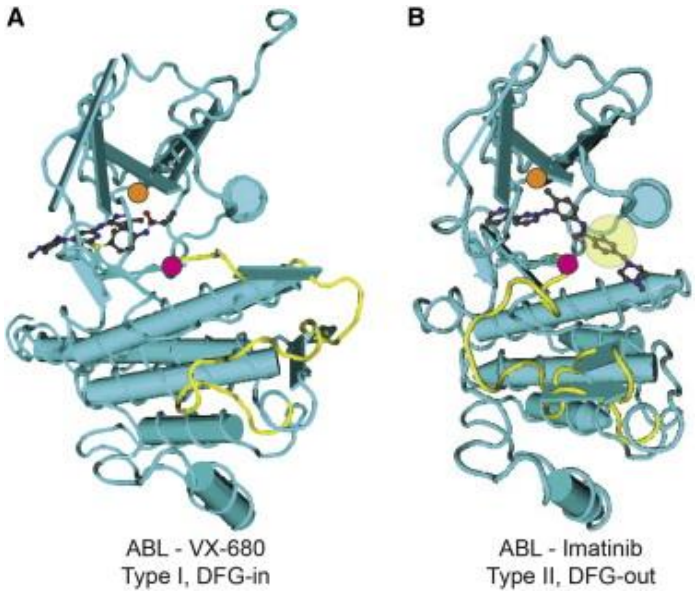

Figure 1-7. DFG-In and -Out conformations of inhibitor bound ABL. Figure adapted from Treiber, D. K. Shah, N. P. Chem Biol. 2013. (A) Type i tyrosine kinase inhibitor, VX-680, favors "DFG-in" conformation; (B) Type ii tyrosine kinase inhibitor, Imatinib, favors "DFG-out" conformation.

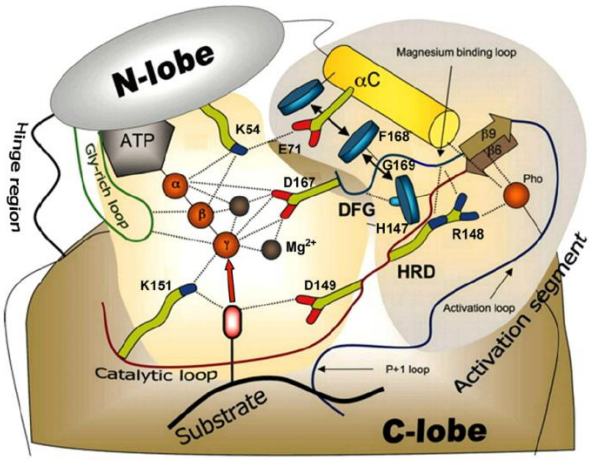

Figure 1-8. Diagram of the inferred interactions between the human ERK2 (MAPK1) kinase catalytic core residues, ATP, and the protein substrates. Figure adapted from Kornev *et al.,* PNAS, 2006.

.

Table 1-1 Classification of eukaryotic protein kinases (ePKs)

Group	Symbols	Number of kinases
Containing PKA, PKG, PKC families	AGC	63
Calcium/calmodulin-dependent protein kinase	CAMK	74
Casein kinase 1	CK1	12
Containing CDK, MAPK, GSK3, CLK families	CMGC	61
Homologs of yeast Sterile 7, Sterile 11, Sterile 20 kinases	STE	47
Tyrosine kinase	TK	90
Tyrosine kinase–like	TKL	43
Other	Other	83

1.2 Skeletal muscle insulin resistance in obesity and Type 2 diabetes

1.2.1 Global epidemic: Obesity and Type 2 diabetes

Obesity, defined as Body Mass Index ≥ 30 kg/m^2, is one of the world epidemics: according to the datasheet from World Heath Organization (WHO), there were almost two billion adults are overweight (BMI≥ 25 kg/m^2), and more than 600 million of these were obese in the world in 2014; what's more, 41 million children (under age of 5) were overweight or obese in the same year. The population on the earth was 7.347 billion (World Bank, United States Census Bureau) in 2015, which means approximately 28% of the world population were overweight and 8.1% were obese. The prevalence of obesity in the United States is even worse, 70.7% of U.S. adults population were overweight (including obesity); more than one third (37.9%) U.S. adults were obese; 9.4% of children (age 2-5 years) in the U.S. were obese in 2013-2014, as reported by Centers for Disease Control and Prevention (CDC). The trends of obesity prevalence in the U.S. has been substantially increased during the past few decades. In Figure 1-9, only 10-14% U.S. adults suffered obesity in 1990 and this number increased to around 20% in 2000 (Figure 1-10); Surprisingly, the prevalence of obesity experienced rapid upsurge to more than 35% among U.S. adults in 2010 (Figure 1-11). Therefore, it is critical to prevent obesity and understand the cellular mechanism of obesity.

Obesity is a known risk factor for many diseases, such as diabetes (X. M. Liu, Liu, Zhan, & He, 2015; Walsh & Vilaca, 2017), cardiovascular disease (X. M. Liu et al., 2015; Ortega, Lavie, & Blair, 2016; Rippe & Angelopoulos, 2016), and

some types of cancer (Cao & Giovannucci, 2016; Goodwin & Chlebowski, 2016; Nunez, Bauman, Egger, Sitas, & Nair-Shalliker, 2017). Importantly, insulin resistance has a strong correlation between obesity and type 2 diabetes (T2D) (Lackey & Olefsky, 2016; Wu & Ballantyne, 2017). Diabetes is a world burden that affects 422 million adults (age 18 years and above) global wide in 2014 (WHO facts report); critically, lower limb amputation rates are 10 to 20 times higher in the diabetic patients than normal population (Moxey et al., 2011). The global prevalence of diabetes is steadily increasing from 4.7% in 1980 to 8.5% in 2014. Similarly to the prevalence of obesity, the developed and rich countries, such as the United States, have higher diabetes rates than the world average. In 2012, National Health and Nutrition Examination Survey reported that 29.1 million people (i.e., 9.3% of U.S. population) had diabetes, and 8.1 million people with diabetes were not diagnosed. Importantly, approximately 95% of the diabetes were T2D (CDC reported in 2014), which has been often undiagnosed and underestimated; however, T2D may leads to a variety of serious medical complications (e.g., loss of vision, heart diseases, stroke, renal diseases, low limb amputations) (Acosta et al., 2000; Khalil, 2016; Papatheodorou, Papanas, Banach, Papazoglou, & Edmonds, 2016; Porte & Schwartz, 1996). Moreover, the number of U.S. adults with diagnosed diabetes has been increased from 5.1 million in 1980 to 21.3 million in 2012 (Figure 1-12); especially, the percentage of diabetic population located in the southeastern region of the U.S. has been elevated from 6.2% in 2000 to 15.2% in 2012 (Figure 1-13).

In summary, obesity and diabetes are global epidemics that affect a large portion of the human population; especially, the United States. Years of studies have demonstrated the clear link between insulin resistance, obesity, and type 2 diabetes.

1.2.2 Insulin resistance in skeletal muscle

Food intake leads to the increase of plasma blood glucose. In order to maintain the plasma glucose level, insulin is produced in the beta-cells of the pancreas and released to signal insulin sensitive tissues/organs to absorb excessive plasma glucose. Human skeletal muscle is responsible for approximately 75% of insulin-stimulated glucose uptake and is also the main site where insulin resistance takes place in obesity and T2D (Bjornholm & Zierath, 2005; Zierath, Krook, & Wallberg-Henriksson, 2000). Using hyperinsulinemic euglycemic clamp technique (Diamond, Jacob, Connolly-Diamond, & DeFronzo, 1993), researchers found that brain, splanchnic area, adipose tissues have similar insulin-stimulated glucose uptake in T2D patients and non-diabetic controls; however, insulin-dependent glucose uptake in skeletal muscle tissue was dramatically reduced among T2D subjects (Figure 1-14). These results suggested that skeletal muscle resistance to insulin is a primary defect in T2D (DeFronzo, 2004).

1.2.3 Cellular mechanism of insulin resistance in skeletal muscle.

1.2.3.1 Cellular mechanism of Normal Insulin Signaling

The principal pathways contributed to insulin resistance might be insulin signaling pathways activated by the insulin receptor, and one of the most extensively studied insulin signaling pathways is PI3K/AKT. The insulin signal transduction begins with ligand (insulin) binding to the insulin receptor (IR) which activates IR, a receptor tyrosine kinase. The activated IR phosphorylates insulin receptor substrate 1 (IRS1) and tyrosine phosphorylated IRS1 recruits PI3K, resulting in the activation of downstream kinases, such as AKT. Activated AKT induces glycogen synthesis via inhibition of glycogen synthase kinase 3 (GSK3); increases the glucose transporter type 4 (GLUT4) translocation to plasma membrane by blocking the activity of AKT substrate of 160 kDa (AS160); and promote the protein synthesis via activation of mammalian target of rapamycin complex (mTOR) pathway (Figure 1-15) (Prada & Saad, 2013; Puigserver et al., 2003; Sano et al., 2003; Taniguchi, Emanuelli, & Kahn, 2006).

1.2.3.2 Cellular mechanism of Insulin resistance in skeletal muscle

The molecular mechanism of skeletal muscle insulin resistance remains unclear. In the IR-PI3K/AKT pathway, serval key regulatory protein kinases have been well investigated. Knocking out Akt2, for example, in mice has been reported to induce insulin resistance and metabolic syndrome (Cho, Mu, et al., 2001; Cho, Thorvaldsen, Chu, Feng, & Birnbaum, 2001); similarly, George S and colleagues (George et al., 2004), using genomic technique, revealed that a family with mutation in kinase domain of AKT2 led to impaired insulin sensitivity (insulin

resistance). These results implied that AKT2 is an essential modulator to phosphorylate downstream proteins in insulin signaling.

IRS is an essential initiator in the upstream of insulin signaling. Figure 1-16 (Copps & White, 2012) showed the pathway initiated by IRS and three tyrosine phosphorylation domains binding to p85 (subunit of PI3K), growth factor receptor-bound protein 2 (GRB2) and SH2 domain-containing protein tyrosine phosphatase-2 (SHP2), and reduced tyrosine phosphorylation of IRS1 has been widely accepted (Copps & White, 2012) in insulin resistant states. In contrast, several studies showed that serine/threonine phosphorylation of IRS1 was significantly elevated in obese or T2D mice or rats, which suggests that increased serine/threonine phosphorylation of IRS1 may reduce its binding capacity to PI3K, and eventually inhibit AKT activity (Morino et al., 2005; Yu et al., 2002).

1.2.4 Inflammation of skeletal muscle insulin resistance in obesity

Skeletal muscle insulin resistance association with chronic inflammation has been widely recognized (Hotamisligil, 2006; Lumeng & Saltiel, 2011; McNelis & Olefsky, 2014; Osborn & Olefsky, 2012). Despite increasing evidence has implied that skeletal muscle inflammation occurs in obesity, the molecular mechanism is still not fully understood. Increased immune cells accumulating in myocytes of obese and T2D individuals has been reported (Fink et al., 2014; Fink et al., 2013; Khan et al., 2015; Patsouris et al., 2014; Varma et al., 2009), and high fat diet increased macrophage markers in insulin resistant obesity (Boon et al., 2015; Tam et al., 2014). One theory of skeletal muscle insulin resistance

development is the activation of immune cells in the myocytes. For example, in figure 1-17, very few immune cells are resting in the skeletal muscle (panel A) in lean muscle, while macrophages and T cells, releasing cytokines, infiltrate into expand adipose depots (or called intermyocellular and perimuscular adipose tissue, IMAT) in obese skeletal muscle, which causes inflammation (panel B) (Wu & Ballantyne, 2017). The cytokines, including IFN-γ and TNF-α, can activate IκB kinase/NF-κB (IKK/NF-κB) and JNK pathways. Evidence showed that IKK/NF-κB pathway was elevated in obesity with T2D (Green, Pedersen, Pedersen, & Scheele, 2011), and overexpression of IKK induced insulin resistance (Yuan et al., 2001). Furthermore, Hirosumi J and colleagues (Hirosumi et al., 2002) reported activated JNK pathway in obese individuals with insulin resistance; similarly, Chiang *et al.*, (Chiang et al., 2009) indicated that JNK signaling was increased in obese mice. Therefore, in figure 1-18, cytokines activated signaling pathways, such as IKK/NF-κB, SAPK/JNK and JAK/STAT, impaired insulin sensitivity might via reduced insulin-stimulated tyrosine phosphorylation and increased serine/threonine phosphorylation of IRS (Wu & Ballantyne, 2017).

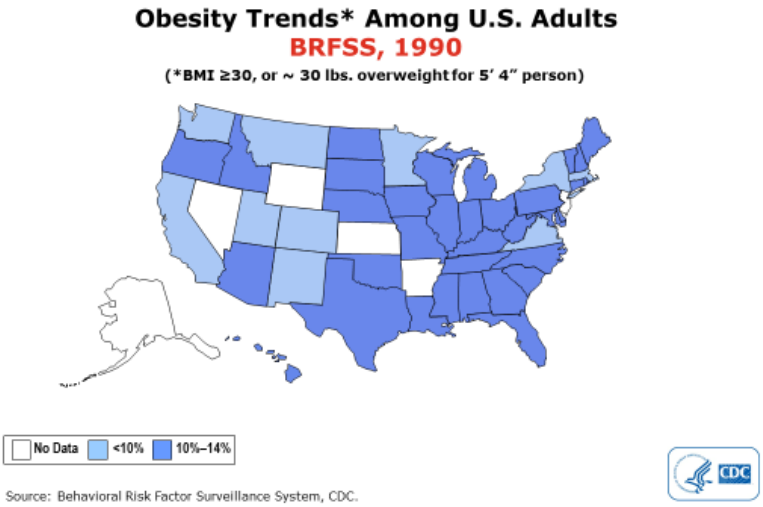

Figure 1-9. Obesity trends among U.S. adults in 1990. Figure adapted from CDC.

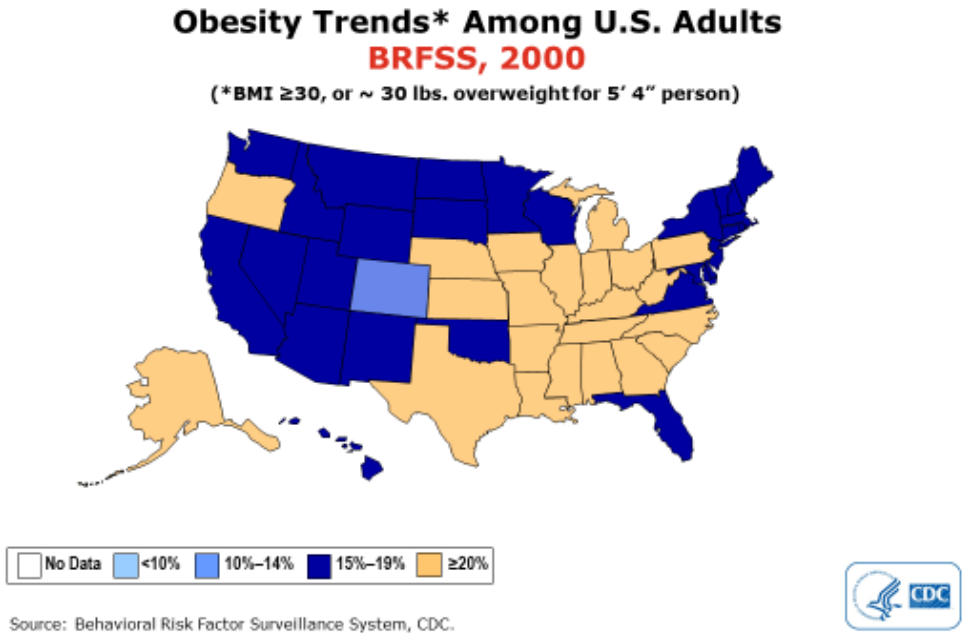

Figure 1-10. Obesity trends among U.S. adults in 2000. Figure adapted from CDC.

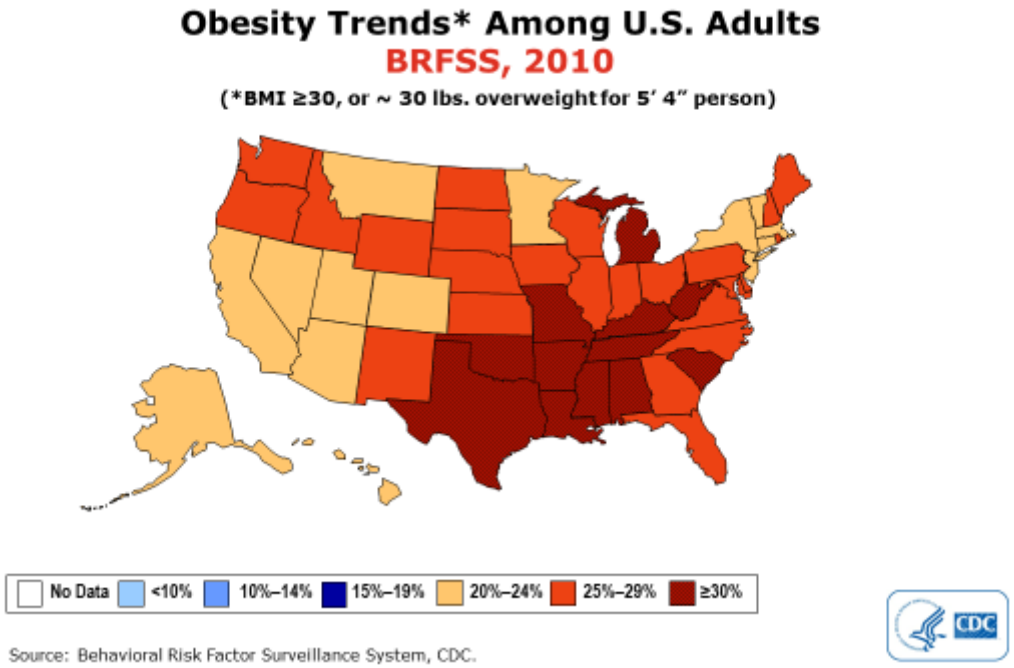

Figure 1-11. Obesity trends among U.S. adults in 2010. Figure adapted from CDC.

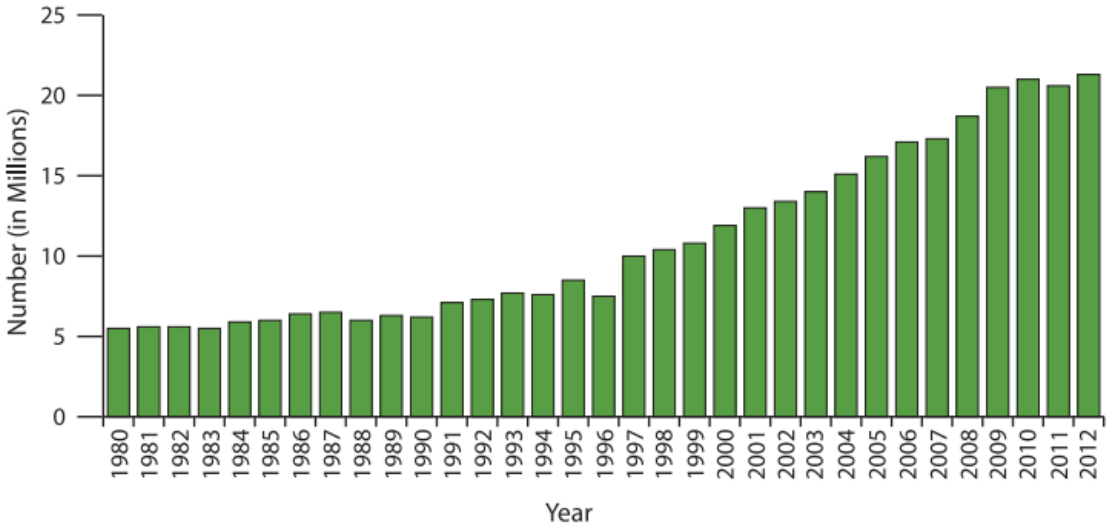

Figure 1-12. Number of US Adults Aged 18 or Older with Diagnosed Diabetes, 1980-2012. Figure adapted from Diabetes Report Card 2014, CDC.

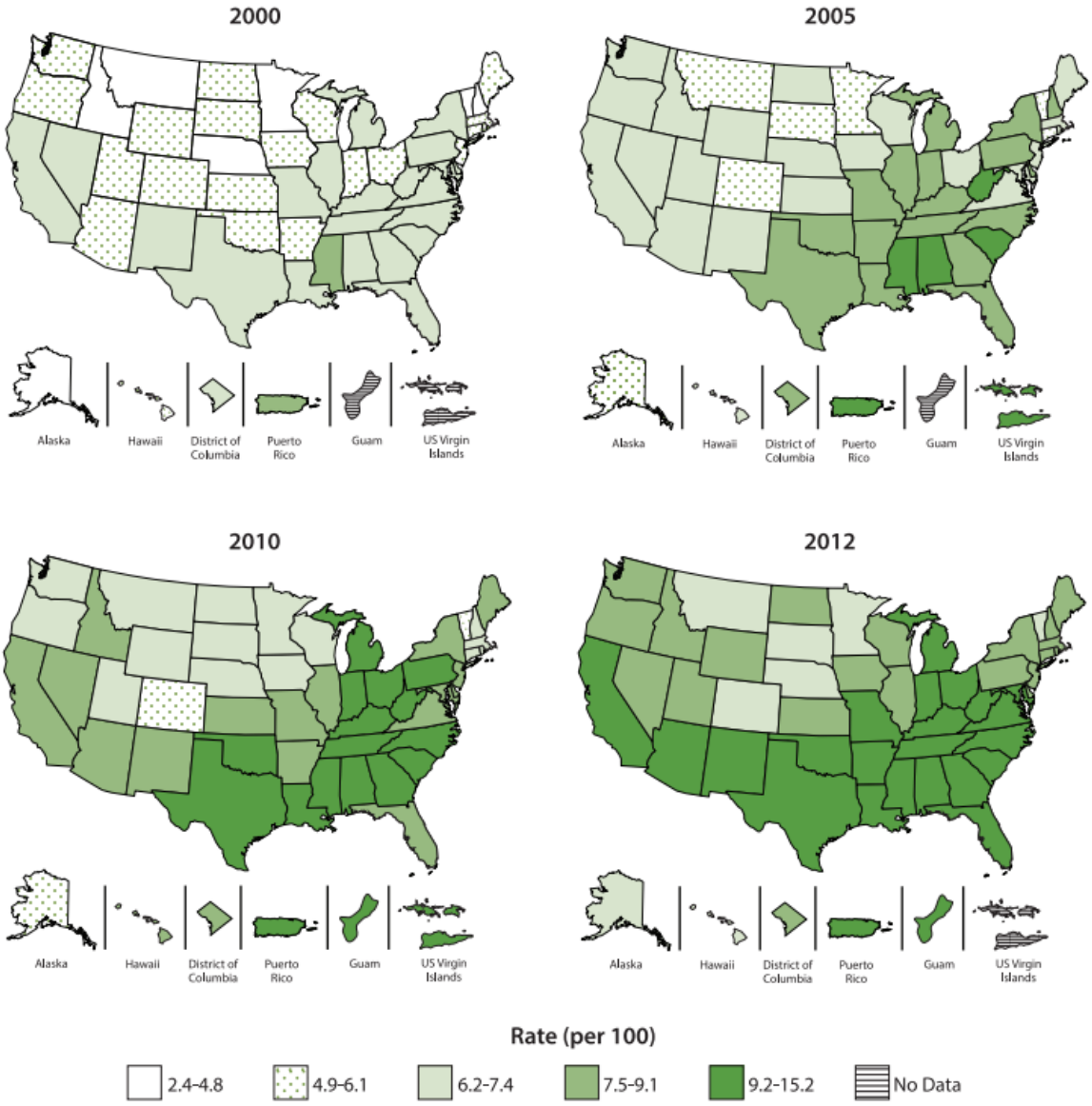

Figure 1-13. Geographic Distribution of Diagnosed Diabetes in the United States, 2000-2012. Figure adapted from Diabetes Report Card 2014, CDC.

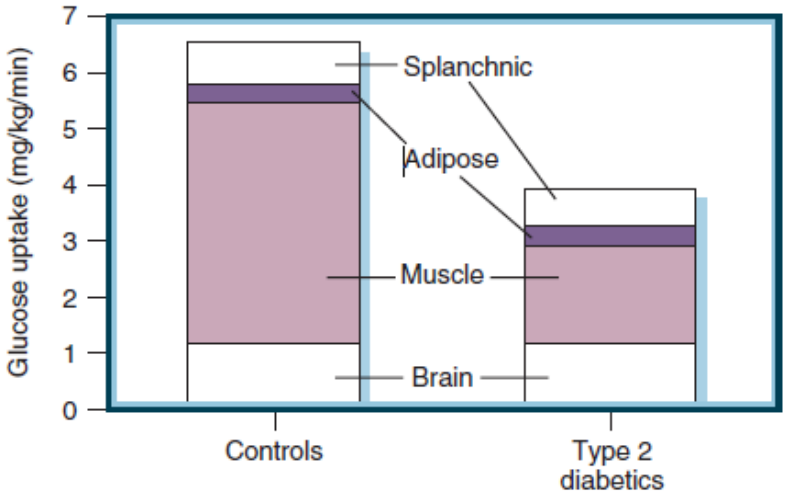

Figure 1-14. Insulin-stimulated glucose uptake rates in various tissues in human. Figure adapted from DeFronzo, R. A. Med Clin North Am, 2004.

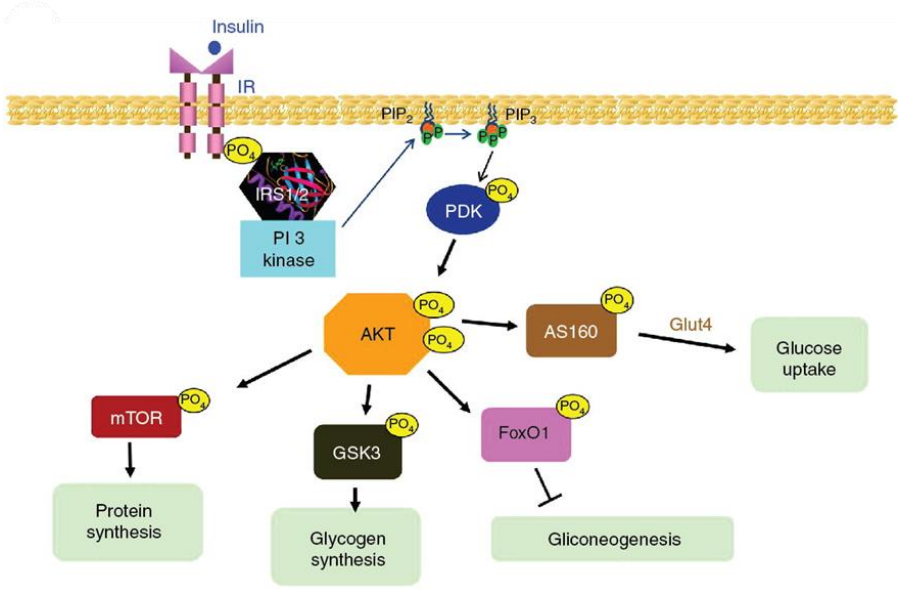

Figure 1-15. PI3K/AKT signal transduction pathway of insulin signaling. Figure adapted from Prada *et al*., Expert Opin Investig Drugs. 2013.

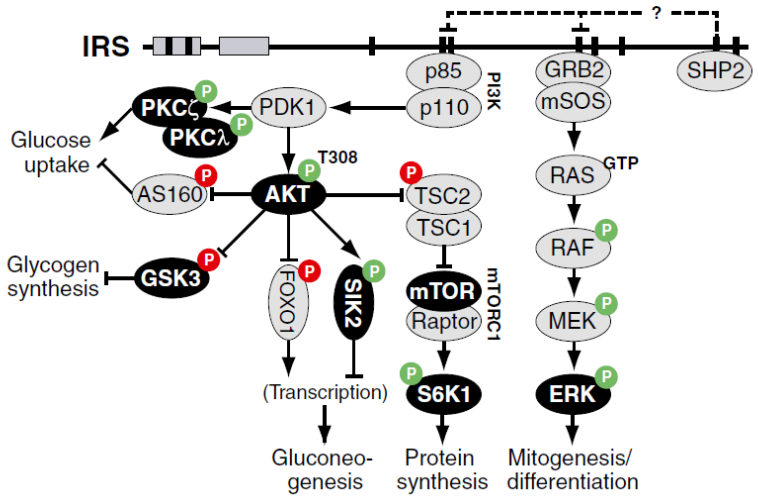

Figure 1-16. Insulin signaling and feedback pathways initiated by IRS. Figure adapted from Copps, K. D. White, M. F. Diabetologia. 2012.

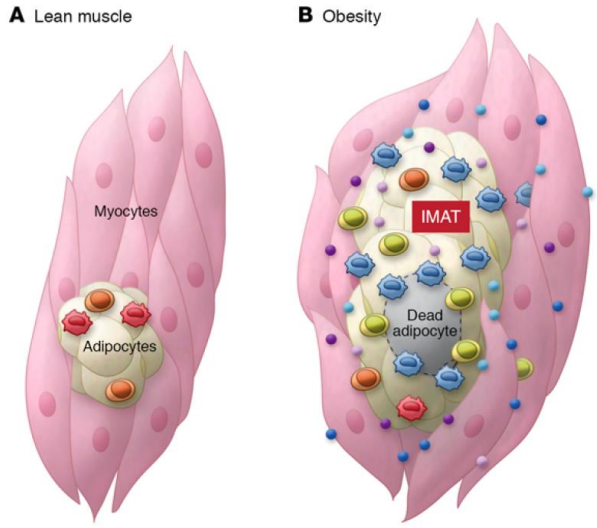

Figure 1-17. Inflammation in skeletal muscle in obesity. Figure adapted from Wu, H. Ballantyne, C. M. J Clin Invest. 2017.

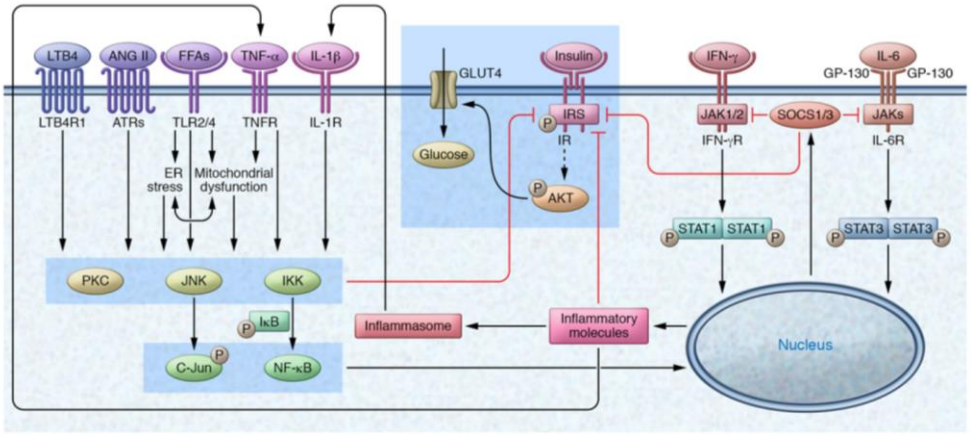

Figure 1-18. Inflammatory signaling mediates insulin resistance in myocytes via IRS/AKT pathway. Figure adapted from Wu, H. Ballantyne, C. M. J Clin Invest. 2017.

1.3 Activity-based kinome profiling

Human kinome consists of more than 500 protein kinases which constitute 1.7% of human genome, so high-throughput protein kinases enriching and profiling are highly demanded. Without kinome enrichment, traditional immunoblots technique (i.e., western blotting) requires to probe one kinase at a time with specific antibody against that kinase, and many kinases are not detectable due to the low protein abundance in the complex matrix (e.g., muscle tissue). Despite the immunoblotting is able to detect the protein kinases abundance, assessing the active form of kinase (i.e., certain serine/threonine or tyrosine phosphorylation of that kinase) might not be achievable due to lack of the phosphor-protein antibodies.

Therefore, activity-based ATP probes were developed for high-throughput enrichment of active protein kinases with the conserved kinase catalytic core, specifically, the 478 ePKs in human kinome.

1.3.1 Kinase activity assay

The traditional kinase function/activity assays (e.g., radiometric filtration binding assay, Figure 1-19) require radioisotope labeled ATP (H. Ma, Deacon, & Horiuchi, 2008), as well as specific substrate proteins which may not be commercially available. The enzyme activity is proportional for the utilized amount of ATP, calculating by initial ATP subtracted by the remaining ATP after the reaction. Other types of kinase functional assays are existing, such as fluorescence intensity assay, fluorescence polarization assay, scintillation proximity assay (von Ahsen & Bomer, 2005); yet, all the assays require prior knowledge on the kinase of interest and availability of corresponding substrates.

1.3.2 Chemical structure and reaction of the activity-based probes

Quantitative proteomics is primarily used to assess protein abundance in the cells or tissues; however, it becomes possible to detect proteins (enzymes) activities by coupling with activity-based enzyme enrichment. In 1999, Yongsheng Liu *et al*., (Y. Liu, Patricelli, & Cravatt, 1999) first synthesized the activity-based chemical probes for serine hydrolases enrichment of which a biotinylated fluorophosphonate (FP-biotin) was designed specifically for the active sites of serine hydrolases (Figure 1-20). Researchers developed various activity-based probe to assess enzyme activities (Bogyo, Verhelst, Bellingard-Dubouchaud, Toba,

& Greenbaum, 2000; Greenbaum et al., 2002; Okerberg et al., 2005; Saghatelian, Jessani, Joseph, Humphrey, & Cravatt, 2004).

In 2007, the same research group (Patricelli et al., 2007) synthesized novel nucleotide acyl phosphates probes (also called kinase probes) that selectively bind to ATP binding pocket (in the kinase core) of eukaryotic protein kinases (Figure 1-21). The kinase probes are constituted by an ATP group (adenosine ring and three phosphates) which selectivity binds to the ATP binding cleft, an acyl phosphate reaction group that forms an irreversible covalent bond with the conserved lysine, and a six carbon linker with a biotin tag which can be pulled down by the biotin affinity agarose beads (Avidin or Streptavidin). When the active-site directed probes bind to the active kinases, the conserved lysine residues can be labeled with biotin tags; subsequently, the labeled active kinases were digested by trypsin (a digest enzyme that cleaves specifically on lysine and arginine residues), and biotin tagged peptides of active kinases were enriched and analyzed by mass spectrometry. Figure 1-22 indicated two conserved lysine residues which are closed to the three phosphate groups in the ATP probe: one is K^{33} which is the conserved lysine on the N-lobe to stabilize the orientation of alpha- and beta-phosphates, and the other is K^{129} which is located at the catalytic loop (2^{nd} residue from HRD motif) and is key residue to transfer the gamma-phosphate to substrate peptides. Both lysine residues are highly conserved in nearly all the ePKs. Furthermore, the authors identified 3 conserved motif for kinase probe binding (Figure 1-23), where the size of the letter in given position represented the

proportion of that residue in the sequence; generally, bigger size of the letter the higher degree of conservation. A1 panel represented the conserved lysine in N-lobe, and A2 & A3 panel showed the lysine in catalytic loop.

Since the discovery of the activity-based kinase profiling, increased studies adopted this technique coupled with proteomics to perform kinase functional assay at large scale. Patricelli, M.P. and colleagues (Patricelli et al., 2011) revealed functional proteome of more than 200 native kinases against several well studied kinase inhibitors. Using activity-base kinase probe, recently, Okerberg et al., (Okerberg et al., 2016) identified a novel tumor-specific active site of casein kinase 1α (CSNK1A1). Figure 1-24 showed peptide sequence of active site of CSNK1A1 (panel A) and ion intensity of the mutated active site of CSNK1A1 (panel B).

In summary, activity-based protein profiling selectively targets active site of protein kinases, which allows for studying functional kinome in biological matrix.

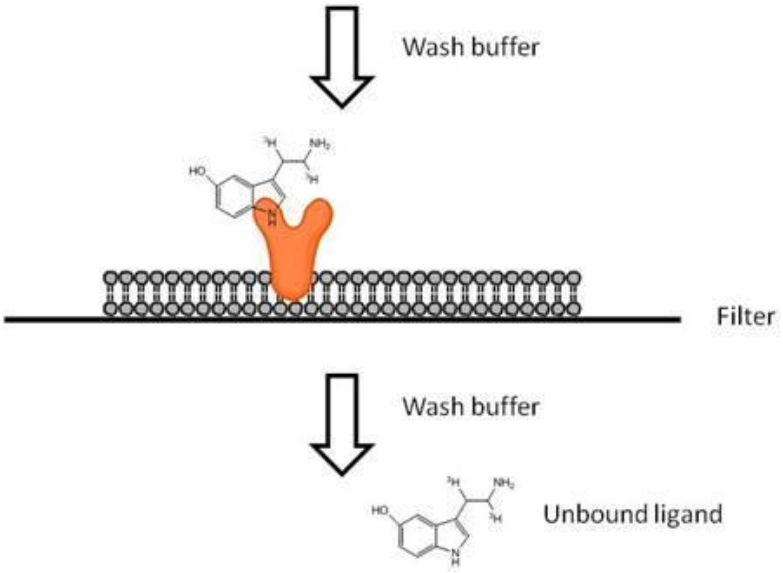

Figure 1-19. Diagram of radiometric filtration binding assay. Figure adapted from http://www.perkinelmer.com.

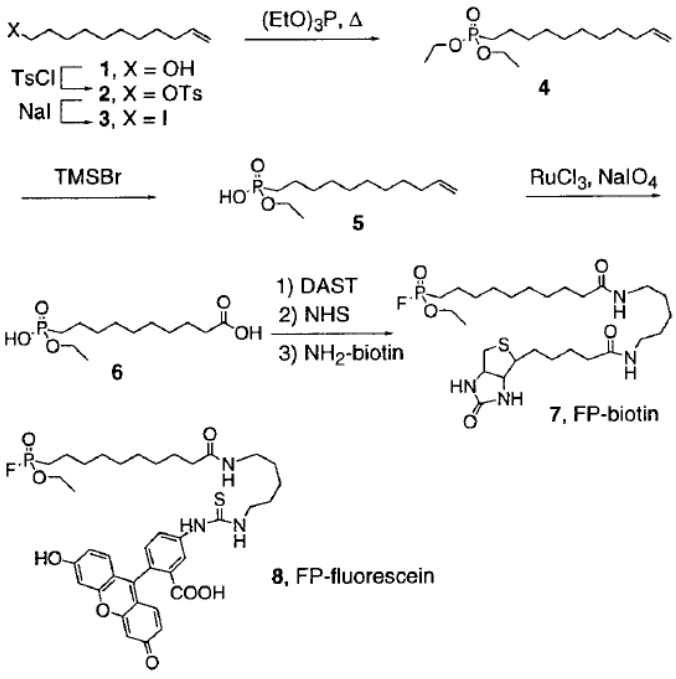

Figure 1-20. Route for the synthesis of FP-biotin. Figure adapted from Liu *et al*., PNAS. 1999.

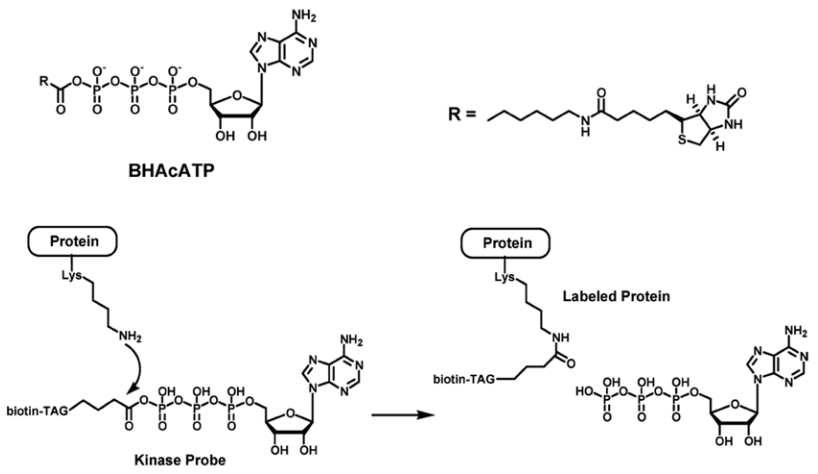

Figure 1-21. Structure and mechanism of kinase probes. Figure adapted from Patricelli *et al.,* Biochemistry. 2007.

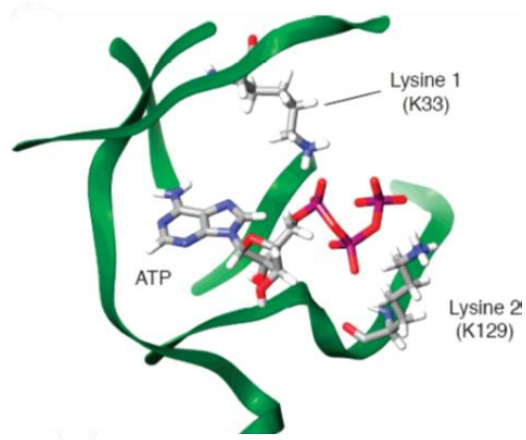

Figure 1-22. Conserved lysine residues in Cyclin-dependent kinase 2. Figure adapted from Patricelli *et al.,* Biochemistry. 2007.

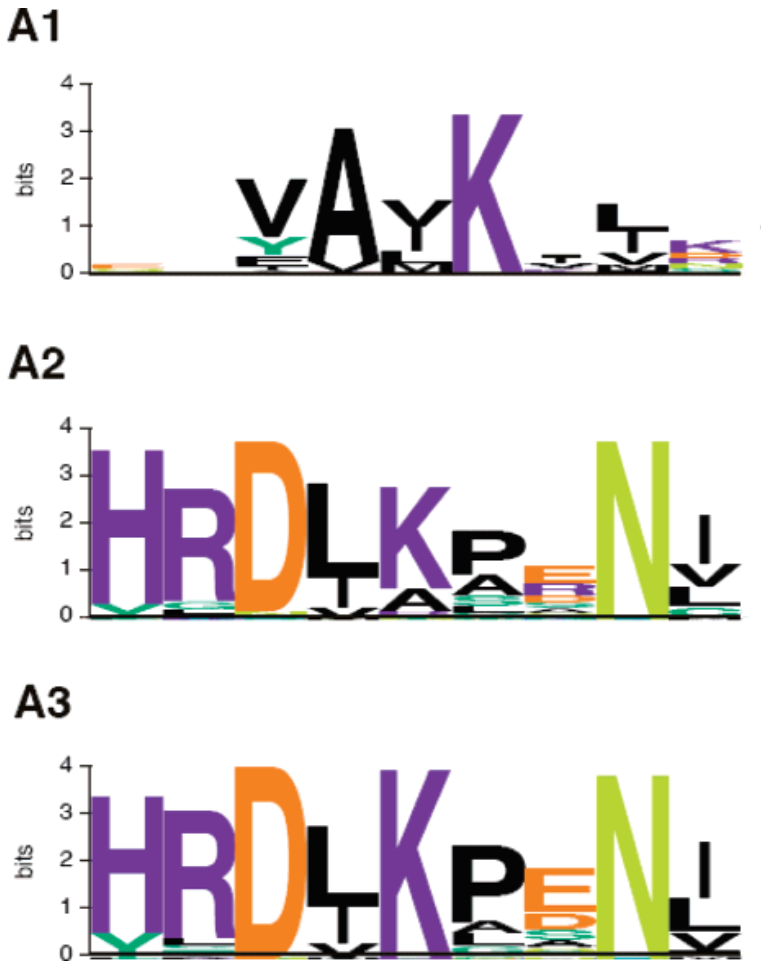

Figure 1-23. Three highly conserved kinase probe binding motifs. (A1) ATP binding site motif; (A2) Catalytic binding motif 1; (A3) Catalytic binding motif 2. Figure adapted from Patricelli *et al.,* Biochemistry. 2007.

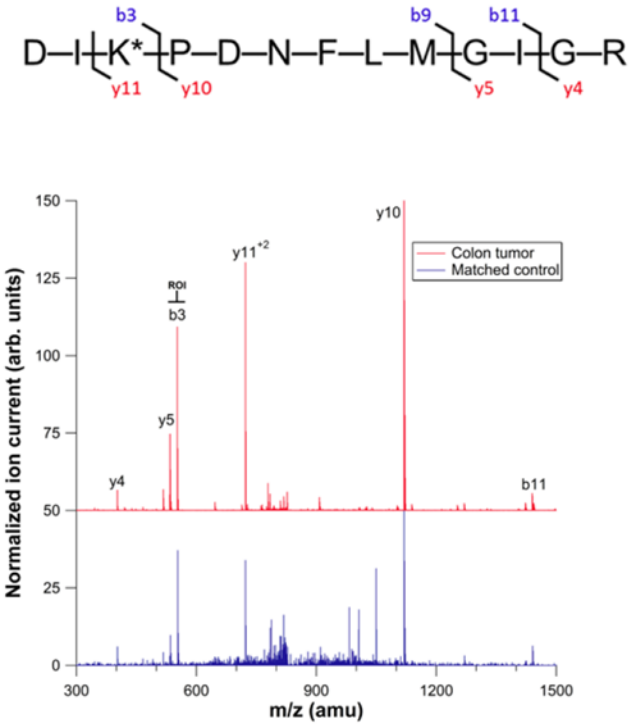

Figure 1-24. Analysis of a CSNK1A1 active-site peptide in both colon tumor and matched control samples. Figure adapted from Okerberg *et al.,* PLoS One. 2016.

1.4 Mass spectrometry-based quantitative proteomics

Proteome represents complete set of proteins in organisms. Proteomics is a technique, coupled with biology and mass spectrometry (MS), to identify and quantify as many proteins as possible in organisms. Even though around 20,000 genes in human genome has been sequenced, how many proteins (est. 1,000,000) and protein post-translational modifications in human remains unknown (Figure 1-25) (Mayne et al., 2016).

1.4.1 Protein immunoblotting versus MS-blotting

Protein immunoblotting (i.e., Western blotting) is one of the most commonly used methods to assess protein abundance in biological matrix (S. F. Smith, 1989). Western blotting starts with separating the protein mixture in SDS-PAGE system based on their molecular weights, followed by primary antibody probing of the target protein. Using secondary antibody (against the primary antibody) and chemical substrate of the secondary antibody, the target protein can be visualized by colorimetric detection or fluorescent detection. This approach has been used as a fundamental method to study protein abundance and other properties in biology, biochemistry, pathology, etc. Western blotting has numerous advantage over other methods, for example, providing specific and accurate assessment of target protein abundance in complex biological samples (Lustbader & Pollak, 1991). However, immunoblotting techniques are highly dependent on primary antibody; as a result, low quality antibody or lack of specific antibody for bait protein are limiting this method from high-throughput protein detection.

For many years, genomics has been primarily used for high-throughput gene mutation and sequencing study because methods for measuring proteins and metabolites could not achieve the high-throughput and in-depth as genomics techniques. However, quantitative proteomics started to provide global profiling of thousands of proteins in few hours. In 2015, Richards *et al.,* reported that a one-hour MS run could identify more than 4,000 proteins in yeast (Richards et al., 2015). The typical workflow for quantitative proteomics adapted the similar concepts of protein immunoblotting. The first step is separating the proteins (or peptides) mixture in high-performance liquid chromatography instruments (HPLCs). Second step is to analyze the extremely accurate molecular weight of each protein or peptides in a high resolution mass spectrometer (i.e., Oribtrap (Makarov, 2000)). The last step is to search the mass spectra against the known databases containing protein sequencing information (e.g., Uniprot). The protein abundance usually need to be normalized by internal or external standards. One of the biggest advantage of quantitative proteomics is that no specific antibody is required to identify the target proteins, and it can identify and quantify hundreds/thousands of proteins, protein phosphorylation and other post-translational modifications (PTMs).

Another crucial application for quantitative proteomics (also known as MS-blotting) is that MS-blotting could be applied for protein-protein interaction studies. In figure 1-26, we compared the advantages of MS blotting over the traditional immunoblotting. For the western blotting, bait protein and partner protein need to

be probed separately; however, both bait and partner proteins can be identified by MS-blotting simultaneously because MS doesn't require antibody probing. What's more, in the protein-protein interaction experiments, the MS based method can detect hundreds of protein interaction partners, and identify novel partners that have not been found by the immunoblotting (Caruso et al., 2015).

1.4.2 "Bottom-up" proteomics

Today, proteomics is a powerful tool to profile comprehensive proteomes in various biological samples (e.g., cells, tissues, blood, etc.) (Cheung & Juan, 2017; W. Liu et al., 2017; Tsolis & Economou, 2017). Two basic classes of proteomics analysis are commonly employed to system biology: "Top down" and "bottom-up" proteomics where "top-down" means to analyze the intact proteins directly by MS whereas "bottom-up" refers that proteins are first digested by specific protease (e.g., trypsin), and the resulting peptides are analyzed by MS (Gregorich, Chang, & Ge, 2014). The main defect of "Top-down" proteomics is that large protein molecules are difficult to be separated, fractionated, and ionized. Therefore, "Top-down" proteomics is not commonly used for large scale profiling. In contrast, "bottom-up" approach generates the relatively small peptides which can be easily separated and analyzed by MS, and the raw MS files containing the peptides information can be mapped and assigned to protein based on protein sequencing databases; hence, "bottom-up" proteomics is a primary proteomics method for high-throughput protein or/and PTMs profiling. For instance, Sacco, F. and colleagues were able to map 8,000 proteins and more than 16,000

phosphoproteins in breast cancer cells using “bottom-up” proteomics (Sacco et al., 2016).

1.4.3 “SILAC” based quantitative proteomics

Stable isotope labeled amino acid in cell culture (also known as SILAC) has been widely used for quantitative proteomics (Doherty, Hammond, Clague, Gaskell, & Beynon, 2009; Duan, Kelsen, Clarkson, Ji, & Merali, 2010; Schwanhausser, Gossen, Dittmar, & Selbach, 2009). In 2002, Ong *et al.,* first reported a SILAC method in which the two cell lines were cultured in two growth media containing two different isotopic labeled amino acids, the light (leu-d0) and heavy (leu-d3). Equal amount of the cell lysates from the light (leu-d0) and heavy (leu-d3) media were combined and analyzed together in one single MS-run (Figure 1-27). Because of the high resolution mass spectrometer, light and heavy labeled peptides were differentiated and compared their ion intensity in one MS raw file. Proteins from the two different cell lines can be compared side by side, leading to reduced experimental error.

In traditional SILAC experiments, up to three cell lines can be labeled and compared simultaneously, which is known as multiplex SILAC labeling. Seyfried *et al.,* (Seyfried et al., 2010) reported to perform quantitative “SILAC” proteomics to enrich Sumolyation in three cell lines. In order to apply this technique to the biological samples that are difficult to be labeled, such as tissue or plasma, a novel modified “SILAC” called super-SILAC was developed to explore the tissue based proteomics (T. Geiger, Cox, Ostasiewicz, Wisniewski, & Mann, 2010; Neubert &

Tempst, 2010; Pozniak & Geiger, 2014). Figure 1-28 is showing that the primary human skeletal muscle cells were labeled by $^{13}C_6$ L-Arginine as heavy cells, and the skeletal muscle tissues were not labeled (non-labeled tissues were considered as light tissue). Then equal amount of heavy labeled cells was spiked into different light tissue samples, and the ratio of light/heavy of each sample was obtained. The relative quantification of the tissue samples was based on “ratio of ratio” comparisons. Using Super-SILAC, Noberini, R. and T. Bonaldi (Noberini & Bonaldi, 2017) were able to largely profile histone post translational modifications in breast cancer tissues.

In summary, super-SILAC based “bottom-up” proteomics is a promising approach to accurately identify and quantify proteome and post translation modification-proteome in complex biological tissue samples.

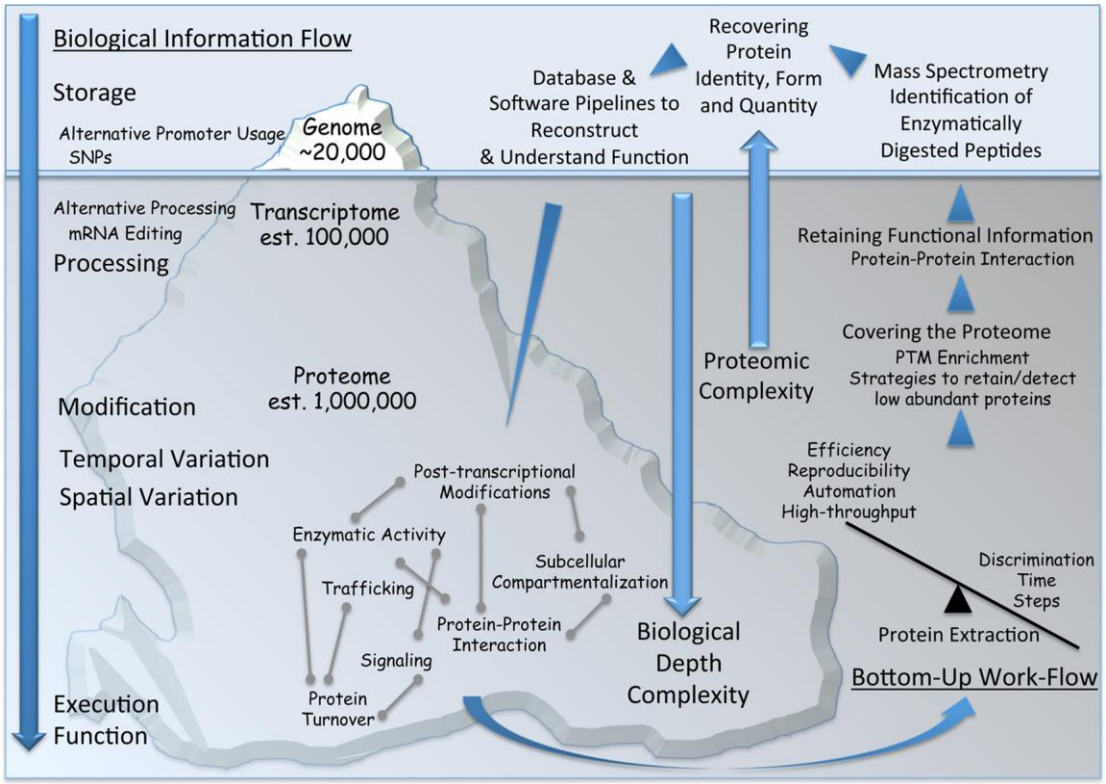

Figure 1-25. Schematic representation of the flow of bottom-up proteomics. Figure adapted from Mayne *et al.,* Anal Chem. 2016.

.

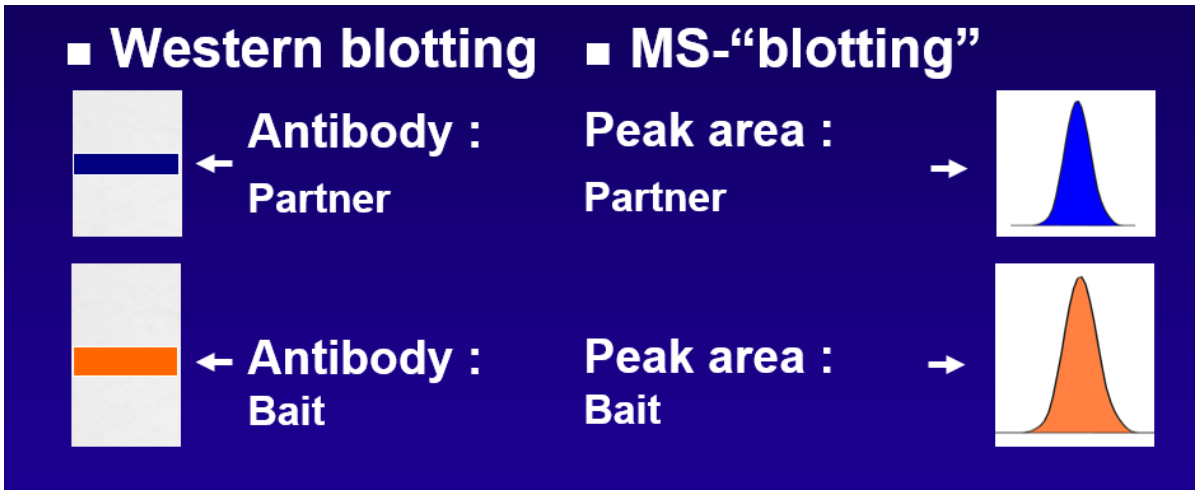

Figure 1-26. Western blotting versus MS-blotting in the protein-protein interaction studies.

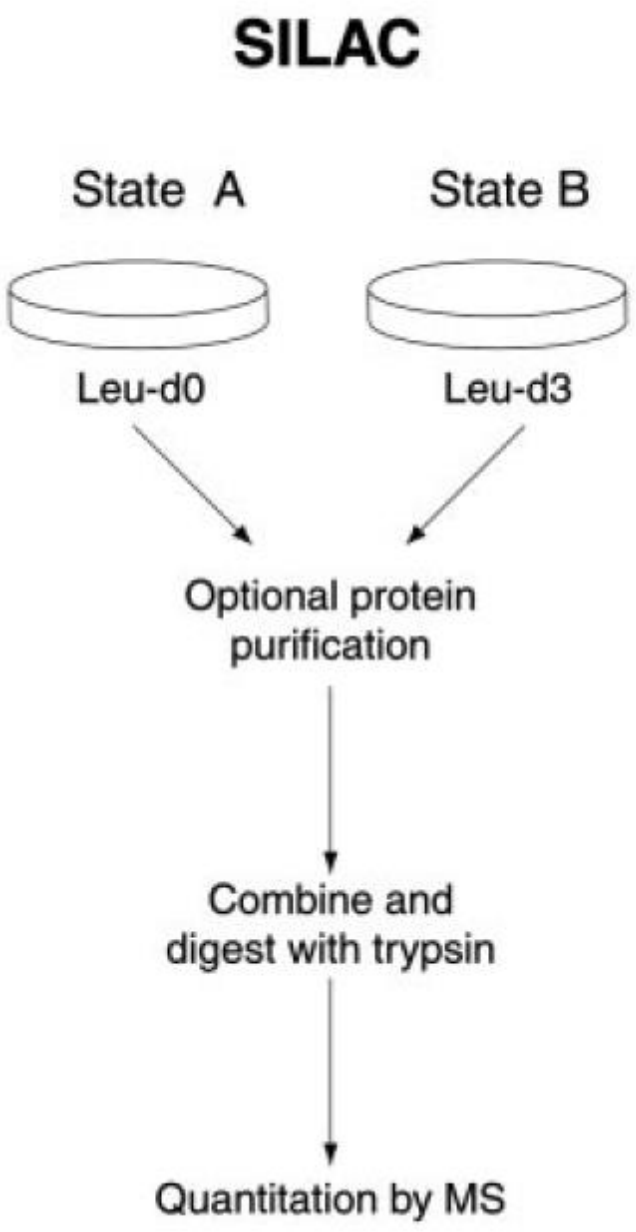

Figure 1-27. Diagram of SILAC labeling and workflow in MS. Figure adapted from Ong et al., Mol Cell Proteomics. 2002.

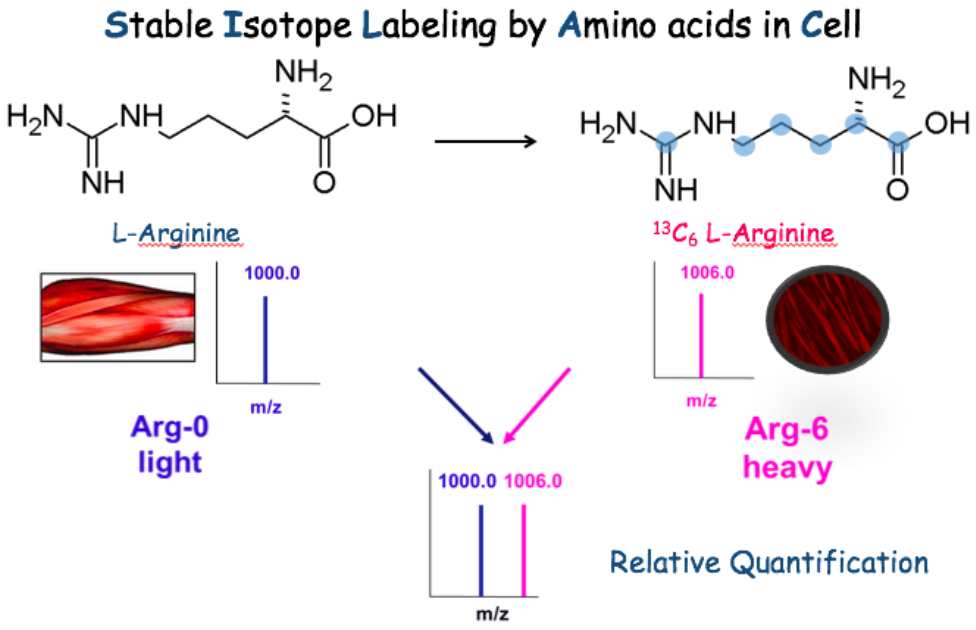

Figure 1-28. A schematic of Super-SILAC. Take $^{13}C_6$ L-Arginine as an example.

CHARTER 2. HYPOTHESES, SPECIFIC AIMS AND EXPERIMENTAL DESIGN

2.1 Hypotheses

Although skeletal muscle insulin resistance is a primary contributor to the development of metabolic abnormalities and chronic diseases, such as type 2 diabetes (T2D), the molecular mechanisms of its pathogenesis remain elusive (Abdul-Ghani & DeFronzo, 2009; Biddinger & Kahn, 2006; Cersosimo, MAndarino, & DeFronzo, 2011; DeFronzo & Abdul-Ghani, 2011; B. B. Kahn & Flier, 2000; Rask-Madsen & Kahn, 2012). A number of kinases, involved in insulin signaling, have been shown to have abnormal protein abundance and/or activity levels in insulin resistance (Taniguchi et al., 2006). However, these studies are mainly performed in cell cultures or animal models, targeting only a limited number of known kinases. The combination of kinase enrichment technologies with tandem mass spectrometry based proteomics offers a powerful approach for studying global profiles of kinases in human health and disease states. However, no kinome profiling in insulin resistant skeletal muscle in humans have been reported so far**. We hypothesize that there are abnormal kinome and kinome inteactome profiles in skeletal muscle of insulin resistant human participants (OBi) as compared to insulin sensitive subjects (LC).** The goal of the project is to identify novel kinase-based molecular mechanisms responsible for skeletal muscle insulin resistance in humans, providing new kinase targets for prevention and treatment of insulin resistance and T2D.

2.2 Specific aims

Specific Aim 1: Assess differences in kinome profiles in skeletal muscle from lean healthy insulin sensitive (LC) and obese insulin resistant human participants (OBi).

Specific Aim 2: Assess differences in kinome-interactome profiles in skeletal muscle from lean healthy insulin sensitive (LC) and obese insulin resistant human participants (OBi).

2.3 Experimental design

In figure 2-1, the two specific aims described in the overall experimental design flowchart demonstrate our research plan and strategy. Clinical studies were performed as we described (Caruso, Ma, Msallaty, Lewis, Seyoum, Al-janabi, Diamond, Abou-Samra, Højlund, et al., 2014). In brief, extensive subject recruitments were followed by comprehensive screening tests (e.g., oral glucose tolerance test (OGTT), body mass index (BMI), medical/health history, blood chemistry, ECG, etc.) at the clinical research center at Wayne State University. Eligible subjects underwent in-patient clinical tests: a 2 hour hyperinsulinemic-euglycemic clamp to assess insulin sensitivity with muscle biopsies. Muscle biopsy was quickly cleaned of connective tissue and fat (~30sec). Biopsy was frozen in liquid nitrogen and was used for kinome/kinome interactome analysis by the Universal-SILAC approach developed in Dr. Yi's laboratory (X. Zhang et al., 2014). Briefly, the study started with biopsy homogenization and spike-in standards (super-SILAC) to minimize experimental variation. The tissue and SILAC labeled cell lysate mixture was desalted by Zeba spin desalting columns to remove the

endogenous free ATP and salts in the lysis buffer. The desalted mixture lysate was labeled with ActivX ATP probes with desthiobiotin tag in the present of $MgCl_2$, while, for the kinome interactiom study, half of the mixture lysate was not labeled with ATP probes. Those lysate without labeling was served as a negative control for eliminating non-specific binding.

For specific aim 1, the labeled proteins were denatured by 8M urea buffer and subsequently reduced by dithiothreitol (breaking the disulfide bonds) and alkylated by iodoacetamide. The proteins were digested by MS-grade trypsin at 37°C shaker overnight. The resulting tryptic peptides were pulled down by streptavidin agarose resin which has high affinity to desthiobiotin to enrich ATP probe labelled peptides (which were from active kinase since active kinases, but not inactive kinases, can be labelled by the ATP probe). The peptides pulled down were washed and eluted from the beads. Enriched ATP probe labelled peptides were desalted by C_{18} ziptip and analyzed by HPLC-ESI-MS/MS, followed by bioinformatics study using different databases (such as Ingenuity Pathway Analysis, Kyoto Encyclopedia of Genes and Genomes and Reactome pathway databases).

For specific aim 2, double amount of tissue and cells as kinome enrichment in Aim 1 were homogenized. Then, half of the mixture (muscle and SILAC cells) lysate were labeled with ActivX ATP Probe whereas the other half won't be labeled (serving as a negative control). Instead of trypsin digestion to generate labeled peptide, we will first pull down ATP probe labelled proteins (in

this case, active kinases, or active kinome) as well as their kinase interaction partners, or kinome interactome. Followed by IP lysis buffer washing, PBS washing and HPLC-grade water washing, three times of each, kinases and their binding partners were reduced and alkylated, then were digested by trypsin “on-beads” overnight. The tryptic peptides were desalted by C_{18} ziptip, followed by HPLC-ESI-MS/MS analysis and bioinformatics study.

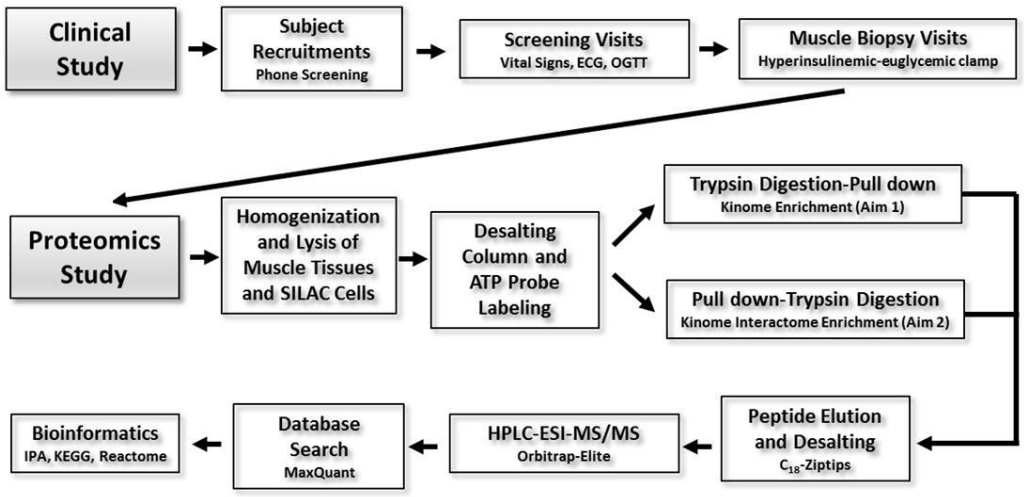

Figure 2-1. Schematic diagram of clinical, biological, and proteomics studies.

CHARTER 3. CLINICAL STUDY PROTOCOL AND CHARACTERIZATION OF HUMAN PARTICIPANTS

3.1 Human participant recruitment and screening visit

The participants for this project were recruited and studied at the clinical research center at the C.S. Mott Center for Human Growth and Development at Wayne State University. We started with initial phone screening to exclude any participants with significant diseases (i.e., cancer, type 1 diabetes, etc.) and inform the subjects study protocol of this clinical research, also schedule them for first on-site visit (Visit 1).

During the visit 1, we hired or collaborated with licensed research nurses (RN) and physicians who eventually determined the eligibility of participants and later perform muscle biopsy during visit 2. Participants were consented first with general introduction of our study and they had to sign the consent form which had been approved by Wayne State University IRB. We excluded participants based on our exclusion criteria, such as significant pulmonary diseases (e.g., COPD), heart diseases, diabetes coma, and extreme obese (BMI>40). Participants also had to pass the urine tests, ECG and routine blood tests. For example, participants with significantly lower than normal hemoglobin and hematocrit were excluded since they may have anemia that might cause bleeding problem during the muscle biopsy procedure (Barany, 2005; Ribeiro-Alves & Gordan, 2014; Torimoto & Kogo, 2006).

For the non-diabetic participants, we had to conduct OGTT which is a test for diabetes diagnosis. Participants were fasting minimal 10 hours, and given glucose tolerance test beverages containing 75g glucose (Thermo Fisher Scientific, Inc) and we drew the blood every 30 minutes up to 2 hours for plasma glucose measurement using YSI 2300 glucose analyzer (Belfiore, Iannello, & Volpicelli, 1998; Fujibayashi et al., 2015). We grouped the participants (non-diabetic, pre-diabetic or diabetic) based on three criteria, HbA1C value, fasting glucose and blood glucose at 2 hours of the OGTT (Figure 3-1) (American Diabetes, 2012). Participants who meet at least one of the three criteria are considered as diabetes, a) A1C≥6.5; b) Fasting Plasma Glucose≥ 126mg/dl; c) 2h-Plasma glucose≥200mg/dl.

3.2 Hyperinsulinemic-euglycemic clamp and muscle biopsies.

The qualified participants were scheduled to the second visits for hyperinsulinemic-euglycemic clamp, the gold standard for insulin sensitivity measurement, and muscle biopsy. They had to be fasting at least 10 hours overnight and stop anticoagulants, which may cause bleeding, 7 days prior to the second visit. Hyperinsulinemic-euglycemic clamp was used to measure the insulin sensitivity of skeletal muscle *in vivo* (Cusi et al., 2000; DeFronzo, Tobin, & Andres, 1979), as described in previous studies (Langlais et al., 2011; Yi et al., 2007). The study started at approximately 8:30 AM (time -60 minute point) in the morning and basal plasma glucose was measured. The blood was drawn through a catheter placed in an antecubital vein on one arm, which was covered by a heating pad

(60 °C), where we also infused saline to avoid dehydration. Another catheter was placed on the other arm for insulin and glucose infusion. The muscle biopsy was performed at -30 min with a percutaneous needle in vastus lateralis muscle of thigh under local anesthesia (use lidocaine). Muscle biopsies were immediately washed with ice-old saline containing proteases and phosphatases inhibitors, separated of connective tissue and adipose tissue then frozen in liquid nitrogen. At time 0 min point, we started the primed regular human insulin (Humulin R; Eli Lilly, Indianapolis, IN) infusion at constant rate 80 mU/m^2/min and variably infuse 20% d-glucose to maintain the plasma glucose at 90 mg/dl. The theory of hyperinsulinemic-euglycemic clamp was described in Figure 3-2 that we continuously infused very high dose of insulin for 120 minutes to overcome the endogenous insulin effect and adjusted glucose infusion rate to target the plasma glucose at roughly 90 mg/dl by monitoring the blood glucose every 5 minutes. The average of glucose infusion rates during the last 30 minutes of the clamp (also known as M value, glucose uptake rate mg/kg.min) is widely used in the literature to represent the insulin sensitivity in skeletal muscle. The higher M value, the higher insulin sensitivity and the lower insulin resistance, vice versa (Caruso, Ma, Msallaty, Lewis, Seyoum, Al-janabi, Diamond, Abou-Samra, Hojlund, et al., 2014). In Figure 3-3, more than 200 participants who completed our clamp studies since 2012 showed significantly different M-value between lean group and overweight/obese and T2D groups; however, no significant change of M-value was observed between overweight/obese and T2D group, which indicated that

overweight/obese and T2D participants were insulin resistant but lean group maintained normal insulin sensitivity.

3.3 Clinical characterization the 16 participants recruited in kinome/kinome interactome study

Totally, 8 lean healthy insulin sensitive and 8 obese insulin resistant participants were recruited this projects. In table 3-1, participants were matched with gender (5 males and 3 females in each group) and age (28.13 years old in lean group versus 33.00 years old in obese group, P>0.05). The BMI and percentage of body fat of these two groups showed significant difference where p-value of BMI was less than 0.001 and p-value of % Fat Mass was less than 0.05 (Figure 3-4); in contrast, their mean hemoglobin A1c % (HbA1c%), fasting blood sugar and 2h OGTT were similar and all were below the ADA's prediabetes and T2D diagnosis cutoffs (Figure 3-5). OGTT was showed in Figure 3-6 where the plasma glucose of both groups reached a peak value (~130 mg/dL) and went down back to normal range at 2 hour time point, which means 8 lean and 8 obese subjects had normal glucose tolerance. In Figure 3-7, fasting plasma insulin levels were significantly elevated in obese insulin resistant subjects (p-value < 0.01), which implied the obese participants suffered from hyperinsulinemia. The lipid profiles were showed in Figure 3-8: A) the total cholesterol levels of obese participants were slightly increased but not significantly changed; (B) the triglycerides levels in insulin resistant obese participants were significantly elevated (p-value<0.05); (C) the high-density lipoprotein (HDL) cholesterol, which

may reduce the risk for cardiovascular disease and diabetes, was slightly but not significantly decreased in obese versus lean healthy participants (Bauer et al., 2017; Rhee, Byrne, & Sung, 2017; Sanguinetti et al., 2001); (D) however, the low-density lipoprotein (LDL) cholesterol, the known “bad” lipoproteins that could be an indicator for risk of cardiovascular disease (McCormack, Dent, & Blagden, 2016; Soltani et al., 2016) and has been observed to be elevated in obese and T2D participants (Marin et al., 2015), was significantly increased in the insulin resistance group compared to lean group (p-value < 0.05).

As described above, the hyperinsulinemic-euglycemic clamp was applied to measure insulin sensitivity. The obese participants for the kinome project were selected based on their M-value, which is the key parameter reflected the insulin sensitivity, and we chose 8 obese participants with significantly low M-value and thus insulin resistance. Figure 3-9 is showing the infusion rate of glucose which compensated the high dose of insulin effect during the 120 minutes clamp. In the diagram, lean group reached a peak infusion rate of glucose and went down to stable stage while obese participants quickly reached to a much lower plateau than lean group without a peak dose of glucose. In figure 3-10, showing the M-value calculated based on the average of last 30 minutes glucose infusion rates, obese participants with insulin resistance had significantly lower M-value than lean healthy participants (p-value < 0.001).

In summary, 8 lean healthy participants with normal glucose tolerance, insulin sensitivity, insulin and lipids, and 8 obese participants with normal glucose

tolerance but hyperinsulinemia and insulin resistance were enrolled in this kinome/kinome interaction partner study.

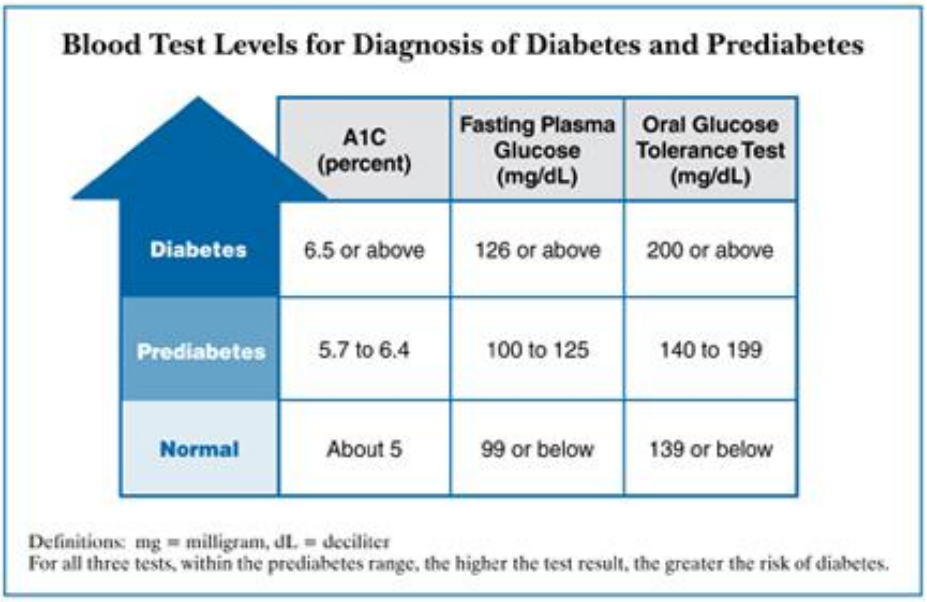

Figure 3-1. The established glucose criteria for the diagnosis of diabetes. Figure adapted from *American Diabetes Association* (American Diabetes, 2012).

.

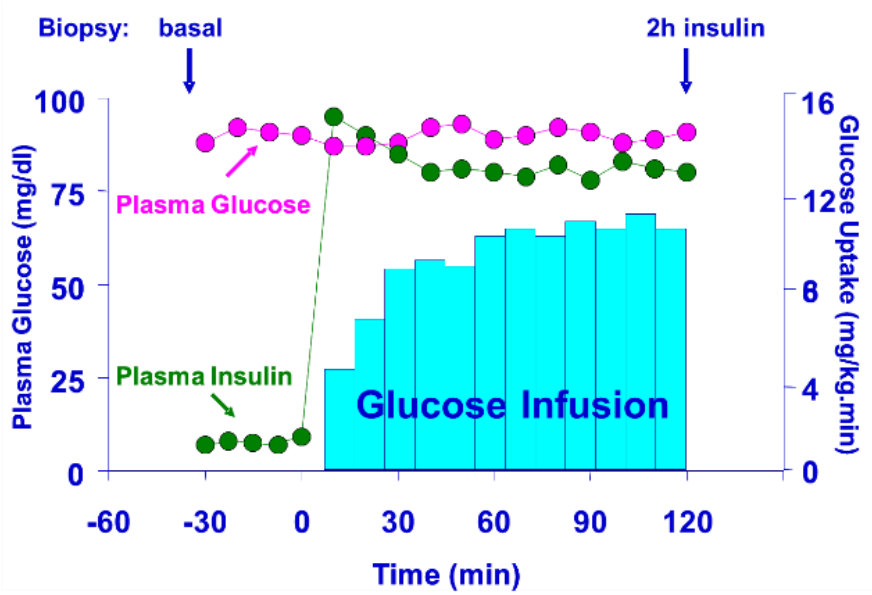

Figure 3-2. Diagram of hyperinsulinemic-euglycemic clamp. Insulin infusion starts at time point 0 minute with constant rate, and adjusted rate of glucose infusion is to compensate the insulin effect. Plasma glucose was maintained at 90mg/dL.

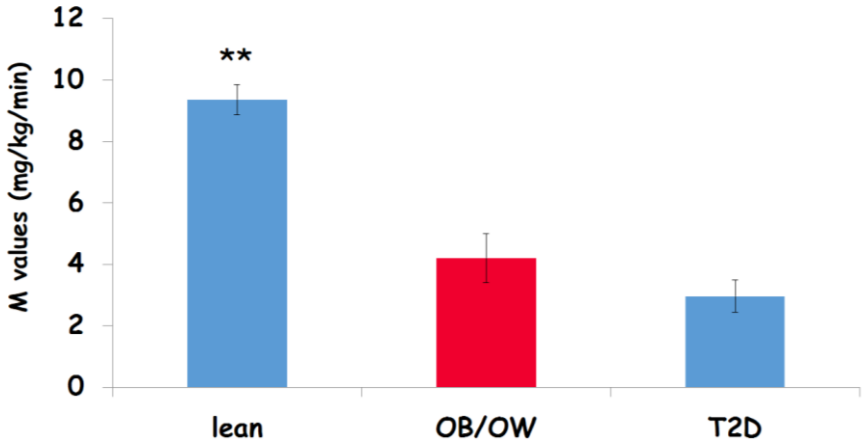

Figure 3-3. Average M-value (mg/kg/min) of the participants completed clamp study. M-value is indicating insulin sensitivity, and more than 200 subjects have completed hyperinsulinemic-euglycemic clamp in our study since 2011.

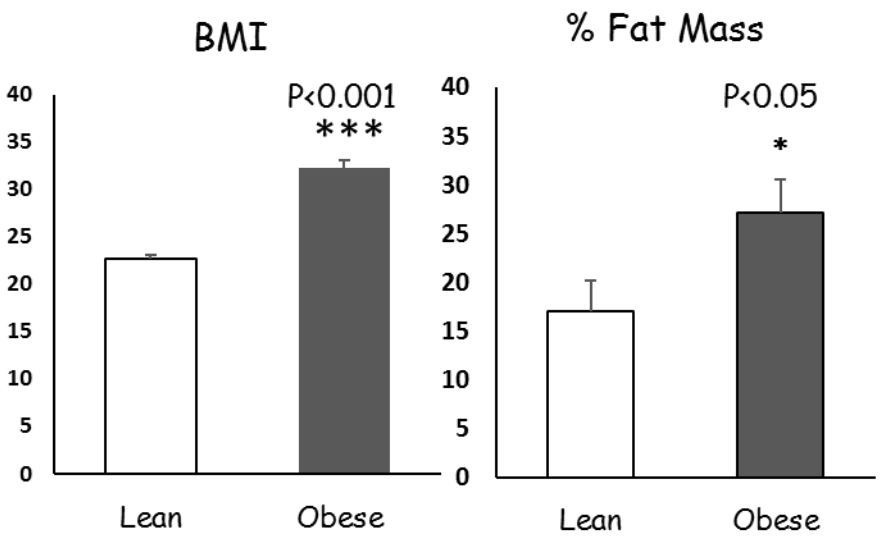

Figure 3-4. The BMI and percentage of body fat of the 8 lean and 8 obese participants. Bar charts are given as mean ± SEM.

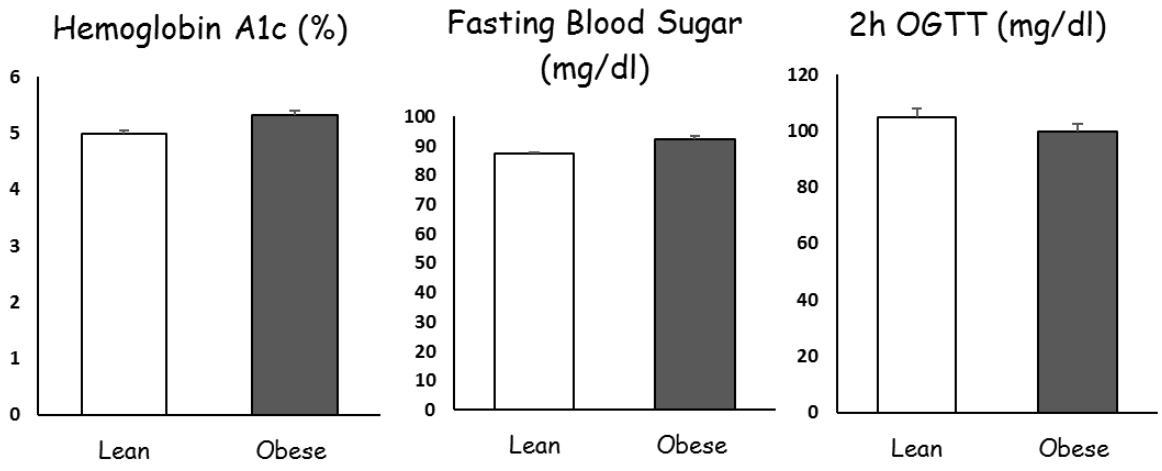

Figure 3-5. The HbA1c% and fasting glucose levels of the 8 lean and 8 obese. Bar charts are given as mean ± SEM.

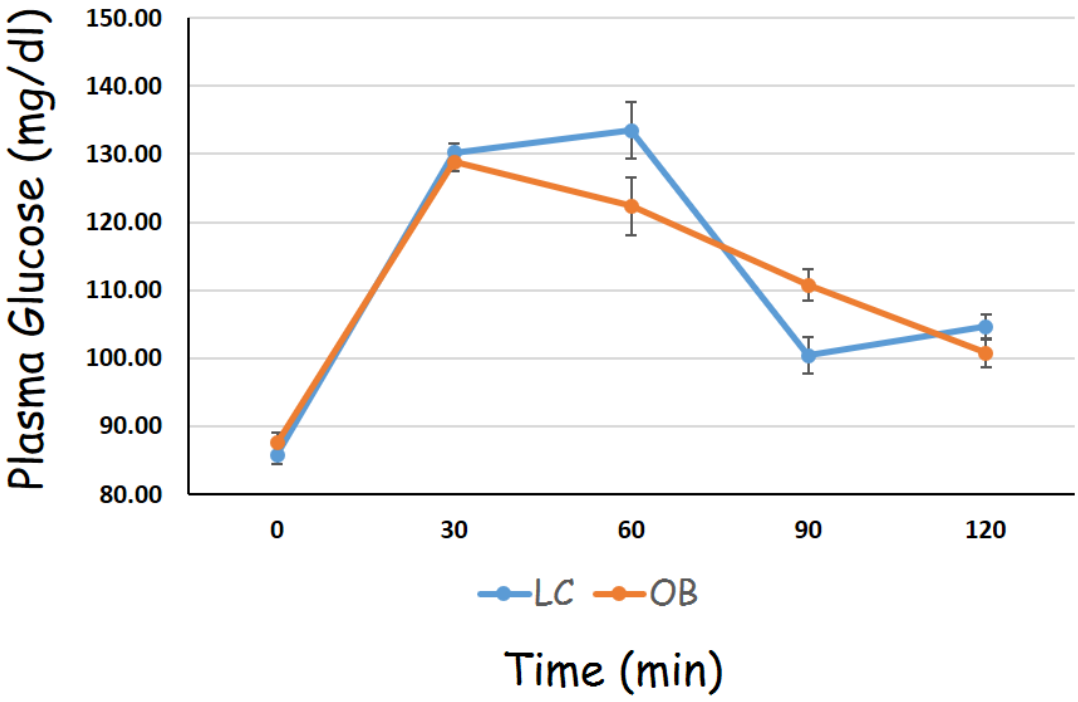

Figure 3-6. Oral glucose tolerance test (OGTT) of the 8 lean and 8 obese participants. Scatter plots are given as mean ± SEM.

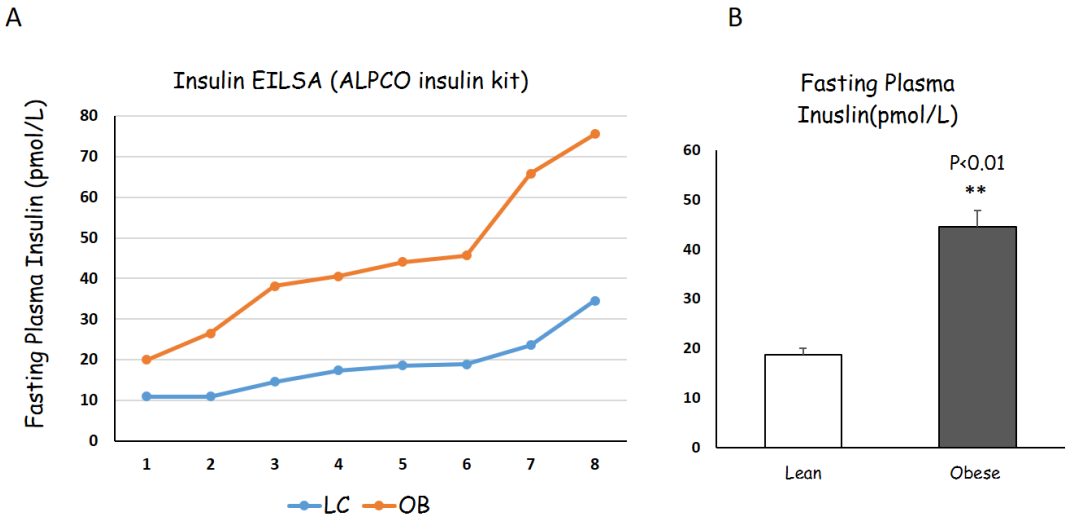

Figure 3-7. Fast plasma insulin level in 8 lean and 8 obese participants.

(A) The scatter plots are showing the individual fasting plasma insulin (pmol/L) of the 8 lean and 8 obese subjects. (B) The bar charts are representing the fasting plasma insulin (pmol/L) in mean ± SEM.

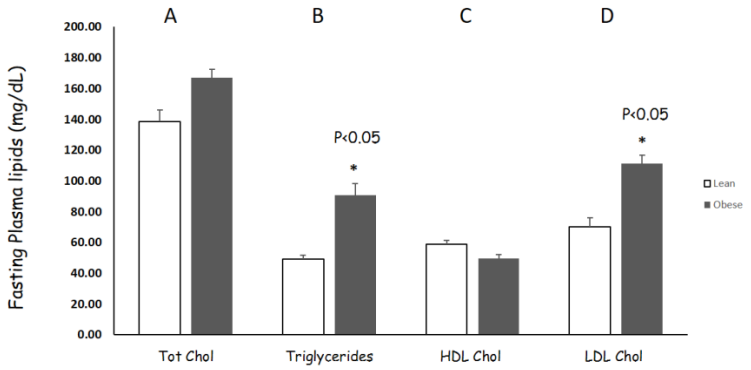

Figure 3-8. Lipid profiles of the 8 lean and 8 obese subjects. Four panels represent: (A) total cholesterol; (B) Triglycerides; (C) HDL cholesterol; (D) LDL cholesterol.

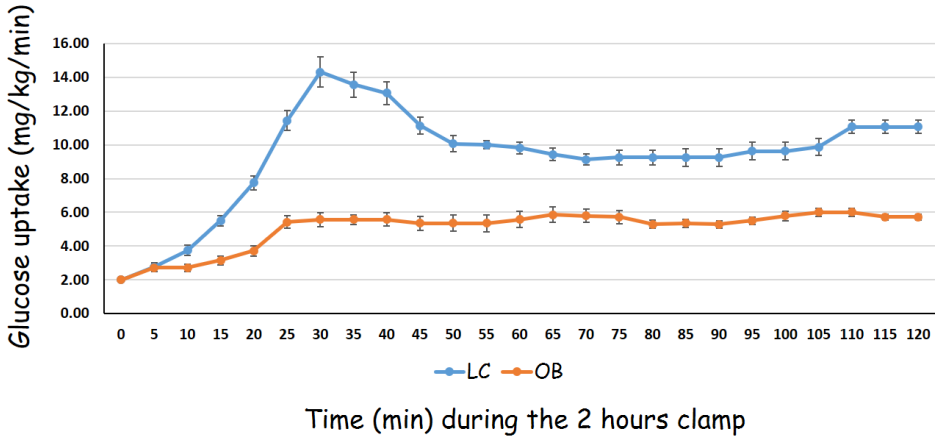

Figure 3-9. Two-hour hyperinsulinemic-euglycemic clamp data points of the 8 lean and 8 obese participants. The blue line represents lean group and orange line stands for obese group (scatter plots are given as mean ± SEM).

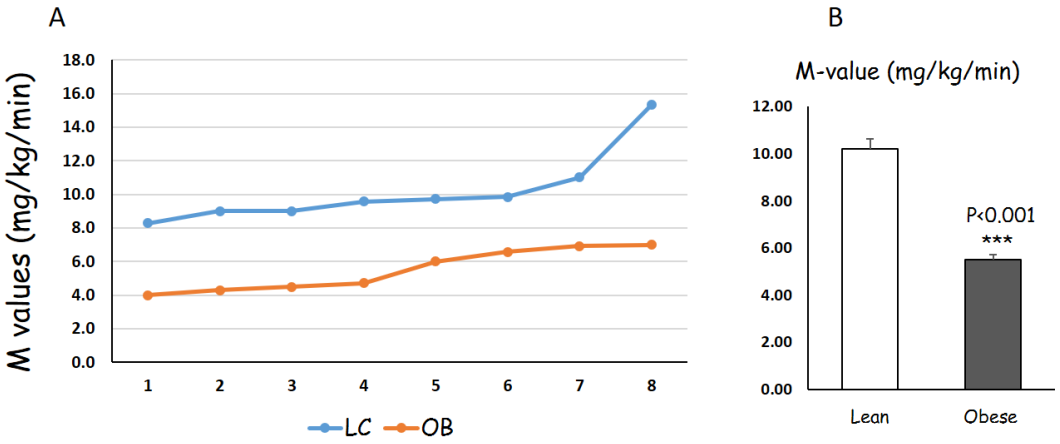

Figure 3-10. M-value of the 8 lean and 8 obese subjects.

(A) The scatter plots are showing the individual M-value (mg/kg/min) of the 8 lean and 8 obese subjects. (B) The bar charts are representing the M-value (mg/kg/min) in mean ± SEM.

Table 3-1. Clinical characteristics of the 8 lean and 8 obese participants.

	Lean (n=8)	Obese(n=8)
Gender (M/F)	5/3	5/3
Age (years)	28.13±3.06	33.00±4.71
BMI at V2 (kg/m2)	22.74±0.68	32.26±1.50***
%Fat Mass	16.95±3.16	27.10±3.38*
HbA1C (%)	5.00±0.11	5.33±0.14
Fasting blood suger (md/dL)	87.34±1.04	93.33±2.19
2h OGTT (mg/dL)	104.65±6.15	99.70±5.07
M value (mg/kg/min)	10.22±0.79	5.50±0.44
Fasting plasma insulin (pmol/L)	19.39±3.13	40.84±7.63**
Tot Chol (mg/dL)	140.38±14.75	166.50±10.30
Triglycerides (mg/dL)	48.50±14.27	89.63±14.57*
HDL Chol (mg/dL)	60.25±5.77	47.50±3.44
LDL Chol (mg/dL)	72.00±11.65	108.50±10.07*

* p-value <0.05

* *p-value <0.01

* **p-value <0.001

Data are given as mean ± SEM

CHARTER 4. HUMAN KINOME PROFILING IN SKELETAL MUSCLE INSULIN RESISTANCE

4.1 Introduction

Protein kinases are the key regulatory modules for variety of biological processes, such as insulin signaling pathway, glucose metabolism and inflammation pathways. Dysregulated protein kinases might induce impaired signal transduction and diseases (e.g., insulin resistance, T2D). As described above, typical protein kinases (or ePKs) have a core structure for catalytic activity, and taking MAPK1 as an example in Figure 4-1, the protein kinase core (shared by majority of typical protein kinases) contains: 1) a conserved lysine (K^{54}), located in N-lobe, for alpha- and beta-phosphates of the ATP binding; 2) a Glycine rich-loop (also known as phosphate-binding loop or P-loop) for ATP binding; 3) another conserved lysine (K^{151}), located in catalytic loop, for gamma-phosphate binding; 4) a DFG motif which is important for kinase activity; 5) a HRD motif in the activation loop which is also regulating the kinase activity, where the aspartate (D^{149}) is responsible for transferring the gamma-phosphate to substrate proteins. In Figure 4-2 (O. Hantschel & Superti-Furga, 2004), tyrosine-protein kinase Lck (Lck) is an example for active conformation of protein kinase core where p-loop is in the “open” position and DFG motif is also in “DFG-in” conformation; in contrast, Proto-oncogene tyrosine-protein kinase Src (Src) is demonstrating the inactive kinase core where p-loop is in “closed” position and DGF motif is in “DFG-out” conformation. The Lck and Src have very similar size (509 amino acids of Lck, 536

amino acids of Src), ATP binding site (K273 in Lck and K298 in Src), and active site (D364 in Lck, D389 in Src); thus, they shared very similar kinase core structure which represents the active and inactive forms of most protein kinases.

The ActivX™ Desthiobiotin-ATP Probes, one type of the activity-based protein profiling probes, consist of 1) a molecule of ATP which can be selectively bound to the ATP binding cleft between the N-lobe and C-lobe; 2) an acyl phosphate contain reaction group which can form a covalent bound with the conserved lysine residues (either the one in ATP binding pocket or the one in catalytic loop); 3) A desthiobiotin-tag which can be pulled down by streptavidin (Figure 4-3).

Skeletal muscle insulin resistance is one of the main defects in T2D, and the molecular mechanism of insulin resistance in human skeletal muscle has not been fully understood. We hypothesized that abnormalities in active protein kinases play key roles in insulin resistance. Therefore, we sought to globally enrich active protein kinases in human skeletal muscle insulin resistance, and discover the abnormalities of protein kinases may contribute to the cellular mechanism and pathogenesis of insulin resistance.

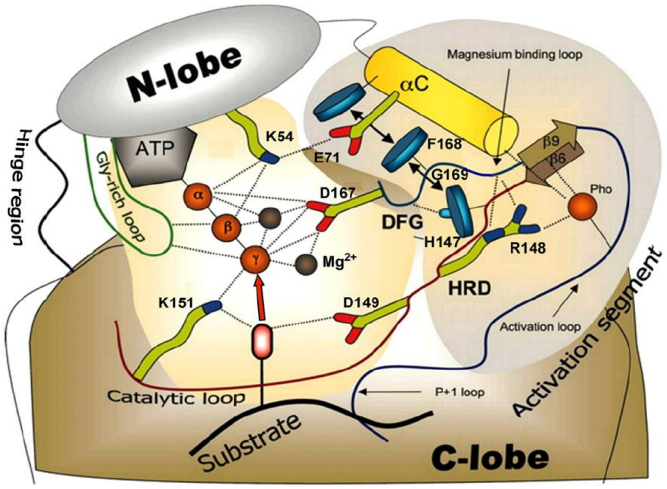

Figure 4-1. Protein kinase core of MAP kinase-1. (Figure adapted from Kornev *et al.,* PNAS, 2006).

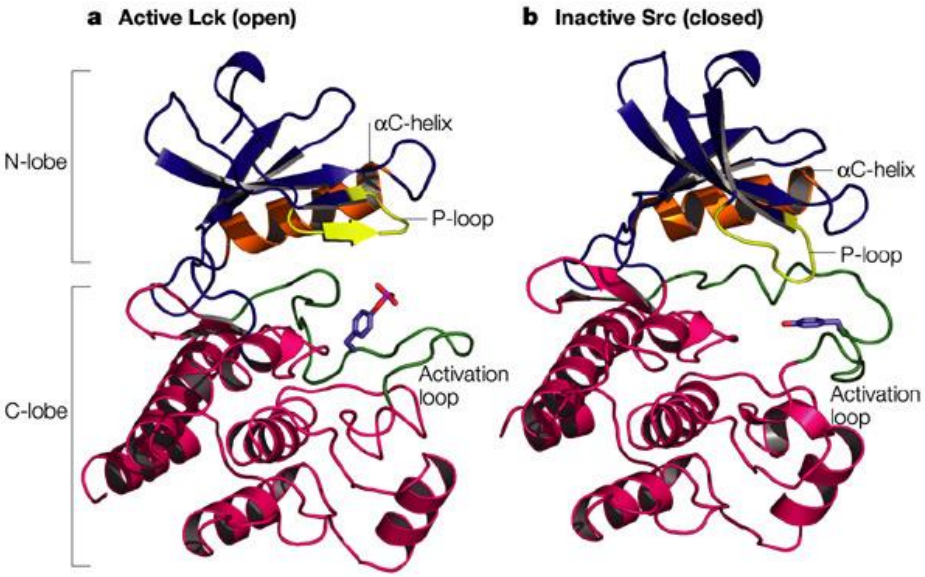

Figure 4-2. Active and inactive protein kinase core.

Lck represents active conformation whearas Src represents inactive conformation of kinase core. Figured adapted from Hantschel, O. Nature Reviews Molecular Cell Biology, 2004.

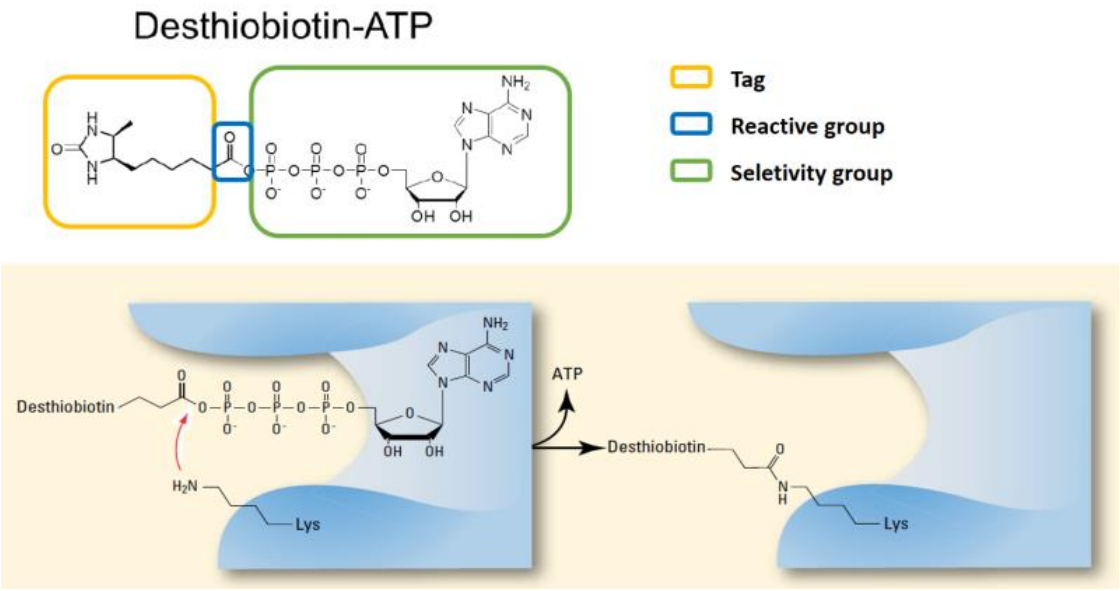

Figure 4-3. Chemical structure of the desthiobiotin-ATP probe. (Figure provided by the vendor).

4.2 Materials and Methods

4.2.1 Primary human skeletal muscle cells for SILAC labelling

Ten to fifteen milligrams of freshly obtained human muscle biopsy were washed 3 times with ice cold Phosphate-Buffered Saline (PBS, pH 7.4, catalog # 10010049, Invitrogen, Carlsbad, CA), and were transferred to a 100mm sterile cell culture dish. The muscle tissue was placed in the center of the dish using sterile forceps, and was minced finely using a small sterile scissors; subsequently, was transferred into a 50 mL conical centrifuge tube with 20 mL digestion solution (0.05% trypsin EDTA (catalog # 25200056, Invitrogen, Carlsbad, CA) in PBS). The tissue was incubated for 60 minutes at 37 °C, and the tube was swirled vigorously every

20 minutes. After the incubation, digested tissue pieces were centrifuged at 3000 rpm for 15 minutes, and the pellet was transferred to a new 50 mL conical centrifuge tube with 10mL human skeletal muscle cells medium, where the based medium was Dulbecco's Modified Eagle's Medium with 1.0 g/L glucose (DMEM, catalog # 11885-092, Invitrogen, Carlsbad, CA) containing 20% Fetal Bovine Serum (FBS, catalog # SH3039603, Fisher scientific, Hampton, NH), 1% Penicillin-Streptomycin-Glutamine (catalog # 10378-016, Invitrogen, Carlsbad, CA), 1% Non-essential Amino Acid (NEAA, catalog #11140-050, Lifetechnologies, Carlsbad, CA), 1% sodium pyruvate (catalog # 11360-070, Lifetechnologies, Carlsbad, CA), 50 µg /mL fetuin (catalog # F2379-1G, Sigma, St. Louis, MO), 10 ng/ML Epidermal growth factor (EGF, catalog # E5036-200UG, Sigma, St. Louis, MO), 0.4 µg /mL dexamethasone (catalog # D4902-100MG, Sigma, St. Louis, MO). The tissue was suspended and mixed 10 times with a 10mL pipette, following by removal of the undigested tissue using a sterile filter membrane. The filtrate containing myoblasts was plated in 100mm cell culture dishes, and primary cultured cells were maintained in a cell culture incubator (37 °C, 5% CO_2).

4.2.2 SILAC labeled skeletal muscle cells

The primary cultured human skeletal muscle cells were sub-cultured in SILAC growth medium which labeled the cells with heavy isotopic amino acids (e.g., lysine, arginine), which are essential for cell growth. The SILAC growth medium included DMEM Media for SILAC (catalog # 88420, Thermo Fisher Scientific, Waltham, MA), 20% dialyzed FBS for SILAC (catalog # 88440, Thermo

Fisher Scientific, Waltham, MA), 0.1 mg/mL L-Lysine-2HCl, 4,4,5,5-D4 for SILAC (catalog # 88438, Thermo Fisher Scientific, Waltham, MA), 0.1 mg/mL L-Arginine-HCl, $^{13}C_6$, $^{15}N_4$ for SILAC (catalog # 89990, Thermo Fisher Scientific, Waltham, MA), 1% Penicillin-Streptomycin-Glutamine (catalog # 10378-016, Invitrogen, Carlsbad, CA), 10 ng/ML Epidermal growth factor (EGF, catalog # E5036-200UG, Sigma, St. Louis, MO), 0.4 µg /mL dexamethasone (catalog # D4902-100MG, Sigma, St. Louis, MO). After 6 doublings of SILAC medium culture, the cells were collected by PBS. The cells were tested to be more than 95% labeled by lysine-4 (4 Da heavier than neutral lysine) and arginine-10 (10 Da heavier than neutral arginine) using HPLC-ESI-MS/MS (Data not shown).

4.2.3 Active protein kinase enrichment for functional kinome

Approximately 60–80 mg frozen muscle biopsies from 8 lean control (LC) and 8 obese insulin resistance (OBi) participants, and mixed SILAC labeled skeletal muscle cells from 2 LC and 2 OBi subjects were homogenized using a Next Advance Bullet Blender (Model BBY5E) and lysed by Pierce IP Lysis Buffer (catalog # 87787, Thermo Fisher Scientific, Waltham, MA) with 8M urea (catalog # BP169-500, Fisher scientific, Hampton, NH) and Halt™ Protease/Phosphatase Inhibitor Cocktail (catalog # 78440, Thermo Fisher Scientific, Waltham, MA). Protein concentration was measured by Bradford protein assay, where Coomassie blue plus Kit with standard (catalog # PI-23236, Fisher scientific, Hampton, NH) was used for this assay. For each sample, 1.0 mg tissue lysate spiked-in with 0.5 mg SILAC cell lysate (Four cell lines from 2 LC and 2 OBi were pooled first) was

aliquoted. Then the mixed lysate went through Zeba™ Spin Desalting Columns, 7K MWCO, 5mL (catalog # 89891 Thermo Fisher Scientific, Waltham, MA) to remove all the endogenous ATP. The filtrate lysate of 8 LC and 8 OBi were diluted with reaction buffer (provided in Pierce™ Kinase Enrichment Kits, catalog # 88310, Thermo Fisher Scientific, Waltham, MA) into 2 mg/mL, and incubated with 10 µL of 1M $MgCl_2$ at room temperature for 1 minute, followed by 10µM ActivX™ Desthiobiotin-ATP Probe (catalog # 88311, Thermo Fisher Scientific, Waltham, MA) incubation at room temperature for 10 minutes. The probe labeled lysate was diluted with 8M urea and underwent reduction (10mM dithiothreitol (DTT) incubation for 30 minutes at 55 °C) and alkylation (50mM iodoacetamide (IAA) incubation for 30min at room temperature in dark). Each sample was digested by 30µg trypsin Protease MS Grade (catalog # PI90058, Fisher scientific, Hampton, NH) for 16 hours at 37°C. The resulting peptides were incubated with 50µL of 50% High Capacity Streptavidin Agarose resin slurry (catalog # 20357, Thermo Fisher Scientific, Waltham, MA) for 1 hour at room temperature on a mixing rotator; subsequently, the resin was washed 3 times with lysis buffer, 3 times with PBS, and 3 times with LCMS-grade water. The final enriched active protein kinase peptides were eluted 3 times with 75 µL Elution buffer (provided in Pierce™ Kinase Enrichment Kits). The eluted peptides were dried with a speedvac, and were reconstituted with 0.1% TFA in water (catalog # LS119 1, Fisher scientific, Hampton, NH) for HPLC-ESI-MS/MS.

4.2.4 HPLC-ESI-MS/MS analysis

The active protein kinase peptides were isolated on a 75 µm ID and 400mm long C_{18} reversed phase analytical column which was in-house packed with ReproSil-Pur C_{18}-AQ µm resin (Dr. Maisch GmbH). The HPLC (UltiMate 3000, Thermo Fisher Scientific, Waltham, MA) was equipped with two nano-flow UHPLC pumps (upper pressure limit 800 bar). A linear HPLC gradient, 2-35% phase B (0.1% FA in acetonitrile, catalog # LS120 1, Fisher scientific, Hampton, NH) was used to separate peptide mixture, where phase A was 0.1% FA in water (catalog # LS118 1, Fisher scientific, Hampton, NH). The LTQ-Orbitrap Elite tandem mass spectrometer (Thermo Fisher Scientific, Waltham, MA) coupled with a nano flex electronic spray ion source was employed to analyze the isolated peptides.

The parameters of nano-ESI was optimized to ionize peptides: spray voltage 2.0 kV, capillary temperature 200 °C, sheath/aux/sweep gas flow rate 0. The MS instrument parameters were setup for “bottom-up” proteomics: 1) A full survey scan 300-1650 Th was acquired using 240,000 resolution power at positive mode; 2) The top 20 most intense the ion peaks were selected for fragmentation (MS/MS) by collision-induced dissociation (CID) with 33.0 normalized collision energy and 1.0 m/z isolation window; 3) 30 seconds dynamic exclusion, a time window in which the same ions are not selected for MS/MS; 4) singly charged ions were excluded for MS/MS.

4.2.5 Database search

The raw MS files generated from Xcalibur (Thermo Fisher Scientific, Waltham, MA) were searched against Uniprot human protein sequences (05/16/2014 version, www.uniprot.org) using MaxQuant software (verison.1.3.0.5) (Cox & Mann, 2008; Cox et al., 2009; Monetti, Nagaraj, Sharma, & Mann, 2011; Neuhauser, Michalski, Cox, & Mann, 2012). In the MaxQuant, besides the default variable modifications (Oxidized Methionine and acetylation at protein N-term), a novel variable modification, Desthiobiotin K, was manually added in the searching engine. The false discovery rate (FDR) for protein and peptides (at least 6 amino acid length) were both set at 1%; the Enzyme type chose “Trypsin”; multiplicity was set at 2 including light labels and heavy Arg10 & Lys4 labels; maximal 2 missed cleavages were allowed; the parent ion mass tolerance was 5 parts-per million (ppm) and fragment ion mass tolerance was 0.5 Da. The MaxQuant generated two main files, a desthiobiotin K peptides file (providing sequence of modified peptides with lysine sites and their intensity) and a protein group file (providing the kinase protein intensity).

4.2.6 Active kinase lysine sites identification and quantification

To be considered as an active kinase identified in the study, at least one of the two conserved lysine residues, one in the ATP-binding pocket and the other in the catalytic domain, of the active kinase lysine sites had to be enriched directly by the ATP-probe. To quantify and compare the active protein kinases between two groups, the enriched lysine sites have to meet the following three rigorous criteria: 1) The localization probability of dethiobiotin modified lysine site must be greater

than 0.75; 2) either identified in at least half of the biopsy samples (i.e., ≥ 8 samples), or identified only in at least half of biopsy samples of LC or OBi group (i.e., ≥ 4 samples); 3) for the kinases identified in both groups, a fold change of OBi/LC greater than 1.5 or less than 0.67 was required. The SILAC labeled heavy lysine sites identified in at least 8 out of 16 samples were used as "Universal" internal standard, and the total peak of the SILAC labeled lysine sites were calculated in each sample. Then, the peak area of each kinase (PAi) was normalized by the sum peak area of universal heavy labeled lysine sites in the same sample:

$$\text{Norm}: i = \frac{\text{PA}i}{\text{Total peak area of SILAC labeled lysine sites identified in } \geq 8 \text{ samples}}$$

The normalized protein kinase lysine site intensity underwent log transformation, and independent two-side *t-test* were employed to assess the significant changes (P<0.05) of active protein kinases in skeletal muscle between LC and OBi. For the kinases only identified in either LC or OBi, the fold changes of the kinases were assigned as infinity (Figure 4-4) and were considered as significant by default.

4.2.7 Bioinformatics

Pathway analysis of functional protein kinome were carried out by two software packages: 1) David bioinformatics (Huang da, Sherman, & Lempicki, 2009; Huang et al., 2007) including variety of databases, such as Gene Ontology (GO) (Ashburner et al., 2000; Gene Ontology, 2015), Kyoto Encyclopedia of Genes and Genomes (KEGG) (Kanehisa & Goto, 2000; Ogata et al., 1999; Wixon & Kell,

2000), Rectome Pathway database (Croft et al., 2011) and PANTHER Pathway (Mi et al., 2017; Mi et al., 2005; Tang & Thomas, 2016); 2) Ingenuity Pathway Analysis (Ingenuity Systems, Redwood City, CA) whose database consists of the high quality knowledgebase of biological functions and molecular networks manually curated by scientists (Jimenez-Marin, Collado-Romero, Ramirez-Boo, Arce, & Garrido, 2009; Kramer, Green, Pollard, & Tugendreich, 2014). Due to the lack of "gold standard" for pathway analysis, multiple software packages might provide comprehensive analysis for functional kinome in skeletal muscle insulin resistance.

4.3 Results

4.3.1 Largest functional kinome in human skeletal muscle

The desthiobiotin labelled lysine, K(de), of the identified protein kinases were manually searched using Uniprot database which provides the knowledgebase ATP binding lysine sites and the 2nd lysine site away from the HRD motif toward the C-terminal (in catalytic domain) (Patricelli et al., 2007). Only kinases identified with a desthiobiotin labelled known conserved lysine were considered as active protein kinases. The modified sequence of the active kinases showed high consistency with three known ATP probe binding motifs (Patricelli et al., 2007). Totally, 71 active protein kinase lysine sites (assigned to 54 protein kinases) were identified in the kinome enrichment (Table 4-1). Seventeen of the 54 kinases were enriched by both conserved lysine residues, and 7 out of the 54 kinases were only bound to lysine residue in the ATP binding pocket while 34

kinases were only bound to the lysine residue located in the catalytic loop. Apparently, the protein kinases with lysine located in catalytic loop were more likely to be enriched by this desthiobiotin ATP probe. Since the reaction group on the probe is more likely to react with the gamma-phosphate which is located closer to the lysine in catalytic loop than the one in ATP binding site, it might be an explanation for why this activity based probe favors the lysine within the catalytic domain over the one in ATP binding site. Surprisingly, 53 of identified 54 protein kinases were serine/threonine kinases; only one tyrosine protein kinase, epidermal growth factor receptor (EGFR), was identified in this dataset. The reason could be the low abundance of tyrosine kinases which only comprises less than 20% of the total ePKs. Additionally, as can be seen in Table 4-1, relatively large protein kinases can also be targeted; for example, microtubule-associated serine/threonine-protein kinase 2 (MAST2, sequence length: 1798 amino acids) was bound to the lysine in catalytic loop, and EGFR (sequence length: 1210 amino acids) was enriched on the lysine in the ATP binding site, which implied the high selectivity of the ATP probes that target the active conformation of protein kinases. In brief, we were able to identify 54 out of the total 478 ePKs (11%) in active conformation, which is largest functional kinome in human skeletal muscle insulin resistance to date.

Canonical pathway analysis on the identified 54 kinases showed MAP kinase pathway, mTOR pathway, Insulin signaling pathway, JNK cascade, Wnt signaling pathway, T cell receptor signaling pathway, etc., were significantly

enriched (P-value < 0.05) (Figure 4-6), and many of the pathways have been reported to regulate muscle function and contribute to the pathogenesis of insulin resistance, obesity and T2D. For example, insulin signaling pathway is one of the best known pathways directly regulates insulin sensitivity, and dysregulation of insulin signaling cascade may lead to insulin resistance and T2D (Kubota, Kubota, & Kadowaki, 2017; Mackenzie & Elliott, 2014). It is noted that enriched pathways could share the same kinases which involve in multiple pathways; for example, MAPK1 and EGFR were highly cited in various signaling pathways. Among the identified kinases involved in insulin pathway, glycogen synthase kinase-3 beta (GSK3β) has been extensively reported as negative regulator of glucose homeostasis. GSK3β phosphorylates and inactivates glycogen synthase and thus attenuates glycogen synthesis. In addition, accumulating evidence suggested that dysregulation of mTOR signaling pathway may induce insulin resistance and T2D (Deblon et al., 2012; Kleinert et al., 2014; Y. Ma et al., 2015; G. I. Smith et al., 2015; Yin et al., 2017).

Since protein kinases are known key regulators in the biofunctions (Figure 4-7), multiple cellular functions were significantly enriched, such as cell activation, apoptosis and migration, which indicated that the active kinome in skeletal muscle is highly responsible for critical cell proliferation, differentiation and programmed cell death. In addition, oxidative stress response and cellular response to stress exhibited high level of significance (p-value < 0.001), which indicated that kinases responsible for cellular stress and survival are highly active and maintain relatively

high abundance in skeletal muscle insulin resistance. Furthermore, the kinases regulated fatty acid oxidation which is essential for acetyl-CoA and NADH generation (Houten & Wanders, 2010).

Protein kinases are increasingly recognized as drug targets by which alternating kinase activity may correct the dysregulation of numerus substrates to exert therapeutic effects treating the various diseases, such as cancer and diabetes. Drugbank (www.drugbank.ca) is an open source database containing 8261 drug entries that either have been approved by the FDA, or are still under experimental development or clinical investigational trails (Knox et al., 2011; Law et al., 2014; Wishart et al., 2008; Wishart et al., 2006). A comprehensive drug target search on the 54 functional protein kinases using Drugbank database suggested that 267 drug-target entries were found. Among them, 28 entries were FDA-approved drugs, 25 were under clinical investigation and 214 were experimental drugs which comprised the largest portion of the chart, which was expected that drug discovery and development requires substantial investments and research efforts (Figure 4-7). Of interest, among the 28 FDA-approved drug-target entries (Table 4-2), metformin-AMPK1 (PRKAA1) was identified as a known anti-T2D agent targeting on AMPK. Metformin is the first line drug for T2D treatment, according to Drugbank data, metformin acts as an AMPK inducer to enhance AMPK activity and therefore improve insulin sensitivity. Interestingly, almost half (13 entries) targeted on EGFR and severed as anti-tumor agents (i.e., tyrosine kinase inhibitor) which mainly treat non-small cell lung cancer (NSCLC).

Due to the high similarities among protein kinases, one drug could target on multiple kinases but the therapeutic effect of the none-target kinases are remain unknown. For example, bosutinib, a Bcr-Abl kinase inhibitor for the treatment of chronic myelogenous leukemia (CML), showed multi-target effect on other kinases including calcium/calmodulin-dependent protein kinase type II subunit gamma (CAMK2G), cyclin-dependent kinase 2 (CDK2), dual specificity mitogen-activated protein kinase kinase 1 (MAP2K1), dual specificity mitogen-activated protein kinase kinase 2 (MAP2K2) and mitogen-activated protein kinase kinase kinase 2 (MAP3K2). Despite a variety of anti-tumor agents primarily target on tyrosine kinases, some drugs designed as serine/threonine kinase inhibitors; for instance, trametinib, targeting on MAP2K1/MAP2K2, treats metastatic melanoma with BRAF V600E or V600K mutations. Other types of drug was also identified, such as lidocaine (local or regional anesthetic agent), lithium (mood stabilizer) and acetylsalicylic acid (pain killer).

4.3.2 Significantly changed active kinases between lean insulin sensitive and obese insulin resistant participants

The quantitative proteomics of functional kinome implied that 22 out of the 54 identified kinases significantly changed comparing LC and OBi group (p-value < 0.05). Among them, 13 kinases exhibited up-regulated levels while 9 kinases were down-regulated in OBi subjects. It is noted that 11 kinases were only identified in OBi group, and 3 kinases were only identified in LC groups because the protein abundance of these active kinases were too low to be detected in the

other group. All the 22 significantly changed kinases were serine/threonine kinases (Table 4-3). It is noted that this is the largest catalog of active protein kinases in human skeletal muscle with a significant change between LC and Obi.

Ingenuity Pathway Analysis (IPA) of the 22 significantly changed protein kinases was performed to identify which cell signal transduction pathways have been significantly enriched, based on the criteria that minimum three kinases identified in each pathway and p-value must be less than 0.0001. Interestingly, the SAPK/JNK and IL-6 signaling were the pathway enriched with highest significant levels ($P< 1.0E-09$), and multiple other pathways were also significantly enriched: AMPK pathway; mTOR pathway; Type 2 diabetes signaling; ErbB signaling; ERK5 signaling; cytokine related pathways (i.e., IL-10 signaling, JAK pathway, STAT3 pathway, IL-17 signaling, IL-1 signaling, etc.); pathways related to oxidative stress and free radicals (e.g., iNOS signaling), etc. Note that the cell signal transduction pathways from different databases (i.e., KEGG and IPA) may contains slightly different entries based on the peer-reviewed functional studies and knowledgebase curated by scientists. In order to visualize the abnormalities of function kinome involved in cell signaling and molecular functions, the quantified protein kinases in human skeletal was manually mapped to several significantly enriched pathways that covered most abnormal active protein kinases in OBi.

Importantly, we performed IPA on the 13 protein kinases with increased activities and 9 kinases with decreased activities separately (Figure 4-9). For the up-regulated protein kinases, JNK signaling, IL-6 signaling, pathway related to

reactive oxygen species (ROS) in macrophages, apoptosis signaling were significantly enriched (P-value < 0.001 and at least 3 kinases involved); on the other hand, AMPK signaling, mTOR signaling, p38 MAPK signaling were significantly enriched in the down-regulated kinases.

MAPK signaling pathway (downloaded from http://www.kegg.jp) (Figure 4-10), including 15 identified protein kinases, was color-coded according to the differential change of functional kinome between OBi and LC. The MAP kinase pathway from KEGG contains three sub-signaling pathways: classic MAP kinase pathway (ERK1/2 pathway), JNK and p38 MAP kinase pathway (involves simplified NF-κB signaling) and ERK5 pathway. First, we mapped EGFR, serine/threonine-protein kinase B-raf (BRAF, also known as RafB), dual specificity mitogen-activated protein kinase kinase 1 (MAP2K1, also known as MEK1), dual specificity mitogen-activated protein kinase kinase 2 (MAP2K2, also known as MEK2), MAPK1 (also known as ERK2) and ribosomal protein S6 kinase alpha-3 (RPS6KA3, also known as RSK2) in the ERK1/2 signaling pathway in which five upstream regulatory kinases of ERK2 (including ERK2 itself) didn't exhibit significant changes; on the contrary, RSK2 was dramatically decreased in OBi. The differences of six kinases between LC and OBi involved in ERK1/2 signaling implied that the upstream signaling remains intact, but the substrate of ERK2 (e.g., RSK2) was suppressed and subsequently might inhibit downstream effectors' activities (i.e., CREB) in the insulin resistance state. Second, there were 5 identified protein kinases mainly affect JNK signaling: mitogen-activated protein

kinase kinase kinase kinase 4 (MAP4K4, also known as HGK), mitogen-activated protein kinase kinase kinase 2 (MAP3K2, also known as MEKK2), mitogen-activated protein kinase kinase kinase 3 (MAP3K3, also known as MEKK3), Mitogen-activated protein kinase kinase kinase MLT (MLTK), dual specificity mitogen-activated protein kinase kinase 4 (MAP2K4, also known as JNKK1 or MEK4). Among the 5 kinases, we observed 4 significantly increased kinases except MLTK, which strongly suggested that JNK signaling was up-regulated in the skeletal muscle insulin resistance. In addition, HGK is a upstream regulator mediating NF-κB signaling pathway. Third, p38 MAP kinases pathway contained 4 identified kinases which were dual specificity mitogen-activated protein kinase kinase 3 (MAP2K3, also known as MKK3), dual specificity mitogen-activated protein kinase kinase 6 (MAP2K6, also known as MKK6), mitogen-activated protein kinase 12 (MAPK12, also known as p38γ or SAPK3) and mitogen-activated protein kinase 13 (MAPK13, also known as p38δ or SAPK4). Although the upstream kinases (MKK3 and MKK6) didn't show significant changes, p38 MAP kinases were reduced significantly in OBi. Last, no identified kinase directly participated in ERK5 pathway, though crosstalk between MAP kinases may indirectly regulate ERK5 pathway (IPA database includes MKK3/6 and RSK2 in ERK5 pathway).

Similarly, in the color-coded Wnt signaling pathway (downloaded from http://www.kegg.jp) (Figure 4-11), three kinases displayed enhanced activities: casein kinase II subunit alpha (CSNK2A1, also known as CK2A1), casein kinase I

isoform alpha (CSNK1A1, also known as CK1α), and calcium/calmodulin-dependent protein kinase type II subunit delta (CAMK2D); three kinases did not show significant change: GSK3β, casein kinase II subunit alpha' (CSNK2A2, also known as CK2A2), calcium/calmodulin-dependent protein kinase type II subunit gamma (CAMK2G); one kinase was down-regulated: calcium/calmodulin-dependent protein kinase type II subunit beta (CAMK2B). Note since CK2A1 and CK2A2 are isoforms of CK2, so half of the CK2 block was colored in red (increased) and half in yellow (no change). Similarly, CAMK2D, CAMK2G and CAMK2B are different subunits of CaMKII, which was colored differently according to the differential changes of its subunits in LC and OBi.

We color-coded mTOR signaling pathway (downloaded from http://www.kegg.jp) (Figure 4-12) using the same approach described above to map functional kinome in human skeletal muscle. Multiple protein kinases in the mTOR signaling have been significantly suppressed, such as serine/threonine-protein kinase STK11 (STK11, also known as LKB1), 5'-AMP-activated protein kinase catalytic subunit alpha-1 (PRKAA1, also known as AMPK1), 5'-AMP-activated protein kinase catalytic subunit alpha-2 (PRKAA2, also known as AMPK2) and RSK2; while Raf, MEK, ERK1/2, and GSK3β did not exhibit significant changes between LC and OBi.

Of interest, significantly changed protein kinases of AMPK signaling pathway (adapted from IPA) was also highlighted. Totally, five kinases, AMPK1,

AMPK2, p38γ, p38δ and LKB1, were involved and all of them were significantly decreased.

Protein kinases are highly regulated by other kinases or autophosphorylation, a significant enriched functional kinome network of the insulin resistance responsible active kinases was constructed by IPA (Figure 4-14). The network is related to post translational modification and cell survival, differentiation and proliferation with score 43 (highest scored network, maximum molecules was set at 70), which contains 21 significantly changed kinases (11 up-regulated kinases highlighted in red and 10 down-regulated kinases highlighted in green) and 13 other known proteins/protein complexes in the IPA database but were not identified in current study.

4.4 Discussion

Protein kinases, enzymes catalyzing phosphorylation, play critical roles in numerous biological processes and molecular functions, such as insulin signaling, glucose uptake, etc. On the other hand, dysregulation of protein kinases might results in variety of unhealthy states and diseases (e.g., obesity, insulin resistance, and T2D). Skeletal muscle insulin resistance has been well defined as a primary defect of T2D. Currently, dysregulation of protein kinases have been reported to lead to skeletal muscle insulin resistance; however, most of the studies only focused on the protein abundance or phosphorylation of few protein kinases in cell or animal models (Sakiyama, Usuki, Sakai, & Sakane, 2014; B. K. Smith et al., 2013; Tunduguru et al., 2014). No high-throughput profiling of active protein

kinases in skeletal muscle biopsies of obese insulin resistant participants has been reported to date. The global functional kinome in human skeletal muscle insulin resistance remains unknown. Therefore, we developed a platform combining activity-based kinase enrichment technique and quantitative proteomics to profile active protein kinases in human skeletal muscle in lean healthy subjects and obese participants with insulin resistance, and sought to unveil novel functional kinome responsible for insulin resistance and obesity. Compared to previous studies, the main innovations were 1) profiling dozens of active kinases other than protein abundance or phosphorylation sites of few kinases; 2) providing a direct and relative global assessment of kinase activities *in vivo* other than traditional radioactive kinase activity assay which requires binding substrates; 3) Improved coverage and accuracy of quantitative proteomics using “Universal” SILAC; 4) providing a comprehensive view of significantly enriched cell signaling pathways by multiple bioinformatics databases. In contrast, the challenges of current study were: 1) highly complex biological samples (i.e., skeletal muscle biopsy) with multiple high abundant contractile proteins (i.e., myosin, nebulin, titin, etc.) may interfere relative low abundant kinome profiling; 2) data dependent acquisition mode of “shotgun” proteomics might miss extremely low abundant proteins compared to target proteomics, which is more sensitive than shotgun proteomics but with relative low throughput. This approach is applicable for functional kinome enrichment in various biological samples in different species.

4.4.1 Inflammatory response pathways in skeletal muscle insulin resistance

Increasing evidence suggests accumulation of immune cells (i.e., T lymphocytes, macrophages, etc.) in skeletal muscle cells (myotubes) in obesity with insulin resistance and T2D (Fink et al., 2014; Fink et al., 2013; Khan et al., 2015; Patsouris et al., 2014; Varma et al., 2009). It is well established that proinflammatory cytokines (e.g., TNFα, IL-1, IL-6) lead to inflammation via inflammatory response pathways, such as JNK signaling, NF-κB signaling, IL-6 signaling, etc (Hou et al., 2008; Sanchez et al., 2012; Spiga et al., 2017; Zhong et al., 2009). In present study, the pathway analysis (Figure4-8) of the 22 protein kinases significantly changed in OBi compared to LC suggested that multiple inflammatory response pathways (e.g., JNK signaling, IL-6 signaling, IL-10 signaling) have been significantly enriched.

JNK has been demonstrated as a critical mediator in insulin resistance and obesity (Chiang et al., 2009; Hirosumi et al., 2002), Senn JJ (Senn, 2006) reported increased JNK activity in insulin resistance myotubes, and Vijayvargia R and associates (Vijayvargia, Mann, Weiss, Pownall, & Ruan, 2010) performed JNK knockdown which enhanced the glycogen storage in skeletal muscle cells from mice. In this study, we found 4 significantly increased active protein kinases (JNKK1, MEKK2, MEKK3 and HGK) in JNK signaling pathway (Figure 4-10) in OBi. JNKK1 directly phosphorylates and activates JNK, and JNNK1 is regulated by MEKK2 and MEKK3 kinase activities. Also, HGK or MAP4K4 has been reported to play a central role in JNK and p38 MAPK signaling, serving as an upstream regulator (Yao et al., 1999). Serine/threonine-protein kinase 38 (STK38) was

significantly increased in OBi (not on the KEGG mapped JNK pathway). Although STK38 was reported as a negative regulator of JNK pathway by inhibiting autophosphorylation of MEKK1/2 (Enomoto et al., 2008), other regulatory compensation may also affect MEKK1/2 activity. Despite we did not observe active JNK directly (might be low abundant), four upstream kinases (especially JNNK1) of JNK with increased activities strongly suggested that JNK signaling was activated in human skeletal muscle insulin resistance. It is noted that hyperglycemia may induce JNK activity (Hein, Xu, Xu, & Kuo, 2016), however, JNK activity could remain unchanged in the current study because the participants in our study have normal glucose homeostasis (normal fasting plasma glucose, HbA1c, and 2-h OGTT) even though their skeletal muscle is insulin resistant. Although, overwhelming evidence implies up-regulated JNK signaling may reduce insulin sensitivity or impair insulin signaling pathway via increased IRS1 S^{307} phosphorylation (Henstridge et al., 2012; Sabio et al., 2010), Zbinden FH and associates (Zbinden-Foncea, Raymackers, Deldicque, Renard, & Francaux, 2012) reported that endurance exercise (likely increases insulin sensitivity) increased JNK and p38 MAPK activity in skeletal muscle from mice with T2D, which seems contrast from our finding and findings from other groups. However, physiological and pathological of mice with T2D might be different from those of human, and majority of the studies are still consistent with our results.

4.4.2 p38 MAPK signaling

p38 MAPK signaling may also contribute to obesity linked insulin resistance. Emerging evidence suggests that inhibition of p38 may results in impaired insulin dependent glucose uptake in skeletal muscle and adipocytes (Sweeney et al., 1999). Furthermore, Somwar *et al.,* (Somwar et al., 2001) observed significantly decreased GLUT4 translocation by p38 inhibitor in L6 rat skeletal muscle cells, which suggested that p38 inhibitors impaired insulin stimulated glucose uptake through a GLUT4 translocation manner. On the other hand, a study showed p38 inducer activated glucose uptake via AMPK-GLUT4 signaling and enhanced insulin sensitivity (P. C. Geiger, Wright, Han, & Holloszy, 2005). However, based on our literature search, no study has been conducted on active p38 MAPK in insulin resistant skeletal muscle from obese participants. In this study, we identified two p38 activation kinases, MKK3 and MKK6, which remained no change; surprisingly, two out of four p38 MAPKs (p38γ and p38δ) were identified in our dataset, and their kinase activity was significantly reduced, which supports the decreased p38 activity may reduce the insulin-stimulated glucose uptake and cause insulin resistance via impaired AMPK (which was found ~ 9.0 fold reduced in our study) mediated glucose transport. Although the molecular mechanism of down-regulated p38 in peripheral insulin resistance is incompletely understood, we provided an evidence of attenuation of p38 MAPK signaling in human skeletal muscle insulin resistance. Not surprisingly, controversial results still exist, for example, it is reported that low dose oxidative stress transiently induced p38

MAPK activity and resulted in insulin resistance in isolated rat skeletal muscle (Diamond-Stanic et al., 2011).

4.4.3 Wnt pathway

Of interest, we identified 7 protein kinases in Wnt pathway, specifically, 4 in Wnt canonical pathway and 3 in Wnt/Ca^{2+} pathway (Figure 4-11). Growing data shows that Wnt signaling was important for development and carcinogenesis, and inhibition of Wnt signaling could suppress various tumor growth (Demagny, Araki, & De Robertis, 2014; M. Kahn, 2015; H. Liu et al., 2014; Morrow et al., 2016; Reno et al., 2016; Uehara, Kage-Nakadai, Yoshina, Imae, & Mitani, 2015; W. Zhang et al., 2016). In addition, Wnt signaling is also activated by anti-inflammatory cytokines (such TGFβ) (Castellone & Laukkanen, 2017; Jardim, Poco, & Campos, 2017). In the canonical pathway, CK1, axin, adenomatosis polyposis coli (APC) and GSK3β forms destruction complex which degrades β-catenin via ubiquitination. In the absence of Wnt signaling (Wnt-off), CK1 and GSK3β constantly phosphorylate β-catenin which subsequently undergoes protein degradation; on the other hand, the destruction complex become inactive upon Wnt ligand binding (Wnt-on), and β-catenin is activated and transferred to nucleus (Minde, Anvarian, Rudiger, & Maurice, 2011; Minde, Radli, Forneris, Maurice, & Rudiger, 2013). Previously reports indicated that beta-catenin gene expression was lower in adipose tissue and skeletal muscle of subjects with low insulin sensitivity compared to those with high insulin sensitivity subjects (Karczewska-Kupczewska, Stefanowicz, Matulewicz, Nikolajuk, & Straczkowski, 2016). In present study, CK1,

a key inhibitor of β-catenin, was significantly increased in OBi, so β-catenin might be suppressed in OBi. Compelling evidence shows β-catenin plays critical role in glucose homeostasis and insulin secretion. Early works (Dabernat et al., 2009) indicated that deletion of β-catenin in mice islet cells induced severe dysregulation of glucose homeostasis. Later on, Elghazi *et al*., (Elghazi et al., 2012) observed that β-catenin knockout in pancreatic progenitors led to impaired glucose tolerance. Recently, Sorrenson, B. and colleagues reported that reduced β-catenin gene expression in β-cell could increase glucose-stimulated insulin secretion. Furthermore, the molecular mechanism of CK1/β-catenin induced abnormal insulin-dependent glucose disposal may be involved in muscle contraction and interaction with actin cytoskeleton (Galli et al., 2012; Nagashima et al., 1997). Therefore, we first reported that decreased CK1/β-catenin complex activity might be responsible for impaired insulin stimulated glucose uptake and hyperinsulinemia in insulin resistant skeletal muscle of obese participants. Noted that some researchers observed up-regulated Wnt signaling in diabetes (Garcia-Jimenez, Garcia-Martinez, Chocarro-Calvo, & De la Vieja, 2014), which provided other possible molecular mechanism of CK1/β-catenin complex regulating insulin resistance and diabetes related pathways.

There were three CaMKII subunits involved in Wnt/Ca^{2+} pathway; however, differential changes of them in OBi (one increase, one decrease and one no change) were observed. CaMKII plays important role in skeletal muscle during

exercise, and exercise induced more than 5 fold changes of phosphorylation at Thr^{287} of CaMKII in skeletal muscle (Rose, Kiens, & Richter, 2006).

4.4.4 mTOR signaling pathway

As described in the introduction part, mTOR is an atypical kinase which lacks of typical kinase catalytic core; therefore, current platform was not capable to enrich active mTOR. As predicted, we did not identify mTOR itself but did identify other upstream regulatory kinases which could affect mTOR activity (Figure 4-12). Among the protein kinases mapped to mTOR pathway, some of them mainly involved in AMPK signaling pathway (Figure 4-13), and rest of them primarily participated in ERK1/2 pathway.

4.4.4.1 AMPK pathway

AMPK is a protein kinase regulated by AMP/ATP ratio in cellular microenvironment, and it could boost ATP generation and reduce utilization of ATP (Carling, Zammit, & Hardie, 1987). Overwhelming evidence indicates AMPK activity was overall attenuated in insulin resistance, obesity and T2D (Coughlan, Valentine, Ruderman, & Saha, 2013; Dzamko et al., 2010; Gauthier et al., 2011; Yamada, Lee, Pessin, & Bastie, 2010). However, whether AMPK exhibiting reduced activity in skeletal muscle insulin resistance mostly yielded the controversial results. Bandyopadhyay *et al.,* (Bandyopadhyay, Yu, Ofrecio, & Olefsky, 2006) suggested decreased AMPK level in skeletal muscle from obesity and T2D; while Liong, S. and Lappas, M. colleagues reported activated AMPK in pregnant women with gestational diabetes (Liong & Lappas, 2015). Similarly,

exercise stimulated AMPK activity in skeletal is still filled up with mixed conclusions. For example, McGee *et al.,* (McGee et al., 2003) stated that acute exercise significantly increased AMPK activity in insulin resistant skeletal muscle, but Sriwijitkamol and associates reported attenuated AMPK activity after acute exercise in skeletal muscle of obese participants with insulin resistance and T2D (Sriwijitkamol et al., 2007). On one hand, numerous controversial studies of AMPK activity in skeletal muscle insulin resistance exist; on the other hand, no study directly assessing the active AMPK in skeletal muscle of obesity with insulin resistance and hyperinsulinemia. Increasing data shows that AMPK is also regulated by inflammation, ER stress and oxidative stress, which are typically increased in obesity with insulin resistance and led to increased AMPK activity (C. C. Chen et al., 2014; Gautam et al., 2016; W. Li et al., 2015; Manna & Jain, 2013). In contrast, decreased AMPK activity reduces glucose uptake in skeletal muscle insulin resistance and T2D. In Figure 4-13, we quantified active LKB1 and AMPK1/2 which were decreased by 11.9 and 9.5 in OBi, representatively. LKB1 is a well-defined AMPK positive regulator that directly phosphorylates AMPK (Forcet & Billaud, 2007; Hardie, 2005; Rider, 2006; Sriwijitkamol et al., 2006) whereas the two p38 MAPKs (decreased in OBi) indirectly mediate AMPK activity via MKK3 (no change). Our results provided evidence that AMPK signaling pathway was significantly attenuated in OBi compared to LC.

4.4.4.2 ERK1/2 signaling

Another pathway mediated mTOR signaling is ERK1/2 pathway which is a central axis for numerous molecular functions (e.g., cell proliferation and differentiation) and cell signal transduction, such as insulin signaling. Multiple studies of the ERK1/2 activity in skeletal muscle of obesity and T2D demonstrated mix results. First, Krook *et al*., (Krook et al., 2000) reported no significant difference of ERK1/2 activity compared lean subjects and T2D, and Cusi *et al.,* (Cusi et al., 2000) observed similar results in human skeletal muscle biopsies; in contrast, other researchers observed increased ERK1/2 phosphorylation in basal state of obesity and T2D (Bandyopadhyay, Yu, Ofrecio, & Olefsky, 2005). In present study, RafB, MEK1, MEK2, and ERK2 did not show significant change; however, RSK2 was attenuated in OBi.

4.4.4.3 AMPK and ERK1/2 signaling crosstalk with mTOR signaling

For the active kinase in the AMPK and ERK1/2 pathway identified in the study, only LKB1, AMPK1/2 and RSK2 were significantly changed (decreased) in OBi compared to LC. Emerging evidence suggests that LKB1/AMPK complex is a negative regulator of mTOR (Dong et al., 2013; D. Han, Li, Zhu, Liu, & Li, 2013; Shaw et al., 2004); however, Han *et al.,* observed unchanged mTOR activity with impaired LKB1/AMPK in rat adipose tissue (J. Han et al., 2016). One of ERK1/2 downstream kinases, RSK2, directly phosphorylates ribosomal protein S6 (RPS6) and Eukaryotic translation initiation factor 4B (EIF4B), and regulates cell proliferation and differentiation. RSK2 inactivates GSK3β which is a negative mediator for glycogen synthesis by which RSK2 is a positive regulator for insulin

sensitivity (Sutherland, Leighton, & Cohen, 1993). MAPK stimulates the mTORC1 activity via RSK1/2 independently of PI3K/AKT pathway. Taken with the findings in this study, mTOR signaling might remain unchanged because, based on the literatures, LKB1/AMPK may up-regulate mTOR while RSK2 (positive regulator) may down-regulate mTOR activity; however, numerous factors could also alter mTOR signaling. Therefore, further validation of mTOR and other key protein kinases are required.

4.5 Summary

In Specific Aim 1, from 8 lean healthy participants and 8 obese participants with insulin resistance using activity-based ATP probes and quantitative proteomics analysis, we identified 54 active protein kinases in human skeletal muscle, which is the largest catalog of experimental determined active kinases to date. Twenty-two out of the 54 active kinases displayed a significant change in insulin resistant obese subjects, including the protein kinases regulate JNK signaling, p38 MAPK signaling, Wnt signaling, AMPK signaling, ERK1/2 signaling and mTOR signaling. We generated a relative global picture of functional kinome in skeletal muscle insulin resistance, providing novel insights into abnormal functional kinome and molecular mechanism of skeletal muscle insulin resistance. These results may facilitate identifying new targets for treating metabolic diseases.

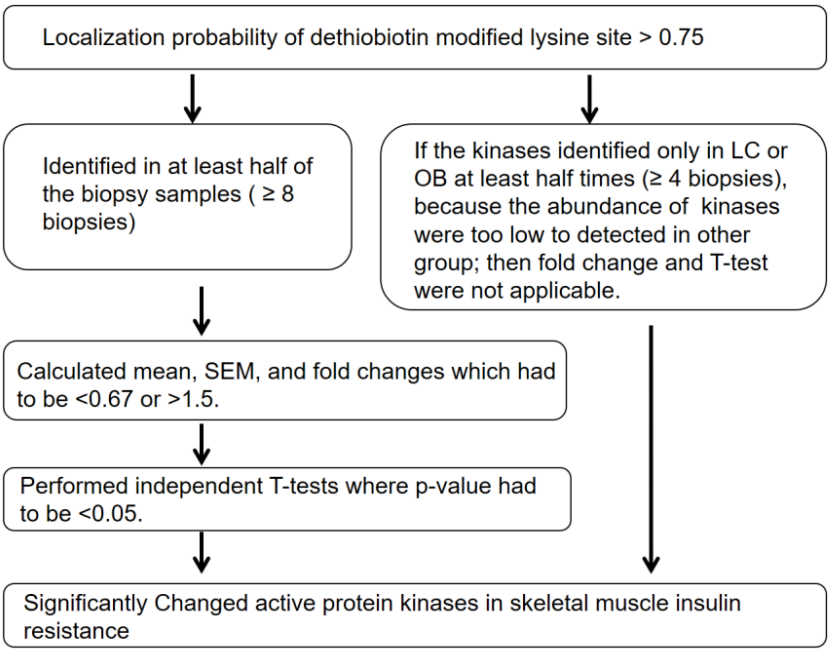

Figure 4-4. Flowchart of active protein kinase identification and quantification.

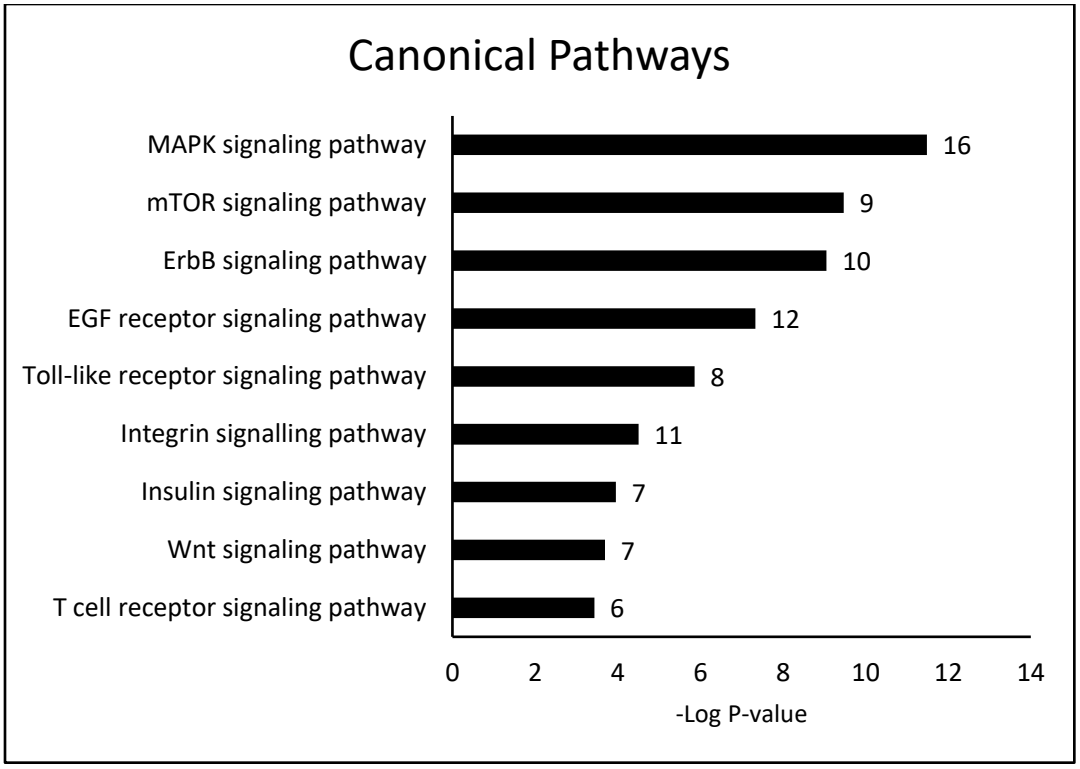

Figure 4-5. Significantly enriched canonical pathways for the 54 identified protein kinases. Data label on the bar represents the number of protein kinases participated in that pathway.

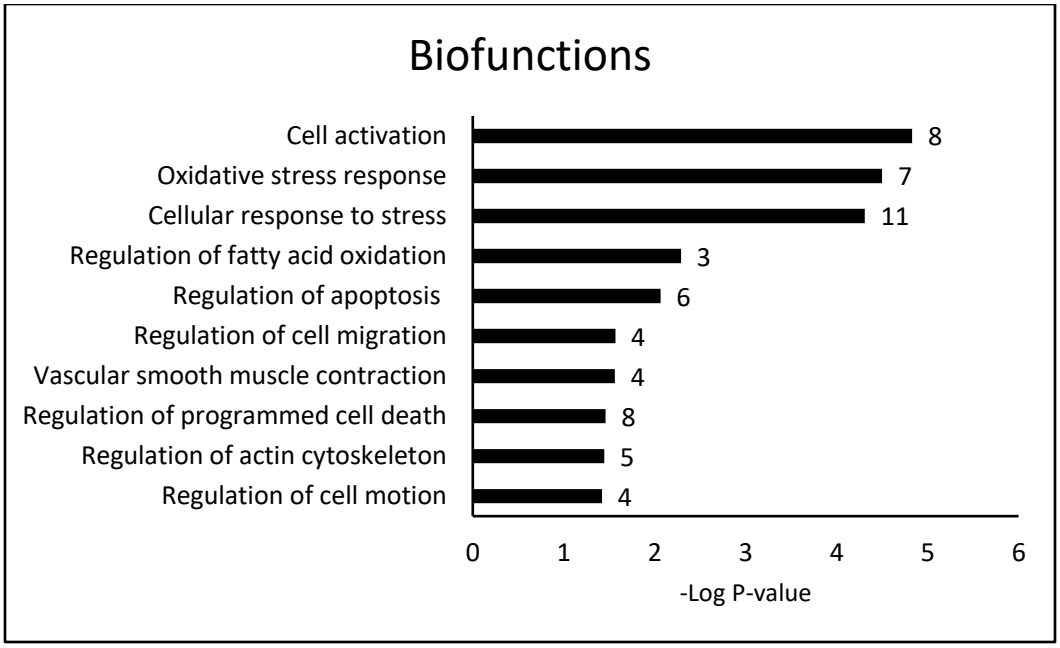

Figure 4-6. Significantly enriched biological functions for the 54 identified protein kinases. Data label on the bar represents the number of protein kinases participated in that biofunction.

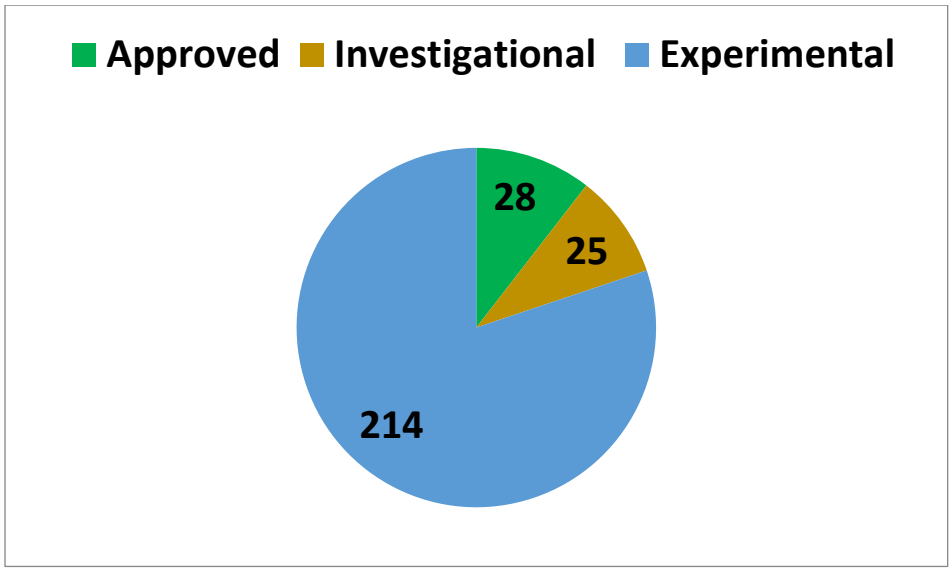

Figure 4-7. Drugbank database search on the 54 identified protein kinases.

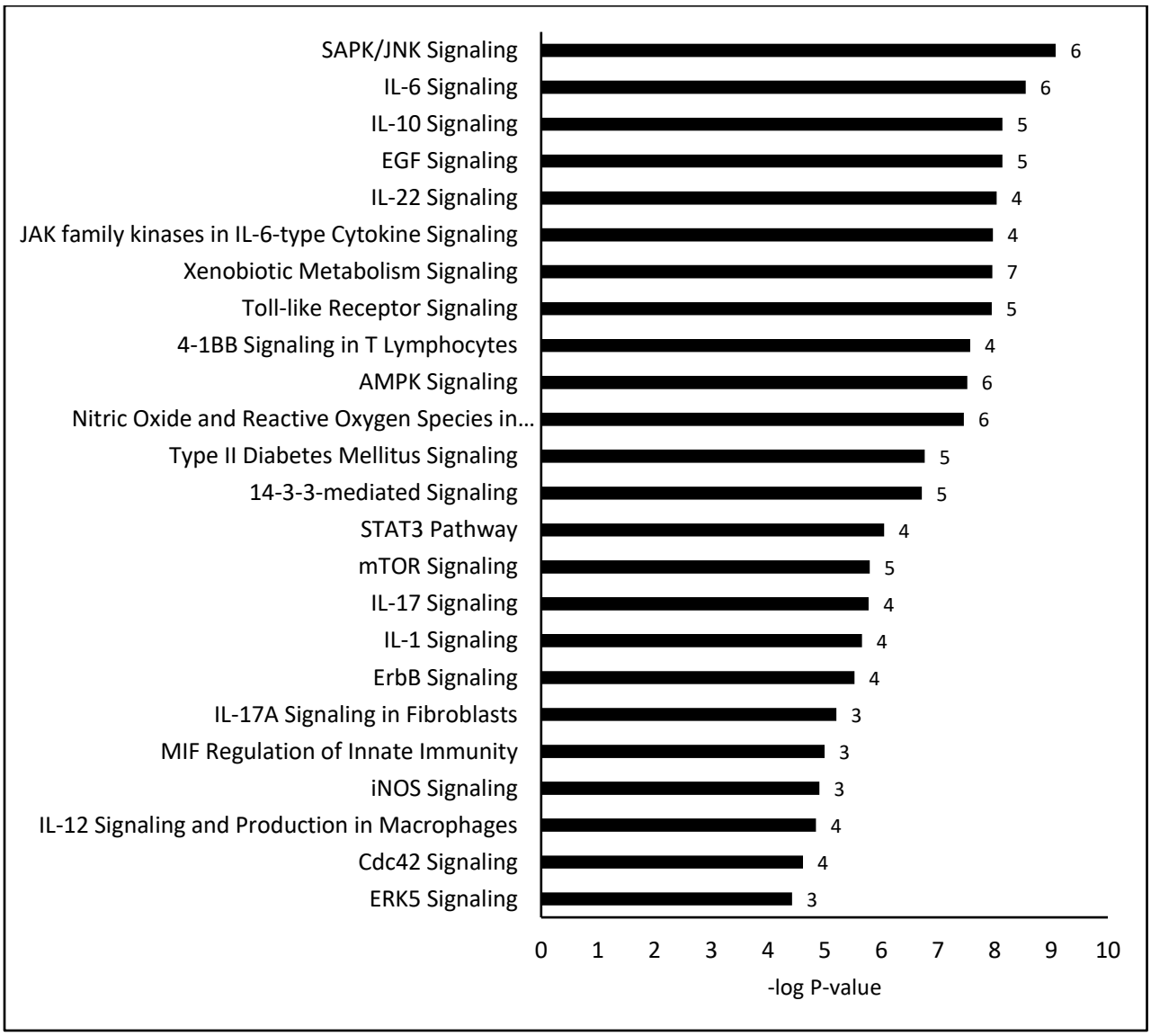

Figure 4-8. Ingenuity pathway analysis on the 22 significantly changed kinases. Data label on the bar represents the number of protein kinases participated in that pathway.

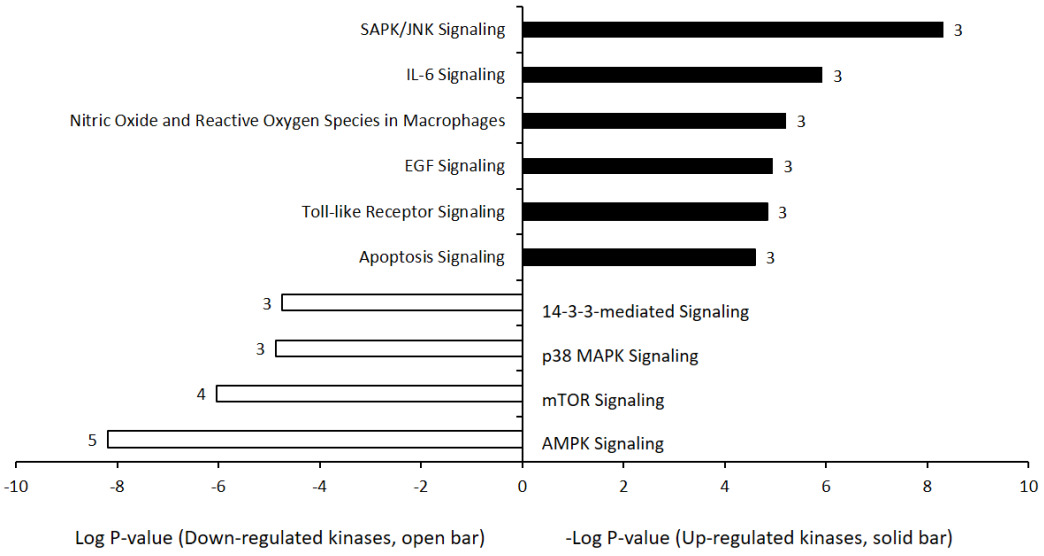

Figure 4-9. Ingenuity pathway analysis on the up-regulated kinases versus the down-regulated kinases. Data label on the bar represents the number of protein kinases participated in that pathway.

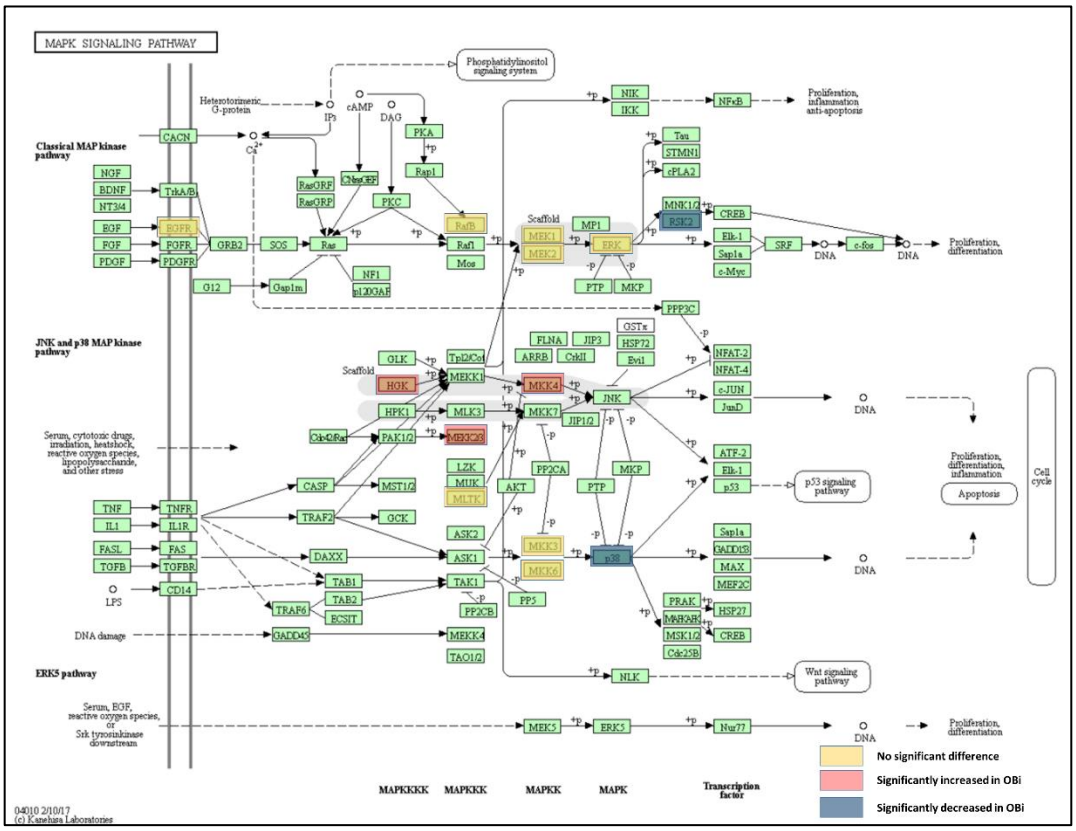

Figure 4-10. Color-coded MAPK signaling pathway of functional kinome according to their differences in LC and OBi. Figure of MAPK signaling pathway was adapted from KEGG.

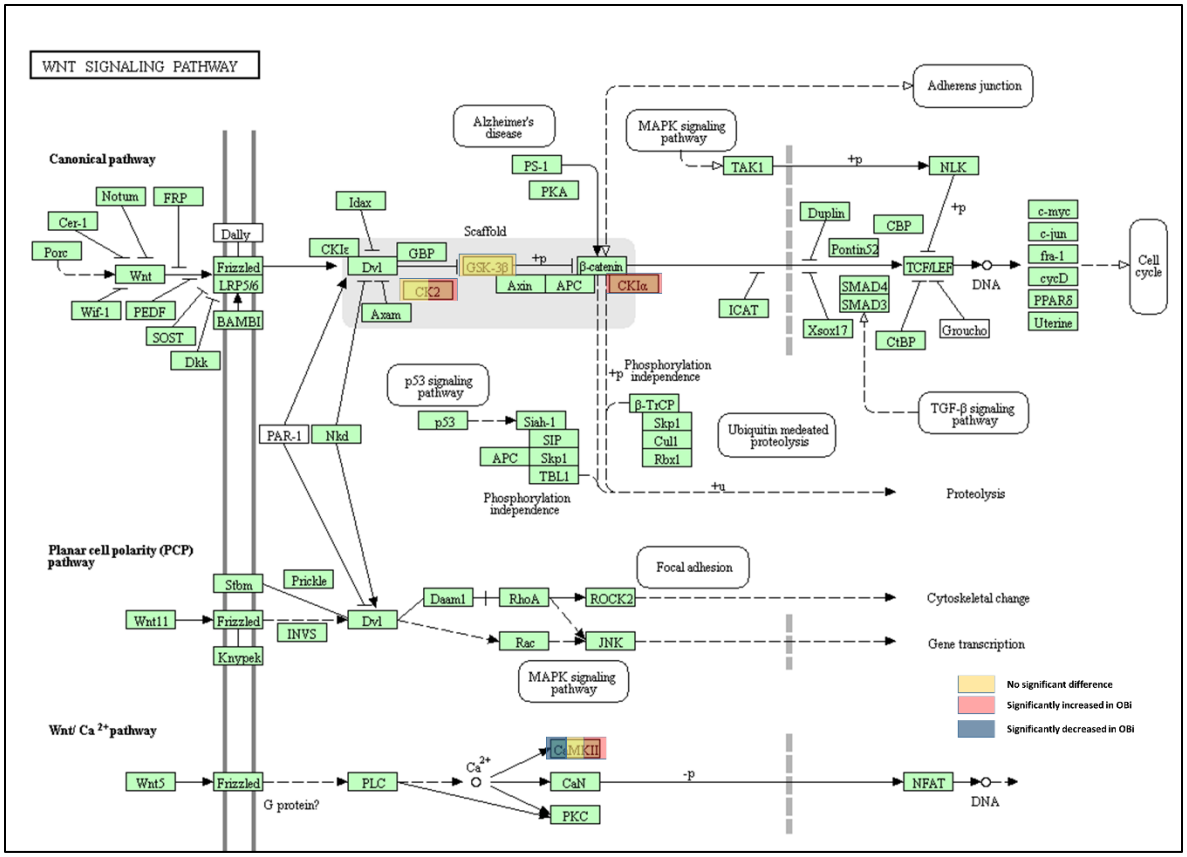

Figure 4-11. Color-coded Wnt signaling pathway of functional kinome according to their differences in LC and OBi. Figure of Wnt signaling pathway was adapted from KEGG.

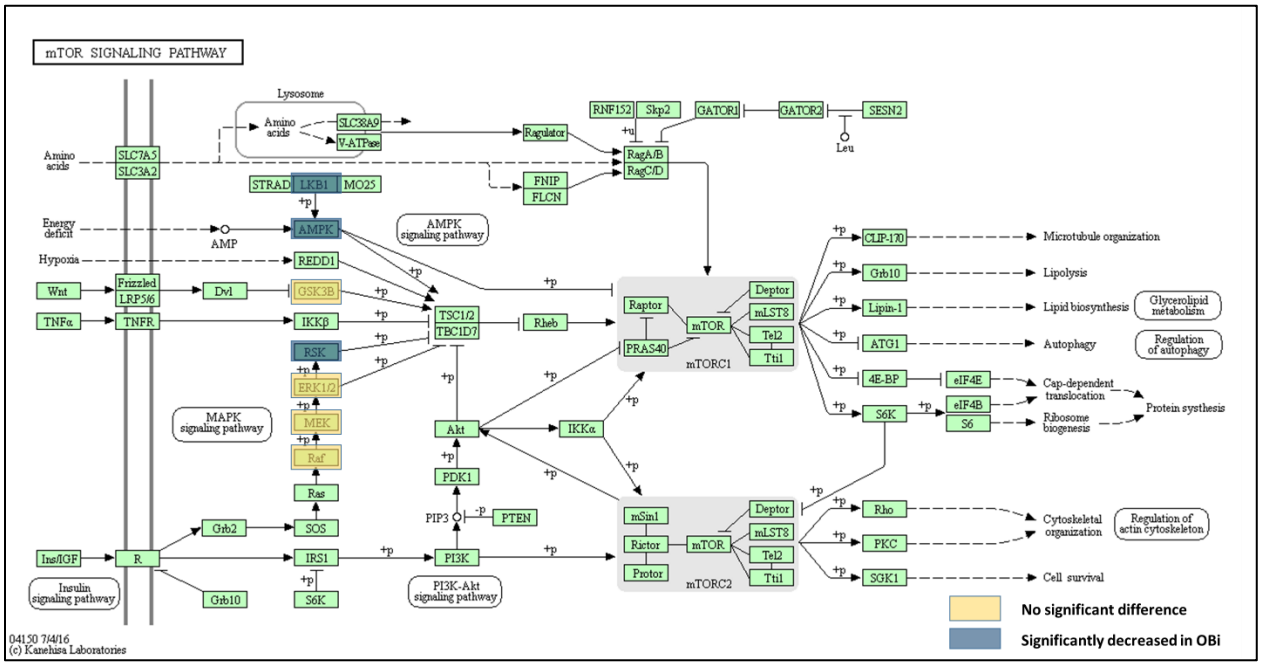

Figure 4-12. Color-coded mTOR signaling pathway of functional kinome according to their differences in LC and OBi. Figure of mTOR signaling pathway was adapted from KEGG.

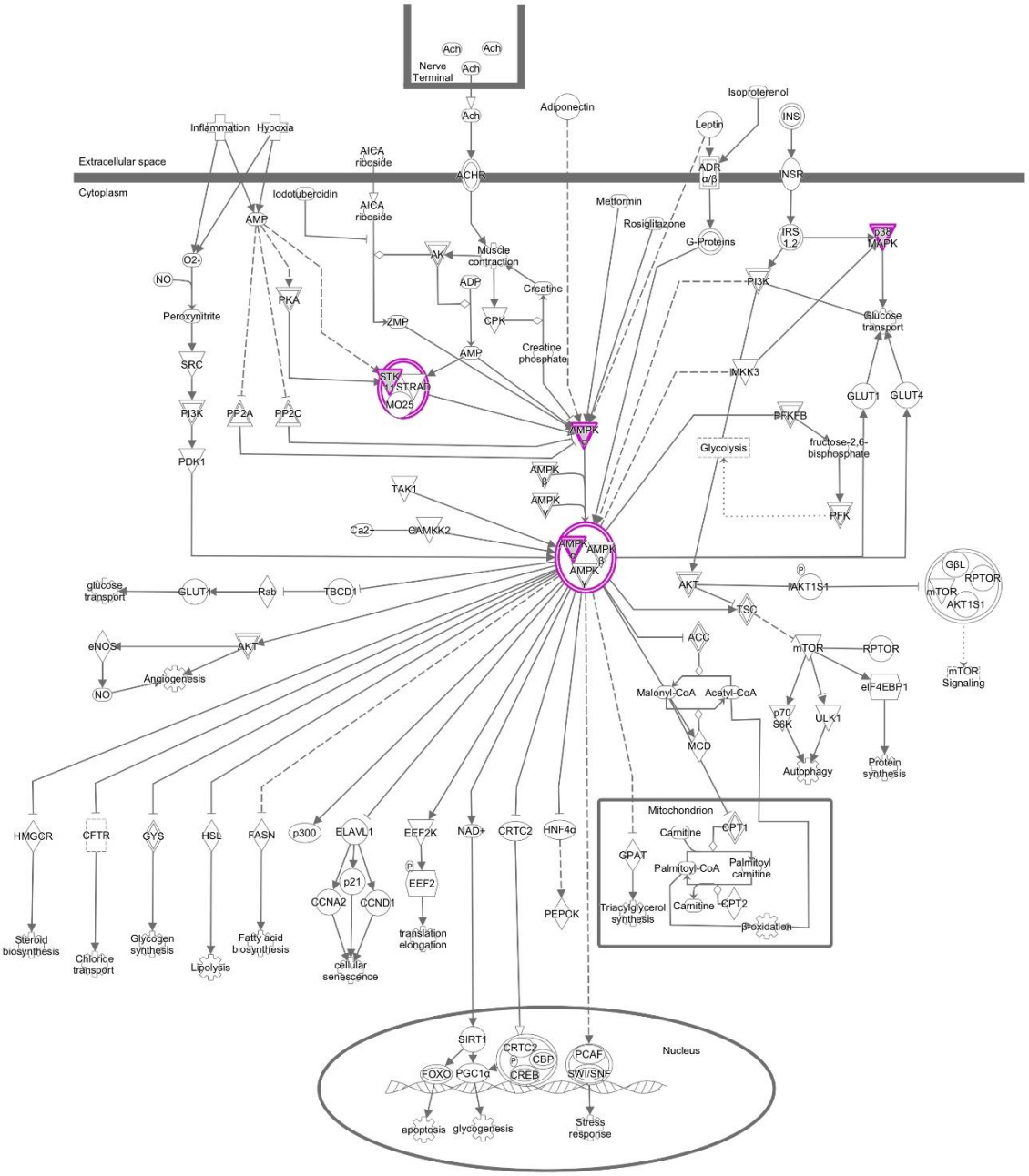

Figure 4-13. Color-coded AMPK signaling pathway of functional kinome according to their differences in LC and OBi. Figure of AMPK signaling pathway was adapted from IPA.

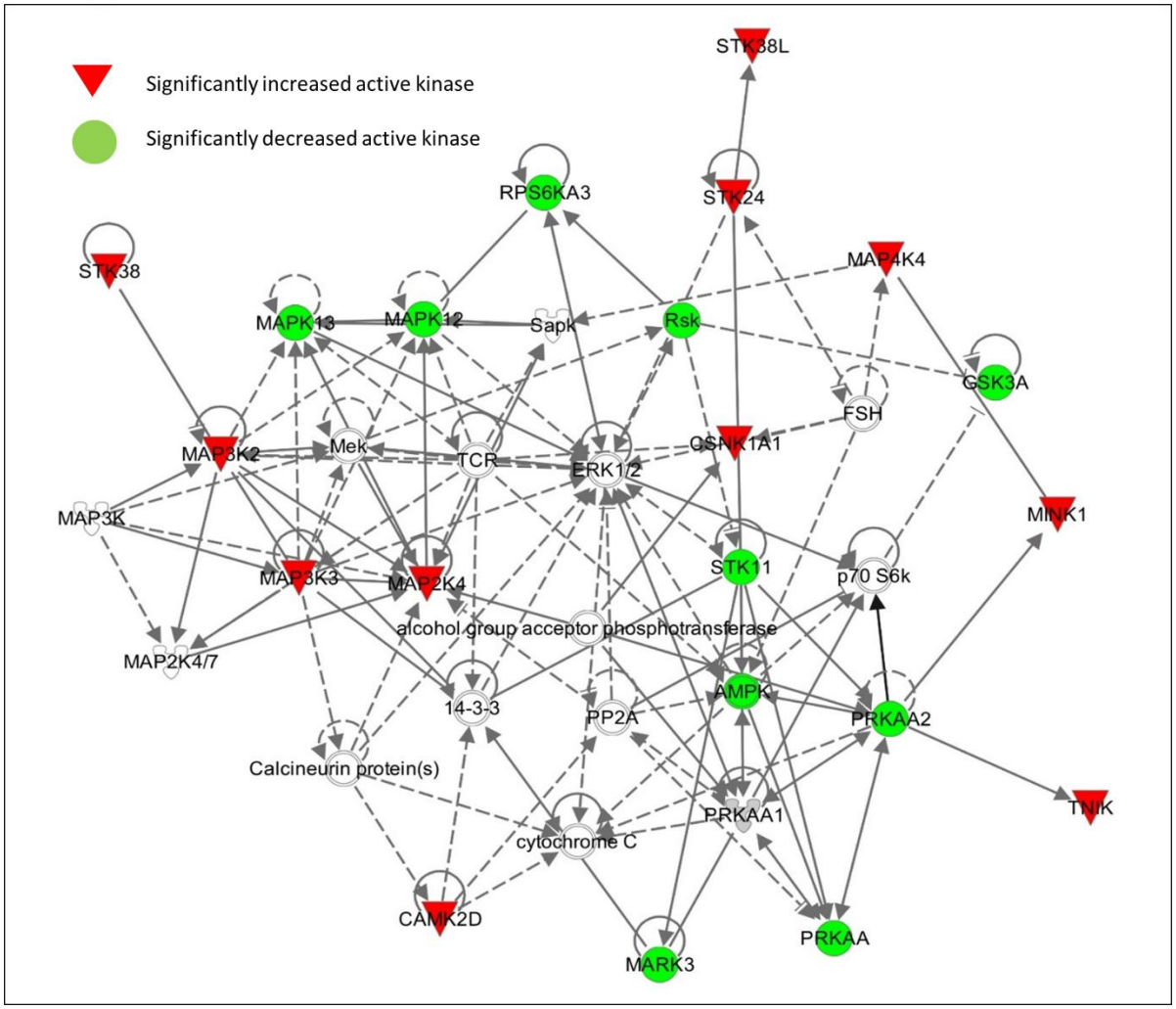

Figure 4-14. A significantly enriched functional kinome network of the differential changed protein kinases in human skeletal muscle insulin resistance. Color-coded network was output from IPA. Solid line is indicating direct interactions and dashed line is indicating indirect interactions.

Table 4-1. Identified 71 active protein kinase lysine sites in skeletal muscle insulin resistance.

Gene Name	Protein Name	Modified sequence	Desthiobiotin K positions within proteins	Binding K type
BRAF	Serine/threonine-protein kinase B-raf	DLK(de)SNNIFLHEDLTVK	578	Catalytic Domain
CAMK2B	Calcium/calmodulin-dependent protein kinase type II subunit beta	LCTGHEYAAK(de)IINTK	43	ATP binding Site
CAMK2D	Calcium/calmodulin-dependent protein kinase type II subunit delta	IPTGQEYAAK(de)IINTK	43	ATP binding Site
CAMK2G	Calcium/calmodulin-dependent protein kinase type II subunit gamma	TSTQEYAAK(de)IINTK	43	ATP binding Site
CDK16	Cyclin-dependent kinase 16	DLK(de)PQNLLINER	288	Catalytic Domain
CDK16	Cyclin-dependent kinase 16	LTDNLVALK(de)EIR	194	ATP binding Site
CDK2	Cyclin-dependent kinase 2	DLK(de)PQNLLINTEGAIK	129	Catalytic Domain
CDK5	Cyclin-dependent kinase 5	DLK(de)PQNLLINR	128	Catalytic Domain
CDK5	Cyclin-dependent kinase 5	NRETHEIVALK(de)R	33	ATP binding Site
CSNK1A1	Casein kinase I isoform alpha	DIK(de)PDNFLMGIGR	138	Catalytic Domain
CSNK2A1	Casein kinase II subunit alpha	DVK(de)PHNVMIDHEHR	158	Catalytic Domain
CSNK2A2	Casein kinase II subunit alpha'	DVK(de)PHNVM(ox)IDHQQK	159	Catalytic Domain
EGFR	Epidermal growth factor receptor	IPVAIK(de)ELR	745	ATP binding Site
EIF2AK2	Interferon-induced, double-stranded RNA-activated protein kinase	DLK(de)PSNIFLVDTK	416	Catalytic Domain
GSK3A	Glycogen synthase kinase-3 alpha	DIK(de)PQNLLVDPDTAVLK	246	Catalytic Domain
GSK3B	Glycogen synthase kinase-3 beta	DIK(de)PQNLLLDPDTAVLK	183	Catalytic Domain

MAP2K1	Dual specificity mitogen-activated protein kinase kinase 1	DVK(de)PSNILVNSR	192	Catalytic Domain
MAP2K1	Dual specificity mitogen-activated protein kinase kinase 1	K(de)LIHLEIKPAIR	97	ATP binding Site
MAP2K2	Dual specificity mitogen-activated protein kinase kinase 2	DVK(de)PSNILVNSR	196	Catalytic Domain
MAP2K2	Dual specificity mitogen-activated protein kinase kinase 2	K(de)LIHLEIKPAIR	101	ATP binding Site
MAP2K3	Dual specificity mitogen-activated protein kinase kinase 3	DVK(de)PSNVLINK	192	Catalytic Domain
MAP2K3	Dual specificity mitogen-activated protein kinase kinase 3	HAQSGTIMAVK(de)R	93	ATP binding Site
MAP2K4	Dual specificity mitogen-activated protein kinase kinase 4	DIK(de)PSNILLDR	231	Catalytic Domain
MAP2K4	Dual specificity mitogen-activated protein kinase kinase 4	PSGQIM(ox)AVK(de)R	131	ATP binding Site
MAP2K6	Dual specificity mitogen-activated protein kinase kinase 6	LSVIHRDVK(de)PSNVLINAL	181	Catalytic Domain
MAP2K6	Dual specificity mitogen-activated protein kinase kinase 6	M(ox)RHVPSGQIM(ox)AVK(de)R	82	ATP binding Site
MAP3K2	Mitogen-activated protein kinase kinase kinase 2	DIK(de)GANILR	482	Catalytic Domain
MAP3K3	Mitogen-activated protein kinase kinase kinase 3	DIK(de)GANILR	491	Catalytic Domain
MAP4K4	Mitogen-activated protein kinase kinase kinase kinase 4	DIK(de)GQNVLLTENAEVK	155	Catalytic Domain
MAP4K5	Mitogen-activated protein kinase kinase kinase kinase 5	DIK(de)GANILLTDHGDVK	142	Catalytic Domain
MAP4K5	Mitogen-activated protein kinase kinase kinase kinase 5	NVHTGELAAVK(de)IIK	49	ATP binding Site
MAPK1	Mitogen-activated protein kinase 1	DLK(de)PSNLLLNTTCDLK	151	Catalytic Domain
MAPK12	Mitogen-activated protein kinase 12	DLK(de)PGNLAVNEDCELK	155	Catalytic Domain

MAPK13	Mitogen-activated protein kinase 13	DLK(de)PGNLAVNEDCELK	152	Catalytic Domain
MARK2	Serine/threonine-protein kinase MARK2	DLK(de)AENLLLDADM(ox)NIK	177	Catalytic Domain
MARK3	MAP/microtubule affinity-regulating kinase 3	DLK(de)AENLLLDADM(ox)NIK	180	Catalytic Domain
MARK3	MAP/microtubule affinity-regulating kinase 3	EVAIK(de)IIDK	85	ATP binding Site
MARK4	MAP/microtubule affinity-regulating kinase 4	EVAIK(de)IIDK	88	ATP binding Site
MAST1	Microtubule-associated serine/threonine-protein kinase 1	DLK(de)PDNLLITSM(ox)GHIK	499	Catalytic Domain
MAST2	Microtubule-associated serine/threonine-protein kinase 2	DLK(de)PDNLLITSM(ox)GHIK	637	Catalytic Domain
MAST3	Microtubule-associated serine/threonine-protein kinase 3	DLK(de)PDNLLITSLGHIK	492	Catalytic Domain
MINK1	Misshapen-like kinase 1	DIK(de)GQNVLLTENAEVK	155	Catalytic Domain
MLTK	Mitogen-activated protein kinase kinase kinase MLT	WISQDKEVAVKK(de)	46	ATP binding Site
MST4	Serine/threonine-protein kinase MST4	DIK(de)AANVLLSEQGDVK	146	Catalytic Domain
NEK6	Serine/threonine-protein kinase Nek6	DIK(de)PANVFITATGVVK	174	Catalytic Domain
NEK7	Serine/threonine-protein kinase Nek7	DIK(de)PANVFITATGVVK	163	Catalytic Domain
NEK7	Serine/threonine-protein kinase Nek7	AACLLDGVPVALK(de)K	63	ATP binding Site
NEK9	Serine/threonine-protein kinase Nek9	DIK(de)TLNIFLTK	178	Catalytic Domain
NEK9	Serine/threonine-protein kinase Nek9	LGDYGLAK(de)K	81	ATP binding Site
OXSR1	Serine/threonine-protein kinase OSR1	DVK(de)AGNILLGEDGSVQ	148	Catalytic Domain
PRKAA1	5'-AMP-activated protein kinase catalytic subunit alpha-1	DLK(de)PENVLLDAHMNAK	152	Catalytic Domain
PRKAA1	5'-AMP-activated protein kinase catalytic subunit alpha-1	VAVK(de)ILNR	56	ATP binding Site

PRKAA2	5'-AMP-activated protein kinase catalytic subunit alpha-2	DLK(de)PENVLLDAH MNAK	141	Catalytic Domain
PRKAA2	5'-AMP-activated protein kinase catalytic subunit alpha-2	VAVK(de)ILNR	45	ATP binding Site
RPS6KA1	Ribosomal protein S6 kinase alpha-1	DLK(de)PENILLDEEG HIK	189	Catalytic Domain
RPS6KA2	Ribosomal protein S6 kinase alpha-2	DLK(de)PENILLDEEG HIK	186	Catalytic Domain
RPS6KA3	Ribosomal protein S6 kinase alpha-3	DLK(de)PSNILYVDES GNPESIR	541	Catalytic Domain
RPS6KA3	Ribosomal protein S6 kinase alpha-3	DLK(de)PENILLDEEG HIK	195	Catalytic Domain
SLK	STE20-like serine/threonine-protein kinase	DLK(de)AGNILFTLDG DIK	157	Catalytic Domain
SLK	STE20-like serine/threonine-protein kinase	ETSVLAAAK(de)VIDT K	63	ATP binding Site
STK10	Serine/threonine-protein kinase 10	DLK(de)AGNVLMTLE GDIR	159	Catalytic Domain
STK11	Serine/threonine-protein kinase STK11	DIK(de)PGNLLLTTGG TLK	178	Catalytic Domain
STK24	Serine/threonine-protein kinase 24	DIK(de)AANVLLSEH GEVK	158	Catalytic Domain
STK25	Serine/threonine-protein kinase 25	DIK(de)AANVLLSEQ GDVK	142	Catalytic Domain
STK38	Serine/threonine-protein kinase 38	DIK(de)PDNLLLDSK	214	Catalytic Domain
STK38	Serine/threonine-protein kinase 38	DTGHVYAMK(de)ILR	118	ATP binding Site
STK38L	Serine/threonine-protein kinase 38-like	DTGHIYAMK(de)ILR	119	ATP binding Site
TNIK	TRAF2 and NCK-interacting protein kinase	DIK(de)GQNVLLTEN AEVK	155	Catalytic Domain
TP53RK	TP53-regulating kinase	FLSGLELVK(de)QGAE AR	40	ATP binding Site
ULK3	Serine/threonine-protein kinase ULK3	NISHLDLK(de)PQNIL LS	139	Catalytic Domain
ULK3	Serine/threonine-protein kinase ULK3	EVVAIK(de)CVAK	44	ATP binding Site

Table 4-2. Twenty-eight FDA-approved drug-target entries on the functional kinome in human skeletal muscle insulin resistance.

Gene Name	Protein Name	Approved drug name	Drug Bank ID	Pharmacology
PRKAA1	5'-AMP-activated protein kinase catalytic subunit alpha-1	Acetylsalicylic acid	DB00945	Treatment of mild to moderate pain
PRKAA1	5'-AMP-activated protein kinase catalytic subunit alpha-1	Adenosine monophosphate	DB00131	Nutritional supplementation
PRKAA1	5'-AMP-activated protein kinase catalytic subunit alpha-1	Metformin	DB00914	Treatment of type II diabetes mellitus, kinase inducer
CAMK2G	Calcium/calmodulin-dependent protein kinase type II subunit gamma	Bosutinib	DB06616	Treatment of chronic myelogenous leukemia (CML)
CDK2	Cyclin-dependent kinase 2	Bosutinib	DB06616	Treatment of chronic myelogenous leukemia (CML)
MAP2K1	Dual specificity mitogen-activated protein kinase kinase 1	Bosutinib	DB06616	Treatment of chronic myelogenous leukemia (CML)
MAP2K1	Dual specificity mitogen-activated protein kinase kinase 1	Cobimetinib	DB05239	Treatment of metastatic melanoma, MAPK inhibitor
MAP2K1	Dual specificity mitogen-activated protein kinase kinase 1	Trametinib	DB08911	Treatment of metastatic melanoma with BRAF V600E or V600K mutations
MAP2K2	Dual specificity mitogen-activated protein kinase kinase 2	Bosutinib	DB06616	Treatment of chronic myelogenous leukemia (CML)
MAP2K2	Dual specificity mitogen-activated protein kinase kinase 2	Trametinib	DB08911	Treatment of metastatic melanoma with BRAF V600E or V600K mutations

EGFR	Epidermal growth factor receptor	Afatinib	DB08916	Treatment of metastatic non-small cell lung cancer, Tyrosine kinase inhibitor
EGFR	Epidermal growth factor receptor	Cetuximab	DB00002	Treatment of metastatic colorectal carcinoma, Tyrosine kinase inhibitor
EGFR	Epidermal growth factor receptor	Erlotinib	DB00530	Treatment of metastatic non-small cell lung cancer, Tyrosine kinase inhibitor
EGFR	Epidermal growth factor receptor	Gefitinib	DB00317	Treatment of metastatic non-small cell lung cancer, Tyrosine kinase inhibitor
EGFR	Epidermal growth factor receptor	Icotinib	DB11737	Treatment of metastatic non-small cell lung cancer, Tyrosine kinase inhibitor
EGFR	Epidermal growth factor receptor	Lapatinib	DB01259	Treatment of metastatic breast cancer, Tyrosine kinase inhibitor
EGFR	Epidermal growth factor receptor	Lidocaine	DB00281	Treatment of Local or regional anesthesia
EGFR	Epidermal growth factor receptor	Necitumumab	DB09559	Treatment of non-small cell lung cancer, Tyrosine kinase inhibitor
EGFR	Epidermal growth factor receptor	Olmutinib	DB13164	Treatment of metastatic T790M mutation positive non-small cell lung cancer
EGFR	Epidermal growth factor receptor	Osimertinib	DB09330	Treatment of metastatic T790M mutation positive non-small cell lung cancer
EGFR	Epidermal growth factor receptor	Panitumumab	DB01269	Treatment of EGFR-expressing, metastatic colorectal carcinoma
EGFR	Epidermal growth factor receptor	Trastuzumab	DB00072	Treatment of HER2-positive breast cancer
EGFR	Epidermal growth factor receptor	Vandetanib	DB05294	Treatment of metastatic medullary thyroid cancer
GSK3B	Glycogen synthase kinase-3 beta	Lithium	DB01356	Mood stabilizer, kinase inhibitor
MAPK1	Mitogen-activated protein kinase 1	Arsenic trioxide	DB01169	Treatment of acute promyelocytic leukemia (APL),
MAPK1	Mitogen-activated protein kinase 1	Isoprenaline	DB01064	Treatment of mild or transient episodes of heart block

MAP3K2	Mitogen-activated protein kinase kinase kinase 2	Bosutinib	DB06616	Treatment of chronic myelogenous leukemia (CML)
RPS6KA3	Ribosomal protein S6 kinase alpha-3	Acetylsalicylic acid	DB00945	Treatment of mild to moderate pain

Table 4-3. Twenty-two significantly changed protein kinases in obesity with insulin resistance.

Gene Name	Protein Name	Protein ID	Desthiobiotin K positions within proteins	Binding K Type	Fold Change OBi/LC Mean ± SEM
MAPK12	Mitogen-activated protein kinase 12	P53778	152	catalytic domain	0
MAPK13	Mitogen-activated protein kinase 13	P53778	152	catalytic domain	0
RPS6KA3	Ribosomal protein S6 kinase alpha-3	P51812	541	Catalytic domain	0
CAMK2B	Calcium/calmodulin-dependent protein kinase type II subunit beta	Q13554	43	ATP binding site	0.06 ± 0.01
STK11	Serine/threonine-protein kinase STK11	Q15831	178	catalytic domain	0.08 ± 0.02
PRKAA2	5'-AMP-activated protein kinase catalytic subunit alpha-2	P54646	45	ATP binding site	0.11 ± 0.03
PRKAA1	5'-AMP-activated protein kinase catalytic subunit alpha-1	Q13131	56	ATP binding site	0.11± 0.03
MARK3	MAP/microtubule affinity-regulating kinase 3	J3KNR0	85	ATP binding site	0.22 ± 0.07
GSK3A	Glycogen synthase kinase-3 alpha	P49840	246	catalytic domain	0.30 ± 0.04
CAMK2D	Calcium/calmodulin-dependent protein kinase type II subunit delta	E9PF82	43	ATP binding site	1.74 ± 0.55
MAP2K4	Dual specificity mitogen-activated protein kinase kinase 4	P45985	131	ATP binding site	4.51 ± 0.28
CSNK1A1	Casein kinase I isoform alpha	P48729	138	catalytic domain	Infinity
CSNK2A1	Casein kinase II subunit alpha	P68400	158	catalytic domain	Infinity
MAP3K2	Mitogen-activated protein kinase kinase kinase 2	Q9Y2U5	485	catalytic domain	Infinity
MAP3K3	Mitogen-activated protein kinase kinase kinase 3	Q99759	491	catalytic domain	Infinity

MAP4K4	Mitogen-activated protein kinase kinase kinase kinase 4	G5E948	155	catalytic domain	Infinity
MINK1	Misshapen-like kinase 1	Q8N4C8	155	catalytic domain	Infinity
NEK9	Serine/threonine-protein kinase Nek9	Q8TD19	178	catalytic domain	Infinity
STK24	Serine/threonine-protein kinase 24	Q9Y6E0	158	catalytic domain	Infinity
STK38	Serine/threonine-protein kinase 38	Q15208	118	ATP binding site	Infinity
STK38L	Serine/threonine-protein kinase 38-like	Q9Y2H1	119	ATP binding site	Infinity
TNIK	TRAF2 and NCK-interacting protein kinase	Q9UKE5	155	catalytic domain	Infinity

CHARTER 5. HUMAN KINOME INTERACTOME PROFILING IN SKELETAL MUSCLE INSULIN RESISTANCE

5.1 Introduction

Protein kinases catalyze phosphorylation, one of the most important PTMs, which serves as a switch to turn “on” and “off” of molecular functions. In most of the cases, phosphorylated proteins (adding a phosphate group) become active or “on” mode, dephosphorylated proteins (removing a phosphate group) become inactive or “off” mode. Hence, protein kinases play essential roles in cell signal transduction and biological process, such as insulin signaling, MAP kinase signaling and glucose metabolic process. Protein kinases not only are key regulators for downstream substrate proteins but also highly regulated by phosphorylation; as a result, protein kinases are phosphorylated by other kinases or themselves (also known as autophosphorylation). For example, protein kinase B (or AKT) is highly regulated by upstream kinases, such as PDK1 and mTOR/Rictor, which phosphorylate AKT at Thr^{308} and Ser^{473} (Tsuchiya, Kanno, & Nishizaki, 2014). Receptor tyrosine kinases (i.e., EGFR) typically undergo autophosphorylation where ligand binding leads EGFR dimerization and multiple tyrosine residues are phosphorylated by EGFR (Bae & Schlessinger, 2010). Therefore, intracellular protein-protein interactions of kinase-substrate complexes and kinase-kinase complexes are primarily means but not limited to 1) cell signaling events, such as promotion or inhibition of each other’s activity; 2) transport across membranes, such as cytoplasm to nucleus transport; 3) protein

degradation, such as ubiquitination. Dysregulation of protein-protein interactions involving protein kinases might lead to cell signaling malfunction and diseases, such as insulin resistance and T2D; nonetheless, large scale profiling of active kinome interaction partners in human skeletal muscle insulin resistance remains unreported. Here, we hypothesized that abnormalities of functional kinome interactome may exist in skeletal muscle of obese insulin resistant participants compared to lean healthy insulin sensitive subjects. We developed a new activity-based functional kinome enrichment platform coupling with quantitative proteomics to globally enrich and quantify interaction partners of active kinases in human skeletal muscle in lean controls and obese insulin resistant participants.

5.2 Materials and Methods

5.2.1 SILAC labeled primary cultured human skeletal muscle cells

Ten to fifteen mg of each human muscle biopsy from two lean healthy and two obese insulin resistance subjects were used to generate primary cultured human skeletal muscle cells. Method used was the same as described in 4.2.1.

The primary cells were SILAC labeled with two heavy isotopic labeled amino acids: L-Lysine-2HCl, 4,4,5,5-D4 (Lys4, which is 4 Da heavier than neutral lysine) and L-Arginine-HCl, $^{13}C_6$, $^{15}N_4$ (Arg10, which is 10 Da heavier than neutral arginine). Method used was the same as described in 4.2.2.

5.2.2 Active protein kinases enrichment for functional kinome interactome

Around 120–150 mg frozen muscle biopsy of each sample from 8 lean control (LC) and 8 obese insulin resistance (OBi) participants, and SILAC labeled

skeletal muscle cells as mentioned above were homogenized using a Next Advance Bullet Blender and lysed by Pierce IP Lysis Buffer with 8M urea and Halt™ Protease/Phosphatase Inhibitor Cocktail. Protein concentration was measured by Bradford protein assay, where Coomassie blue plus Kit with standard was used for this assay. For each sample 2.0 mg tissue lysate spiked-in with 1.0 mg SILAC cell lysate (four cell lines from 2 LC and 2 OB were pooled first) was accurately aliquoted. Then the mixed lysate went through Zeba™ Spin Desalting Columns, 7K MWCO, 5mL to remove all the endogenous ATP. The filtrate lysate of 8 LC and 8 OBi were diluted with Reaction buffer into 2mg/mL, and incubated with 10 µL of 1M $MgCl_2$ at room temperature for 1 minute. Before the probe labeling, each sample was evenly divided into two portions, one portion for real kinome interactome enrichment while the other portion served as negative control (without probe labeling to filter out non-specific binding proteins that are not labelled by the probe but pulled down by streptavidin agarose resin). The portion for enrichment was labeled with 10µM ActivX™ Desthiobiotin-ATP incubation at room temperature for 10 minutes, whereas the negative controls were incubated with 10 µL ddH_2O for 10 minutes. The probe labeled lysate and negative control were incubated with 50µL of 50% high capacity streptavidin agarose resin slurry for 1 hour at room temperature on a mixing rotator; subsequently, the resin was washed 3 times with lysis buffer, 3 times with PBS, and 3 times with LCMS-grade water. The agarose resin slurry with pulled down proteins were incubated with 10mM dithiothreitol (DTT) for 30 minutes at 55 °C and 50mM iodoacetamide (IAA)

incubation for 30min at room temperature in dark. “On-beads” digestion was performed with 2µg protease MS grade trypsin incubation for 16 hours at on a thermo shaker at 37°C. The resulting peptides were dried with a speedvac, and were desalted with Zipclean tips and reconstituted with 0.1% TFA in water for HPLC-ESI-MS/MS analysis. Noted that all the catalog number and vendor company are the same as described in 4.2.3

5.2.3 HPLC-ESI-MS/MS analysis

As described in 4.2.4

5.2.4 Database search

As described in 4.2.5

5.2.5 Bait active protein kinome and its interactome identification and quantification

In the desthiobiotin K peptides file generated from MaxQuant software package, which provides sequence of modified peptides with lysine sites and their intensity, a bait kinase has to be identified with at least one of the two lysine residues (#1 in ATP binding site and #2 in catalytic domain) on the desthiobiotin modified lysine site. Because of the high selectivity and sensitivity of the ATP probe, all the bait protein kinases were considered as in their active form. In order to unveil true interaction partners of functional kinome, the identified proteins other than bait proteins (i.e., active kinases in this case) must satisfied the following three rigorous criteria: 1) the protein must be identified with minimum two unique peptides; 2) the protein must be identified with light labeled peak area (PA) in at least half of the

kinome interaction partner enrichments (i.e., ≥8 biopsy samples); 3) those proteins must have an enrichment ratio (Kinome IP/negative control IP) of >10. In order to calculate the enrichment, the PA for each protein identified was normalized against Universal SILAC: the heavy labeled proteins identified in at least 8 out of 16 samples were used as "Universal" internal standard, and the total peak of the SILAC labeled lysine sites were calculated in each sample. Then, the peak area of each kinase (PAi) was normalized by the sum peak area of universal heavy labeled proteins in the same sample:

$$\text{Norm}: i = \frac{\text{PA}i}{\text{Total peak area of SILAC labeled heavy proteins identified in } \geq 8 \text{ samples}}$$

Due to the sensitivity of this platform, non-specific binding partners may result in high discover rate of false-positive. Therefore, we employed negative controls without probe labeling to eliminate nonspecific binding accumulated in the experiment process. The negative control concepts have been widely used and accepted for protein-protein interaction partner identification in our previous work (Caruso, Ma, Msallaty, Lewis, Seyoum, Al-janabi, Diamond, Abou-Samra, Hojlund, et al., 2014; Caruso et al., 2015; X. Zhang et al., 2016). For each sample, the enrichment ratio was calculated as followed: the average of SILAC normalized PA from real enrichment pull down experiment was divided by the average of SILAC normalized PA from negative control. It is noted that if zero identification in negative control, then the enrichment ratio of that protein was manually assigned as infinity. The calculation formula of enrichment ratio listed below:

$$\text{Enrichment\_Ratio}: i = \frac{\text{Average\_Norm: } i\text{\_IP}}{\text{Average\_Norm: } i\text{\_control}}$$

In order to quantify relative protein abundance of the kinome interaction partners, the PAj of each partner protein was normalized against PAj of total bait kinases in the same sample. This normalization approach for protein-protein interaction study has been demonstrated and employed in either quantitative proteomics or western blotting (Caruso, Ma, Msallaty, Lewis, Seyoum, Al-janabi, Diamond, Abou-Samra, Hojlund, et al., 2014; Caruso et al., 2015; Wepf, Glatter, Schmidt, Aebersold, & Gstaiger, 2009; X. Zhang et al., 2016). The normalization formula listed below:

$$\text{Norm}: j = \frac{\text{PAj}}{\text{PAj\_}total\ bait\ kinases}$$

To determine the significantly changed partners, a fold change of OBi/LC greater than 1.5 or less than 0.67 was required, subsequently, p-value of independent two-side *t-test* must be less than 0.05.

5.2.6 Bioinformatics

As described in 4.2.7

5.3 Results

5.3.1 Kinome interaction partners in human skeletal muscle insulin resistance

To determine the true interaction partners of functional kinome in human skeletal muscle insulin resistance, a rigorous identification and quantification procedure was designed in figure 5-1. We first identified 1791 proteins with

minimum two unique peptides and 0.01 false discovery rate (FDR) which has been widely accepted for quantitative proteomics analysis for interaction partners discovery (Wepf et al., 2009). Furthermore, we categorized 18 protein kinases, being identified with at least one conserved lysine residue, which served as bait proteins (Table 5-1); the rest 1773 proteins were potential prey proteins for the 18 active kinases. Then, in order to eliminate the nonspecific binding proteins, we filtered 1580 proteins with enrichment ratios greater than 10. The true interaction partners also need to be identified in at least half sample size (i.e., ≥ 8 muscle biopsies); as a result, there were 616 proteins assigned as true interaction proteins which were, based on our literature search, the first functional kinome interactome in human skeletal muscle. The active kinases or active conformation of the kinases are the real “players” in cellular functions because inactive kinases lose their intrinsic enzyme activity or with very low catalytic level (Chihara-Nakashima, Hashimoto, & Nishizuka, 1977; Phillips, Aponte, Covian, & Balaban, 2011; Ward & O'Brian, 1992); therefore, the proteins interacted with active kinases are important to understand the abnormalities of cell signaling and molecular function in muscle insulin resistance.

First, we analyzed the 18 bait protein kinases which are the key modulators in cell signal transduction. Among the 18 protein kinase, as expected from specific aim 1, only one tyrosine kinase (Tyrosine-protein kinase CSK) was enriched, and the other 17 kinases were all serine/threonine kinases. As we know, each individual kinase may involve in multiple cell signaling pathway but, for most well

studied kinases, has a few primary focuses; for example, AMPK1 is mainly involved in AMPK pathway. Based on Uniprot and Gene Ontology databases, we assigned the 18 protein kinases in 5 primary signaling pathways but 4 kinases were not being assigned to any known signaling pathway based on the database search (Figure 5-2). There were 5 protein kinases were mapped in the ERK1/2 pathway, which is also part of typical insulin signaling and mTOR signaling pathway, and 3 kinases involved in AMPK pathway, which is also part of mTOR signaling; two kinases participate in Wnt signaling; two kinases were assigned to JNK pathway and two kinases involved in p38 MAPK signaling. Furthermore, a biofunction analysis was performed on these 18 kinases (Figure 5-3). As we expected 18 kinases showed phosphotransferase activity; in contrast, three kinases displayed tyrosine kinase activity, but only 1 out of 3 was tyrosine kinase and the other 2 kinases were serine/threonine kinases, serine/threonine-protein kinase Nek6 (NEK6) and dual specificity mitogen-activated protein kinase kinase 6 (MAP2K6 or MEK6). MEK6 has been reported to phosphorylate both serine and tyrosine residue on the p38 MAP kinases (Visconti et al., 2000). Due to the limited number of bait kinases, a large bioinformatics analysis may not show significance on many biofunctions, but these 18 kinases did involve in multiple foundational cell signaling (Figure 5-2) which is highly related to insulin signaling (e.g., ERK1/2 pathway) and glucose uptake (e.g., AMPK pathway).

Second, we analyzed the 616 kinome interaction partners that directly or indirectly bind to the bait active kinases. Noted that protein binding could be transit;

therefore, this analysis may not contain the complete map of the interaction proteome. Also, non-protein kinases and atypical kinases (without kinase core) or other typical kinases, which are either in inactive conformation ("closed" ATP binding site) or their ATP binding sites were blocked in the kinase-kinase complexes, were also considered as interaction partners. Therefore, out of the 616 interaction partners, we identified 26 protein kinases (including 1 regulatory subunit), 12 non-protein kinases, 2 protein phosphatases and 2 protein phosphatase regulatory subunits (Table 5-2), such as MAPK1. MAPK3, tyrosine-protein kinase Fyn (FYN), tyrosine-protein kinase Yes (YES1), integrin-linked protein kinase (ILK), cAMP-dependent protein kinase catalytic subunit alpha (PRKACA), cGMP-dependent protein kinase 1 (PRKG1), hexokinase-1 (HK1), TP53-regulating kinase (TP53RK), serine/threonine-protein phosphatase PP1-alpha catalytic subunit (PPP1CA), protein phosphatase 1 regulatory subunit 12A (PPP1R12A) and serine/threonine-protein phosphatase 2A 55 kDa regulatory subunit B alpha isoform (PPP2R2A). Our finding indicated that dozens of kinase-kinase interactions exist in human skeletal muscle.

Next, we conducted cell signaling pathway (Figure 5-4) and biofunction analysis (Figure 5-5) on the 616 kinome interaction partners using IPA and David bioinformatics online source integrating GOTERM, KEGG and Recatome databases. Diabetes pathway (from reactome database) was significantly enriched with highest -log (p-value) at 15.44, and it covers 72 proteins that may contribute to the pathogenesis of diabetes. For example, cAMP-dependent protein

kinase type II-alpha regulatory subunit (PRKAR2A), (cAMP-dependent protein kinase catalytic subunit alpha (PRKACA) and ras-related protein Rap-1b (RAP1B) was categorized into diabetes pathway. Besides diabetes pathway, mTOR signaling was also enriched with very high significant level. As we described above, mTOR is a critical pathway regulates multiple key players that might involve in insulin resistance and T2D, such as MAPK1, Growth factor receptor-bound protein 2 (GRB2), 40S ribosomal protein S3 (RPS3), 5'-AMP-activated protein kinase subunit beta-2 (PRKAB2), eukaryotic translation initiation factor 3 subunit A (EIF3A) and 40S ribosomal protein S6 (RPS6). Furthermore, insulin signaling pathway with 20 protein interaction partners (from KEGG database) was significantly enriched as well. In addition, multiple essential signaling pathways were also significantly enriched, including p70S6K signaling (downstream of mTOR), Wnt signaling, ILK signaling, and apoptosis related pathway. Figure 5-4 illustrates the top 8 identified pathways related but not limit to insulin signaling, cell growth and programmed death, and diabetes.

The biofunction analysis of the kinome interactome indicated that protein folding, proteasome, positive/negative regulation of ubiquitination and regulation of cytoskeleton were highly enriched. These biofunctions are key molecular processes for protein synthesis and degradation, and cytoskeleton remodeling. Beyond those, glucose, pyruvate and glycogen metabolism play the central roles in glucose homeostasis; similarly, fatty acid and lipid metabolism are critical biological processes for lipid homeostasis. Taken all the biofunction analysis

results, the kinome interaction partners participate in maintaining proteins, glucose, and lipids balances in skeletal muscle, and might be contribute to abnormal metabolism in obese individuals with insulin resistance.

5.3.2 Significantly changed functional kinome interaction partners in skeletal muscle insulin resistance

Importantly, we identified 135 kinome interaction proteins with a fold change greater than 1.5 (i.e., 83 proteins increased in OBi) or less than 0.67 (i.e., 52 proteins decreased in OBi) and also with significant p-value from independent two-side student t-tests ($p < 0.05$) comparing OBi with lean subjects. Of the 135 proteins, 131 were only identified in kinome IPs but not in negative control IPs, which suggested the high confidence of the results. The 135 significantly changed partners might be responsible for abnormal molecular function and cell signaling caused by insulin resistance in skeletal muscle (Table 5-3).

Based on the pathway analysis for the interaction partners, we identified 20 proteins involved in the insulin signaling pathway, which is one of the most studied pathways for abnormal molecular function and cell signaling related to insulin resistance and T2D. We color coded insulin signaling pathway (downloaded from http://www.kegg.jp) with identified partners in that pathway according to their difference in kinome interaction; interestingly, out of the 20 kinome interaction partners, 17 proteins remained unchanged and only 3 proteins (i.e., RPS6, PRKAB2 and PRKAR2A) had significantly increased association to the active kinases (Figure 5-7). Also, we mapped 16 interaction proteins in the MAPK

signaling pathway (downloaded from http://www.kegg.jp); similarly,13 proteins remained intact and 3 partners showed enhanced interactions with active kinases in OBi, which were heat shock-related 70 kDa protein 2 (HSPA2), Voltage-dependent L-type calcium channel subunit beta-1 (CACNB1) and MAPT (Figure 5-8). Furthermore, two increased partners and 4 decreased in OBi compared to LC were mapped into ILK pathway (downloaded from IPA software package) which was significantly enriched in the pathway analysis for kinome interactome (Figure 5-8). In addition, two protein kinases with attenuated interactions to active kinases in OBi were not categorized in any pathway above: YES1 (reduced 3.73 folds in OBi) and TP53RK (reduced 2.67 folds in OBi), which play central roles in cell cycle, cytokine responsive pathway and tumor cell differentiation and proliferation. In addition, no phosphatase was identified with significant changes.

We performed biofunction analysis (Figure 5-6), which suggested abnormal protein degradation and synthesis, apoptosis and cytoskeleton dynamics may contribute to the pathogenesis of insulin resistance in human skeletal muscle. Of interest, 5 out of the 6 proteins (i.e., PSMA1, PSMD14, PSMD11, PSMC3, PSMD7) regulated ubiquitination were significantly increased, which might indicate a trend for up-regulated ubiquitination in OBi.

To elucidate the protein-protein interaction of the 18 active bait kinases and their 135 significant interaction partners, an interaction network was developed using IPA with mapping parameter set at maximum 70 molecules per network (Figure 5-6). We mapped 15 out of the 18 bait protein kinases (highlighted in

yellow), 6 increased kinome interaction partner (highlighted in red) and 7 interaction proteins that showed decreased trend (highlighted in green) in the network. The central core protein is ERK1/2, which has been identified as an interaction partner of kinome, but did not show significant change. In the network, we noticed a few proteins in the center were closely interacted with multiple kinases (e.g., ERK1/2), such as integrin-linked protein kinase (ILK), vimentin (VIM), RPS6, and microtubule-associated protein tau (MAPT).

5.4 Discussion

Intracellular protein-protein interactions mediated cell signal transduction, protein transport, endocytosis and exocytosis of signaling molecules (e.g., insulin granule exocytosis) have been widely accepted and recognized, and protein kinases are known active reaction modules that interact with dozens of substrates or regulatory proteins. High-throughput methods for protein-protein interaction analysis have been broadly used, such as co-immunoprecipitation which allows bait protein binding as well as the interaction proteins bound to the bait. However, the typical Co-IP targets one bait protein which is specifically against the antibody conjugated to the protein A/G beads. Here, we present an ATP probe pull-down assay that enriches dozen of active protein kinases and their interaction partners using activity-based ATP probes instead protein antibodies. Coupling high resolution mass spectrometry with the ATP probe, we identified the first functional kinome interactome (616 proteins) in the human skeletal muscle insulin resistance,

which provided a global picture of kinase interaction complexes including kinase-substrate, kinase-kinase, etc.

5.4.1 Insulin signaling pathway

Insulin signaling pathway is the central and most studied pathway that affects insulin sensitivity and glucose metabolism; and dysregulation of insulin signaling may result in insulin resistance and impaired insulin stimulated glucose uptake. In this study, we identified and quantified 20 kinome interaction partners involved in insulin signaling (Figure 5-8); and majority of them have unchanged association with core active kinases in OBi. For example, the interaction to active kinases for PPP1CA/PPP1CC (two catalytic subunits of protein phosphatase-1), phosphorylase b kinase regulatory subunit alpha (PHKA1), glycogen phosphorylase (PYGB) which directly interact with each other (based on KEGG's data), remained the same in OBi. Also, GRB2 and ERK1 did not show significant difference in their interaction to active kinases between LC and OBi. However, multiple proteins in the insulin signaling pathway exhibited increased interaction with active kinome, such as RPS6, PRKAB2 and PRKAR2A. Of interest, PRKAB2 (AMPK Subunit Beta-2), a non-catalytic subunit of AMPK1/2, which has been shown down-regulated trend in our kinome profiling in Aim 1, has been reported as a scaffold to assemble the AMPK complex which includes α (catalytic), β, and γ subunits (Scott et al., 2004; Xiao et al., 2007). The molecular function of β subunit of AMPK is far from well understood, and it is known that subcellular localization and PTMs of AMPK can influence its activity (Salt et al., 1998; Warden et al., 2001).

Qi *et al.,* reported that ubiquitination of AMPK β subunit exert negative regulation of AMPK1 activity in brown adipose tissue from mice (Qi et al., 2008); furthermore, they proposed that elevated inflammation in the adipose tissue may lead to down-regulated AMPK activity via increased PRKAB2 ubiquitination. In our study, we also demonstrated up-regulated ubiquitination in OBi through the biofunction analysis of the 135 significantly changed interaction partners. Therefore, our finding suggested that increased PRKAB2 association with active kinome might inhibit AMPK1 activity via the ubiquitin-proteasome protein degradation. It is noted that researchers (Rubio, Vernia, & Sanz, 2013) also reported that sumoylation of PRKAB2 enhanced AMPK activity, but they pinpointed that ubiquitination and sumoylation shared the same catalytic lysine residue on PRKAB2, so these two PTMs were competitive binding. Combining our data showing increased regulation of ubiquitination, it seems that PRKAB2 might be a negative regulator of AMPK activity in addition to be a scaffold subunit.

5.4.2 MAPK signaling pathway

MAPK signaling (Figure 5-9), including three sub-pathways: ERK1/2 signaling, JNK signaling and p38 MAPK signaling, is mainly responsible for cell survival, differentiation and proliferation, and inflammation. We identified 16 kinome interaction partners assigned to MAPK signaling, primarily on ERK1/2 signaling (14 partners). GTPase HRas (HRAS) was identified as unchanged partners, and Ras is one of the most important modulators in ERK signaling. Additionally, two RafB regulators, Rap1 and PKA, were also identified, and the

quantified results implied no significant change of Rap1 and PKA when interacting with functional kinome. Combined with our results in specific aim 1 that EGFR, RafB, MEK1, MEK2, ERK2 displayed no changed kinase activity, it seems that ERK1/2 signaling pathway might remain intact in the insulin resistant skeletal muscle, which is in agreement with some literature (Cusi et al., 2000; Krook et al., 2000).

Interestingly, we found three kinome interaction partners (HSPA2, CACNB1 and MAPT) exhibited significant increased binding to active kinases, of which CACNB1 displayed mixed kinome interaction (another subunit CACNA1S showed no change). HSPA2, belonged to HSP70 family, is one of the most universal molecular chaperones that assisting protein folding (Gehrmann et al., 2005; M. Hantschel et al., 2000), and dysregulation of HSP70 leads to various diseases, such as diabetes (Pockley, Henderson, & Multhoff, 2014). Growing evidence indicates increased serum HSP70 level in diabetic patients (Garamvolgyi, Prohaszka, Rigo, Kecskemeti, & Molvarec, 2015; Nakhjavani et al., 2010; Pagetta, Folda, Brunati, & Finotti, 2003); however, its cellular mechanism in skeletal muscle insulin resistance and T2D remains unknown. Previous data suggested that HSP70 promoted muscle regeneration after injury and was responsive to inflammatory cytokines. Emerging data reports that insulin resistance and obesity induce inflammation in skeletal muscle (Hotamisligil, 2006; Lumeng & Saltiel, 2011; McNelis & Olefsky, 2014; Osborn & Olefsky, 2012), and another theory of skeletal muscle inflammation is that immune cells, secreting pro-inflammatory cytokines,

are accumulating in myotubes (Wu & Ballantyne, 2017). Another study reported that HSP70 activated T cells in autoimmune arthritis (Wieten et al., 2010), which supports that the positive correlation between HSP70 and insulin resistance via an inflammatory manner. The current finding that increased HSPA2 association with functional kinome in OBi further supports HSP70's role in skeletal muscle insulin resistance.

5.4.3 ILK signaling pathway

Integrin-linked kinase catalyzes variety of intracellular and extracellular functions, such as cell migration and proliferation, through integrin which is a transmembrane receptors. In this study (Figure 5-10), we observed decreased kinome interaction with ILK, myosin heavy chain 1 (MYH1), vimentin (VIM), actin, cytoplasmic 2 (ACTG1), and increased kinome association level with nascent polypeptide-associated complex alpha subunit (NANA), fibronectin 1(FN1). Of interest, early work reported that ILK is necessary for PI3K mediated AKT signaling, and ILK directly phosphorylates GSK3 (Delcommenne et al., 1998). Recent work suggested that decreased glucose uptake and insulin sensitivity in ILK deficiency mice in a GLUT4-dependent manner (Hatem-Vaquero et al., 2017). Based on our literature search, only one study focused on the ILK function in development of muscle insulin resistance, which was done in mice (Kang et al., 2016), nonetheless, reduced kinome interaction with ILK has not been reported.

5.5 Summary

We identified 616 functional kinome interaction partners in human skeletal muscle from 8 lean healthy and 8 obese insulin resistant participants, which is the largest human kinome interactome to date. Among the 616 interaction partners, 385 has a fold change > 1.5 or <0.67. Out of these 385 kinome interaction partners, 135 displayed significantly difference between the two groups (p-value < 0.05). The kinome interatome participate in various cell signaling pathways (i.e., diabetes pathway, mTOR pathway, insulin signaling pathway, etc.) and biofunctions (i.e., protein synthesis and degradation, cytoskeleton dynamics, and apoptosis). Notably, we developed this ATP probe pull-down platform coupling with quantitative proteomics, which allowed us to globally profile protein interaction partners of dozens of active kinases simultaneously. However, the obvious limitation was that interaction partners cannot be assigned to one particular kinase. Nonetheless, using this approach, we generated the 1st active kinome interactome profile in skeletal muscle of lean heathy individuals, and how it is differ in obese insulin resistant subjects, which offers new information on molecular mechanism of skeletal muscle insulin resistance.

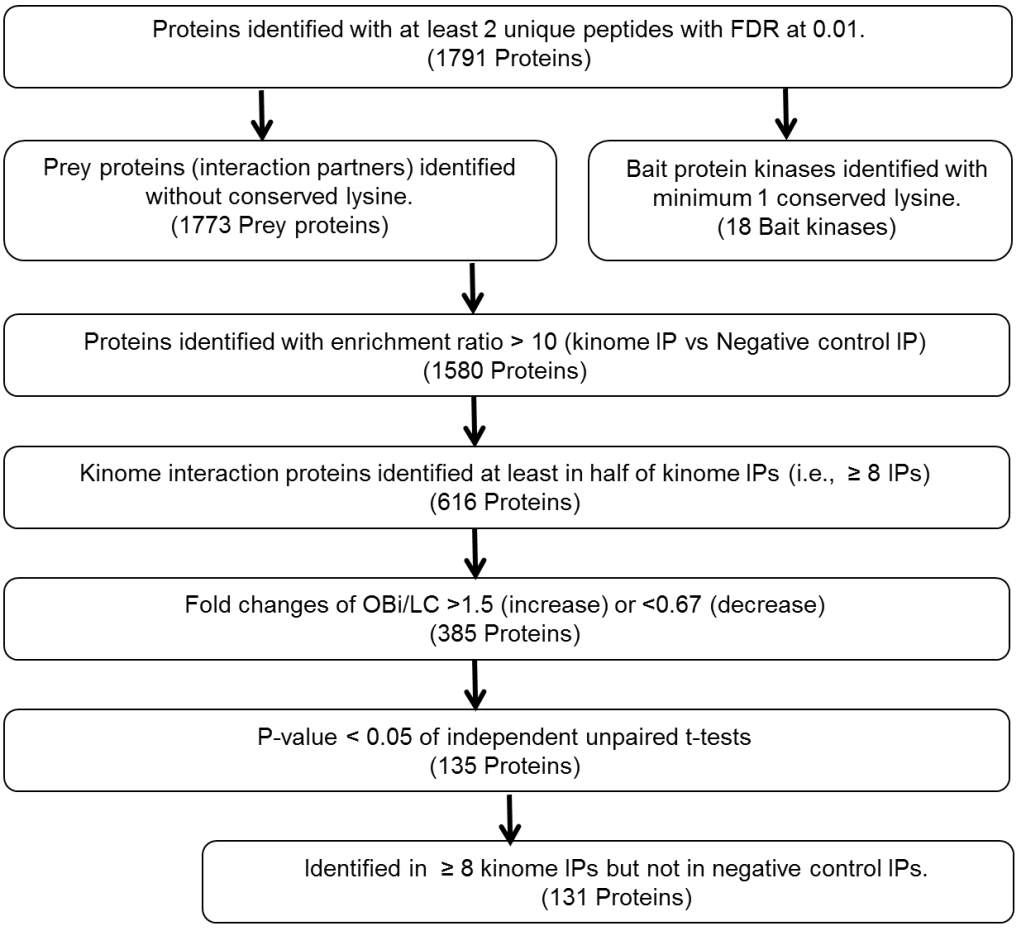

Figure 5-1. Flowchart of kinome interactome identification and quantification procedure.

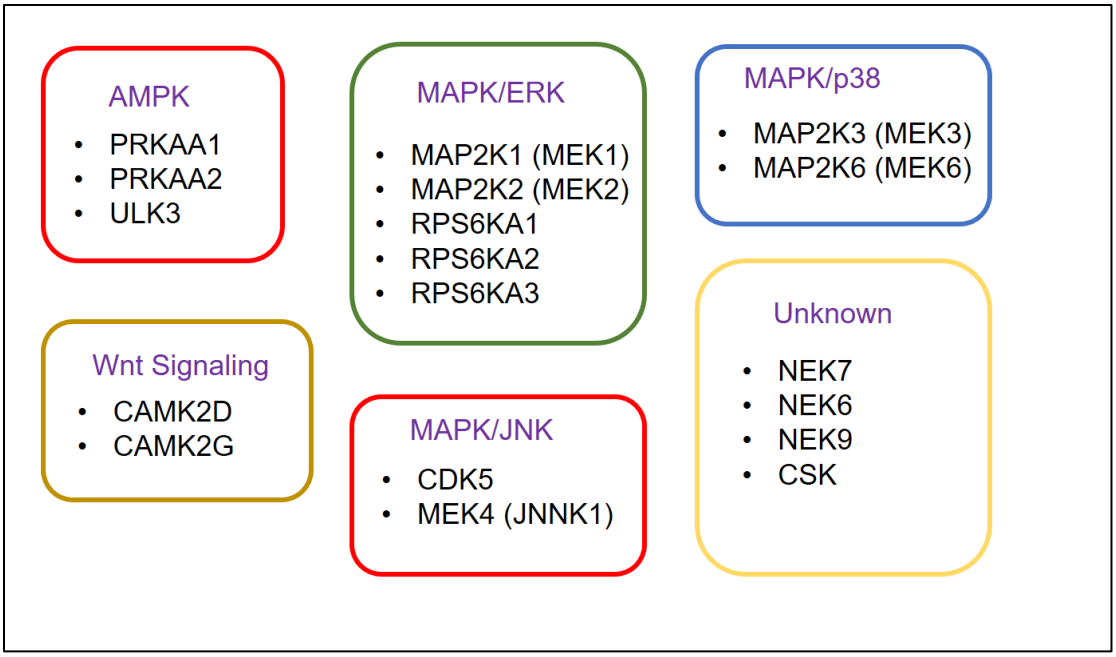

Figure 5-2. Primary cell signaling pathways assigned for the 18 bait kinases.

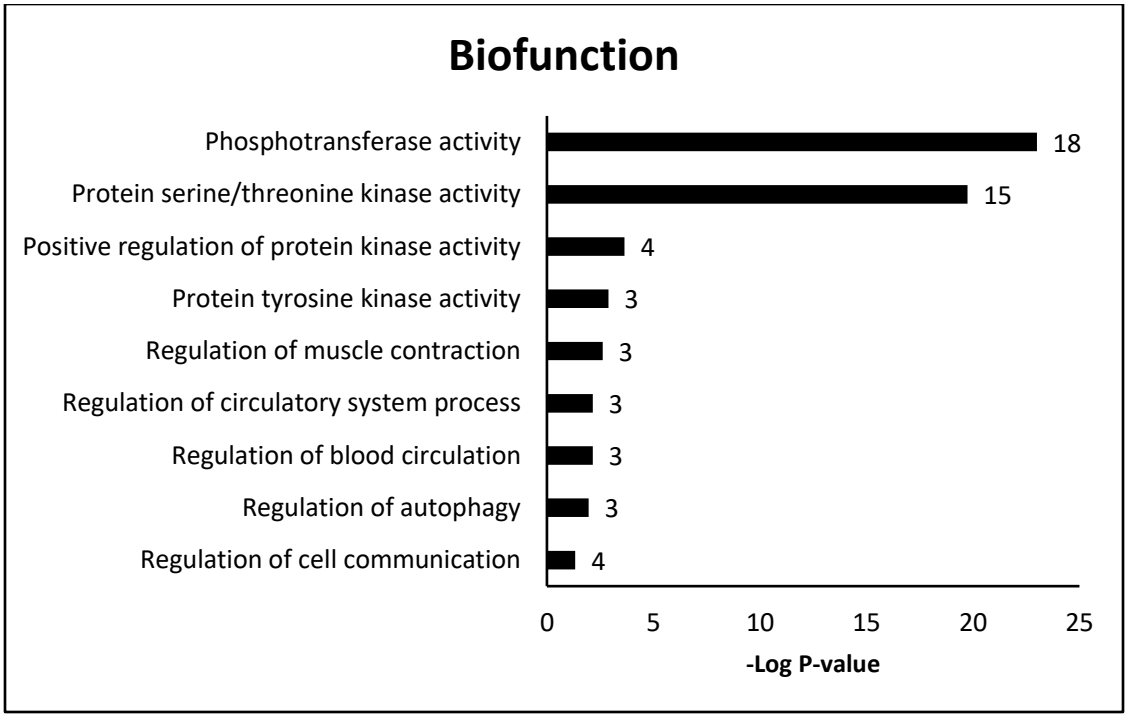

Figure 5-3. Biofunction analysis of the 18 bait kinases. Data label on the bar represents the number of bait protein kinases participated in that biofunction.

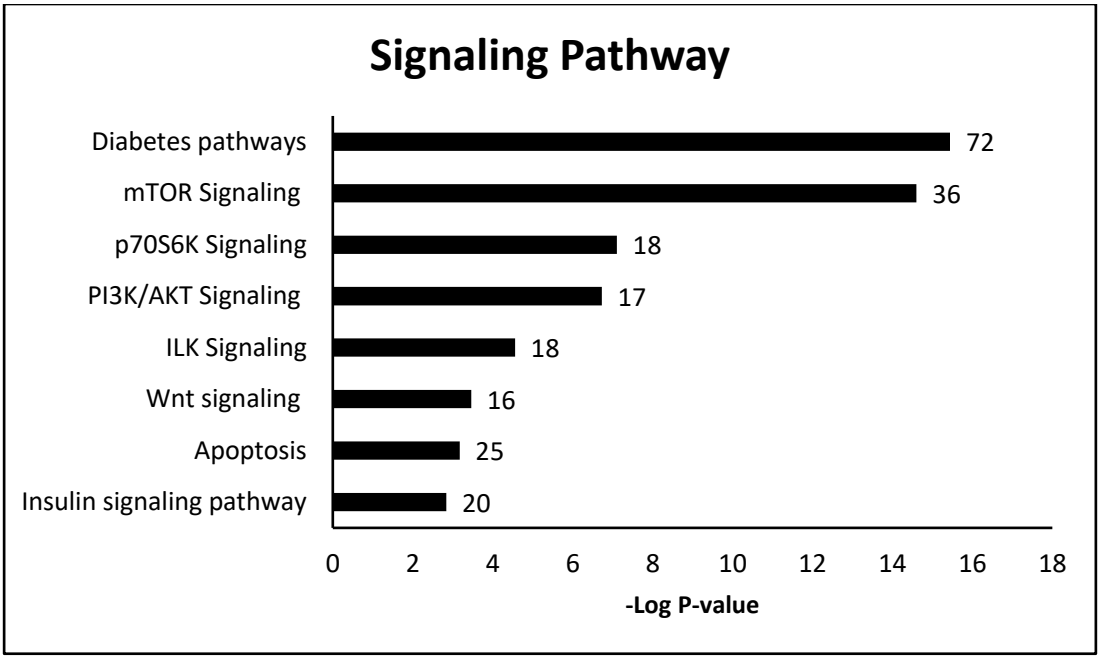

Figure 5-4. Signaling pathway analysis of the 616 functional kinome interaction partners. Data label on the bar represents the number of protein interaction partners participated in that pathway.

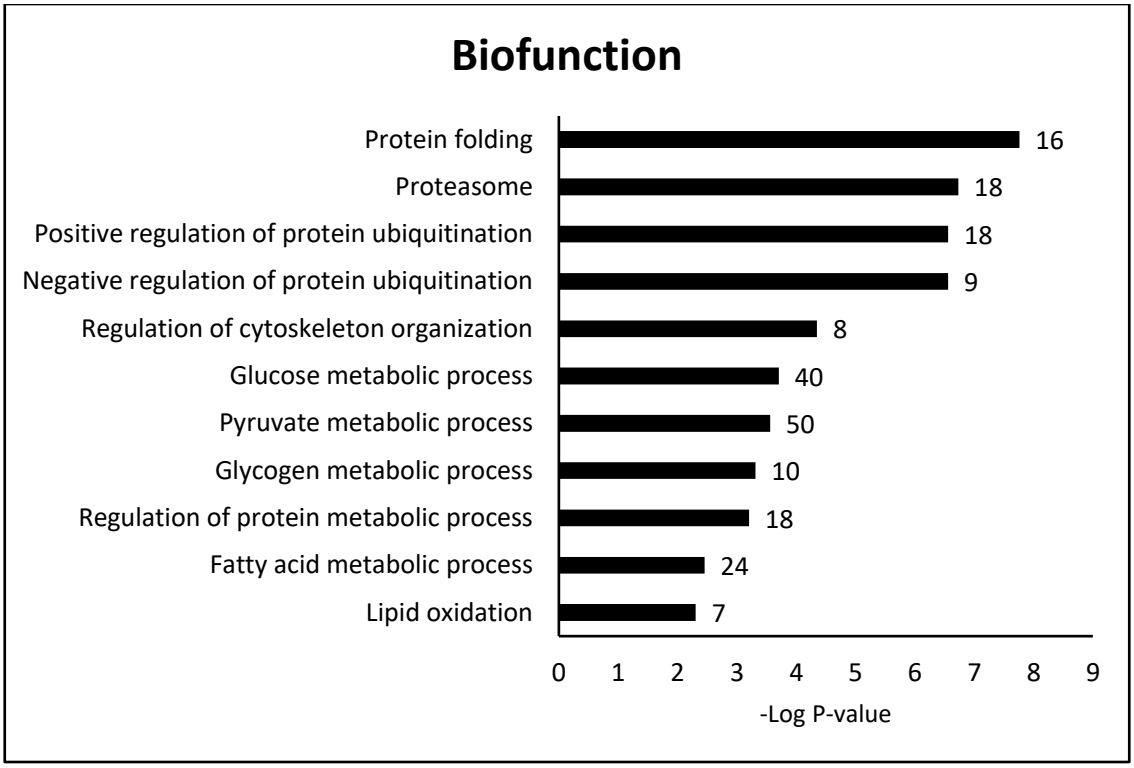

Figure 5-5. Biofunction analysis of the 616 functional kinome interaction partners. Data label on the bar represents the number of protein interaction partners participated in that biofunction.

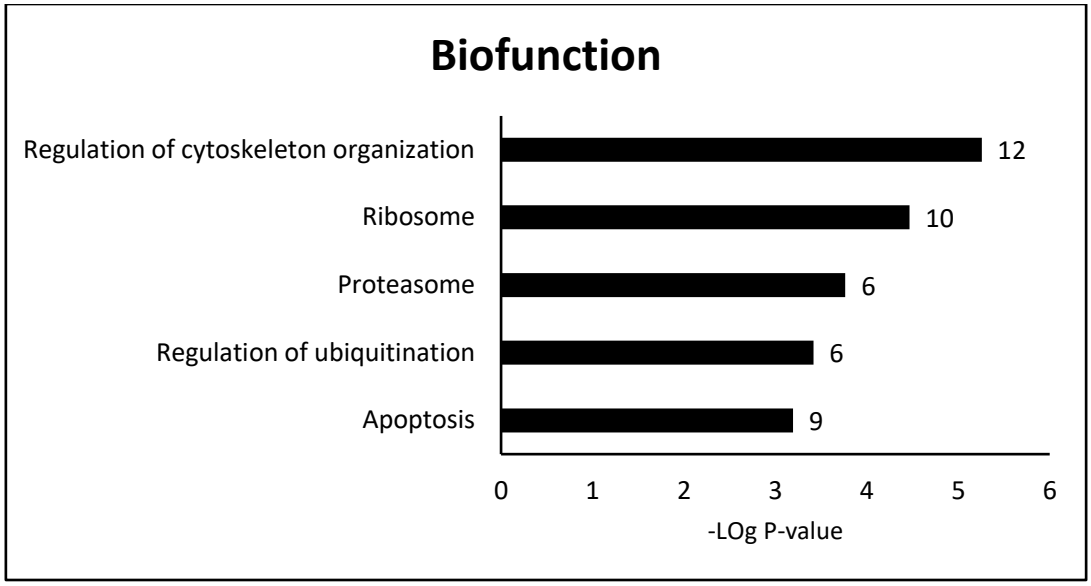

Figure 5-6. Biofunction analysis of the 135 significantly changed functional kinome interaction partners. Data label on the bar represents the number of significantly changed protein interaction partners participated in that biofunction.

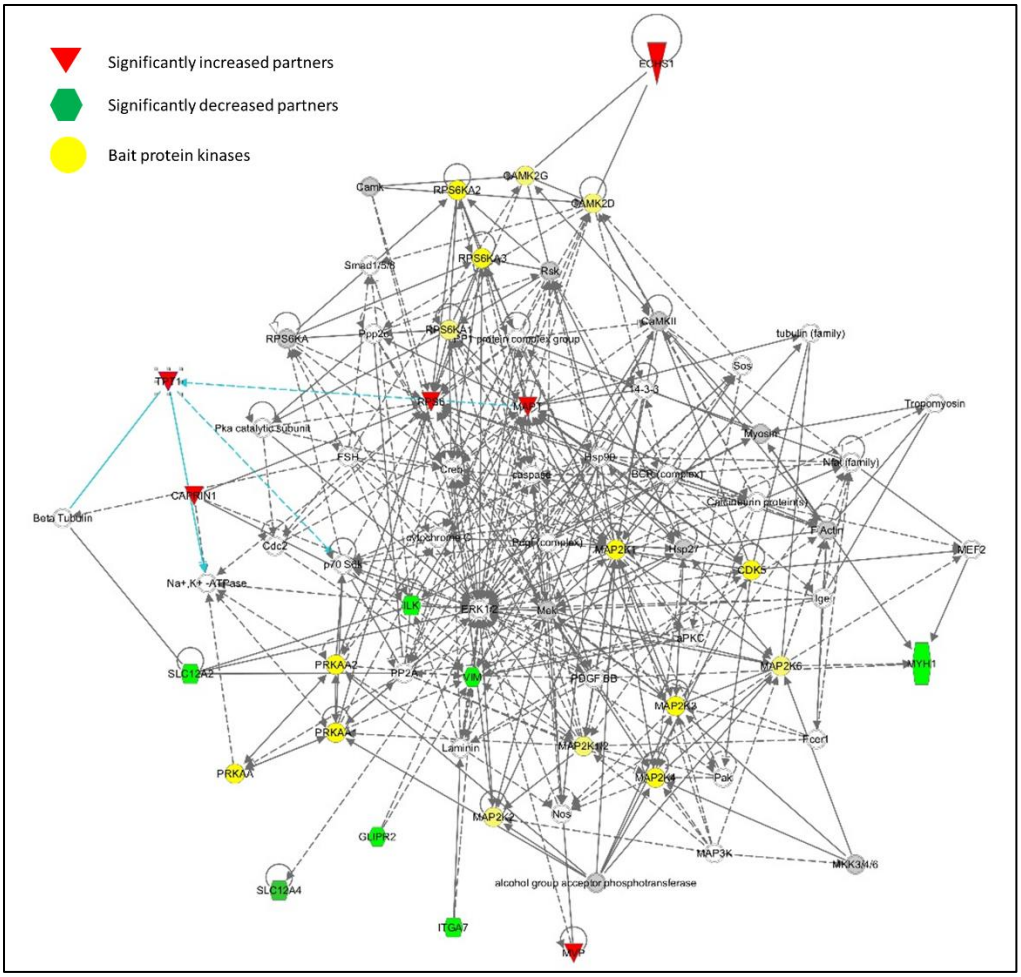

Figure 5-7. Interaction network of the 18 bait protein kinases and significantly changed functional kinome interaction partners. Solid line is indicating direct interactions and dashed line is indicating indirect interactions.

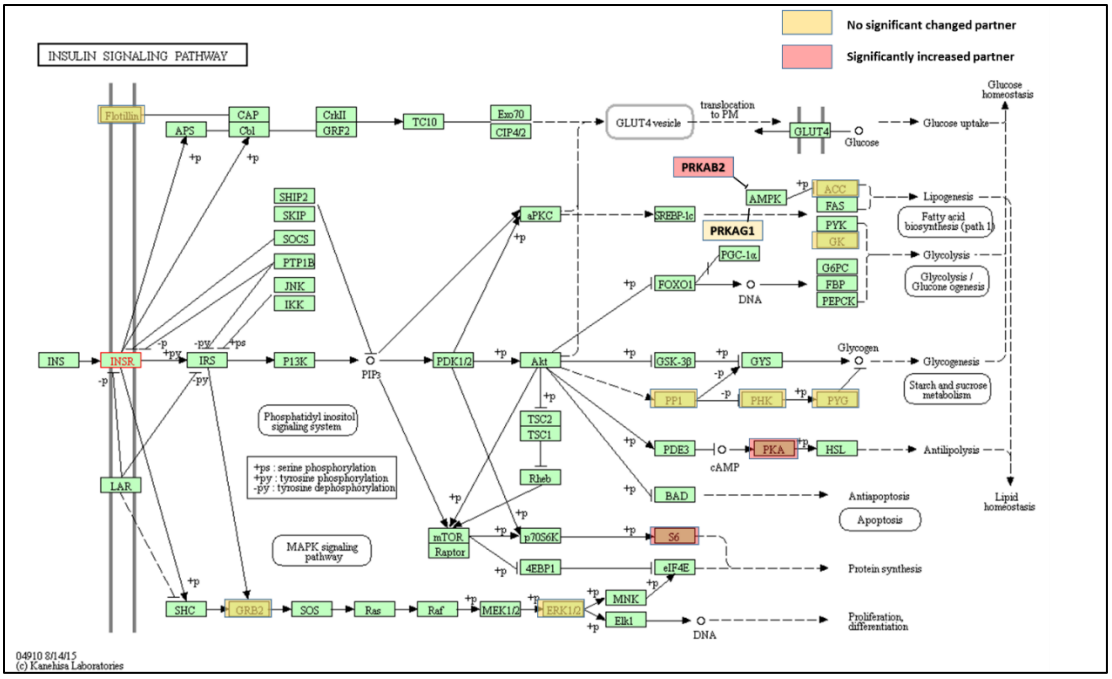

Figure 5-8. Color-coded insulin signaling pathway of kinome interaction partners according to their differences in LC and OBi. Pathway map was downloaded from KEGG.

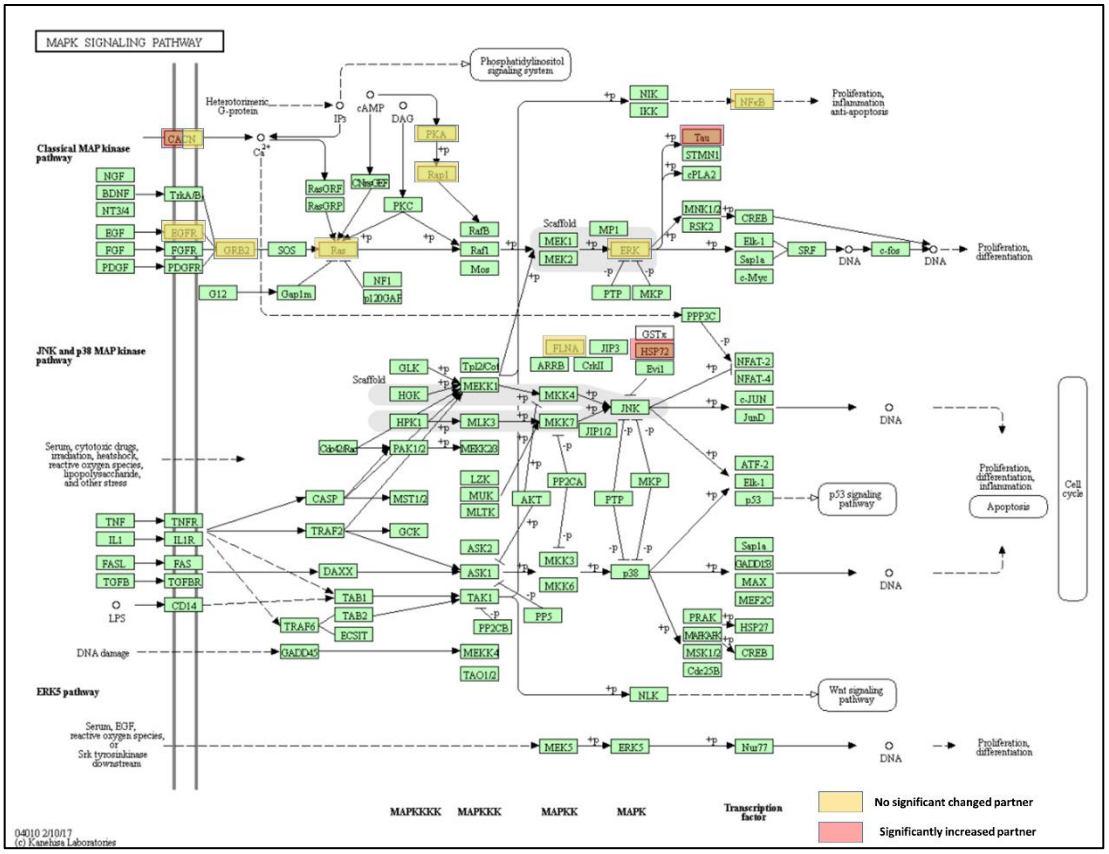

Figure 5-9. Color-coded MAPK signaling pathway of kinome interaction partners according to their differences in LC and OBi. Pathway map was downloaded from KEGG.

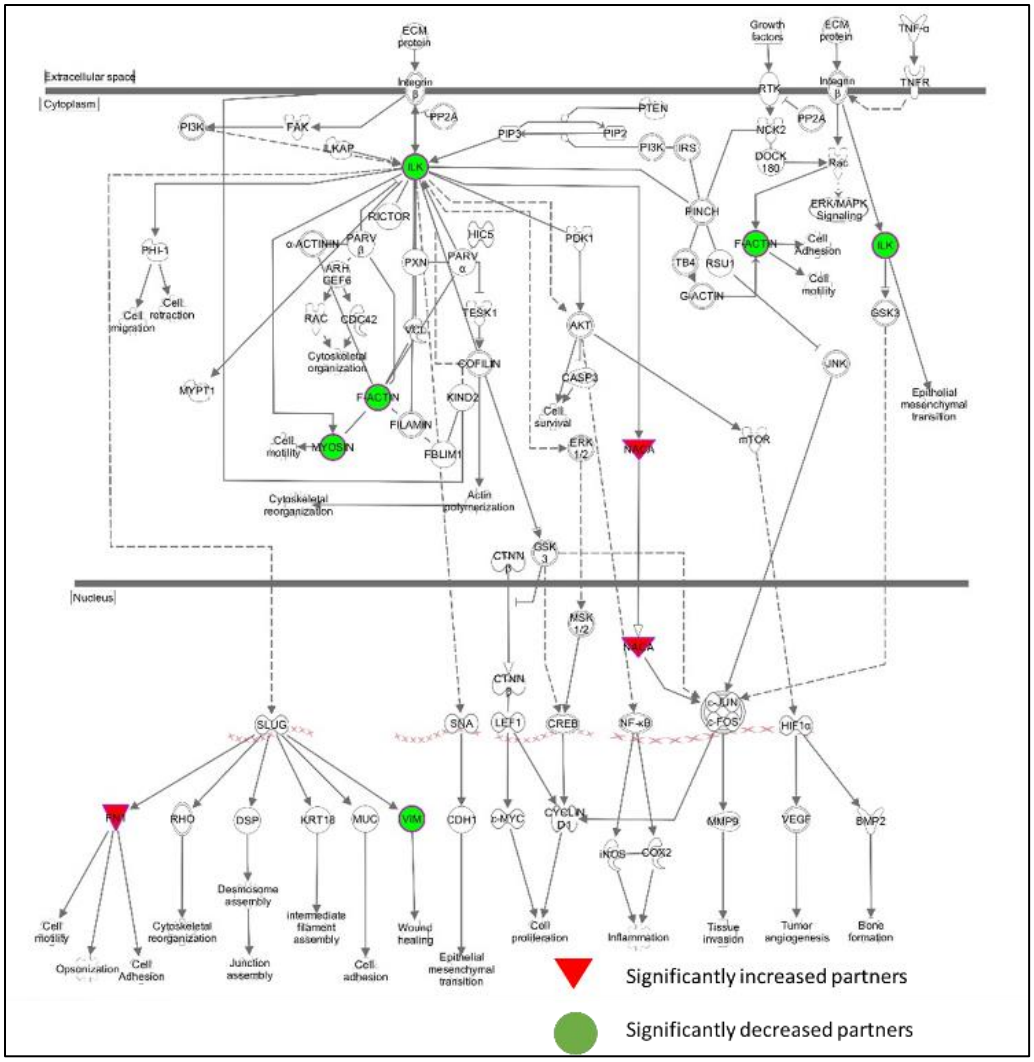

Figure 5-10. Color-coded ILK signaling pathway of significantly changed kinome interaction partners according to their differences in LC and OBi. Pathway map was adapted from IPA.

Table 5-1. Identified active protein kinase lysine sites (assigned to 18 kinases) served as bait proteins in kinome interactome profiling.

Gene Name	Protein Name	Modified sequence	Desthiobiotin K positions within proteins	Binding K type
CAMK2D	Calcium/calmodulin-dependent protein kinase type II subunit delta	IPTGQEYAAK(de)IINTK	43	ATP binding Site
CAMK2G	Calcium/calmodulin-dependent protein kinase type II subunit gamma	TSTQEYAAK(de)IINTK	43	ATP binding Site
CDK5	Cyclin-dependent kinase 5	DLK(de)PQNLLINR	128	Catalytic Domain
CSK	Tyrosine-protein kinase CSK	VSDFGLTK(de)EASSTQDTGKLPVK	337	Catalytic Domain
MAP2K1	Dual specificity mitogen-activated protein kinase kinase 1	K(de)LIHLEIKPAIR	97	ATP binding Site
MAP2K1	Dual specificity mitogen-activated protein kinase kinase 1	DVK(de)PSNILVNSR	192	Catalytic Domain
MAP2K2	Dual specificity mitogen-activated protein kinase kinase 2	K(de)LIHLEIKPAIR	101	ATP binding Site
MAP2K2	Dual specificity mitogen-activated protein kinase kinase 2	DVK(de)PSNILVNSR	196	Catalytic Domain
MAP2K3	Dual specificity mitogen-activated protein kinase kinase 3	DVK(de)PSNVLINK	192	Catalytic Domain
MAP2K3	Dual specificity mitogen-activated protein kinase kinase 3	HAQSGTIMAVK(de)R	93	ATP binding Site
MAP2K4	Dual specificity mitogen-activated protein kinase kinase 4	DIK(de)PSNILLDR	231	Catalytic Domain
MAP2K4	Dual specificity mitogen-activated protein kinase kinase 4	PSGQIM(ox)AVK(de)R	131	ATP binding Site
MAP2K6	Dual specificity mitogen-activated protein kinase kinase 6	LSVIHRDVK(de)PSNVLINALGQVK	181	Catalytic Domain
MAP2K6	Dual specificity mitogen-activated protein kinase kinase 6	M(ox)RHVPSGQIM(ox)AVK(de)R	82	ATP binding Site
NEK6	Serine/threonine-protein kinase Nek6	DIK(de)PANVFITA	174	Catalytic Domain
NEK7	Serine/threonine-protein kinase Nek7	DIK(de)PANVFITATGVVK	163	Catalytic Domain

NEK9	Serine/threonine-protein kinase Nek9	LGDYGLAK(de)K	81	ATP binding Site
PRKAA1	5'-AMP-activated protein kinase catalytic subunit alpha-1	VAVK(de)ILNR	56	ATP binding Site
PRKAA2	5'-AMP-activated protein kinase catalytic subunit alpha-2	VAVK(de)ILNR	45	ATP binding Site
RPS6KA1	Ribosomal protein S6 kinase alpha-1	DLK(de)PENILLDEEGHIK	189	Catalytic Domain
RPS6KA2	Ribosomal protein S6 kinase alpha-2	DLK(de)PENILLDEEG	186	Catalytic Domain
RPS6KA3	Ribosomal protein S6 kinase alpha-3	DLK(de)PENILLDEEGH	195	Catalytic Domain
ULK3	Serine/threonine-protein kinase ULK3	NISHLDLK(de)PQNILLSSLEKPHLK	139	Catalytic Domain

Table 5-2. Kinases and phosphatases identified as functional kinome interaction partners.

Gene name	Protein name	Category
ALDH18A1	Glutamate 5-kinase	Non-protein kinase
BCKDK	[3-methyl-2-oxobutanoate dehydrogenase [lipoamide]] kinase, mitochondrial	Non-protein kinase
CAMK2A	Calcium/calmodulin-dependent protein kinase type II subunit alpha	Protein kinase
CAMK2B	Calcium/calmodulin-dependent protein kinase type II subunit beta	Protein kinase
CMPK1	UMP-CMP kinase	Non-protein kinase
CSNK2A1	Casein kinase II subunit alpha	Protein kinase
CSNK2A2	Casein kinase II subunit alpha	Protein kinase
EIF2AK2	Interferon-induced, double-stranded RNA-activated protein kinase	Protein kinase
FAM20B	Glycosaminoglycan xylosylkinase	Non-protein kinase
FN3K	Fructosamine-3-kinase	Non-protein kinase
FN3KRP	Ketosamine-3-kinase	Non-protein kinase
FYN	Tyrosine-protein kinase Fyn	Protein kinase
HK1	Hexokinase-1	Non-protein kinase
ILK	Integrin-linked protein kinase	Protein kinase
MAPK1	Mitogen-activated protein kinase 1	Protein kinase
MAPK3	Mitogen-activated protein kinase 3	Protein kinase
MLTK	Mitogen-activated protein kinase kinase kinase MLT	Protein kinase
MYLK	Myosin light chain kinase, smooth muscle	Protein kinase
MYLK2	Myosin light chain kinase 2, skeletal/cardiac muscle	Protein kinase
NME1	Nucleoside diphosphate kinase A	Protein kinase
NME2	Nucleoside diphosphate kinase B	Protein kinase
PANK4	Pantothenate kinase 4	Non-protein kinase
PFKL	6-phosphofructokinase, liver type	Non-protein kinase
PGAM5	Serine/threonine-protein phosphatase PGAM5, mitochondrial	Protein phosphatase
PHKG2	Phosphorylase b kinase gamma catalytic chain, testis/liver isoform	Non-protein kinase
PPP1CA	Serine/threonine-protein phosphatase PP1-alpha catalytic subunit	Protein phosphatase
PPP1R12A	Protein phosphatase 1 regulatory subunit 12A	Protein phosphatase regulatory subunit
PPP2R2A	Serine/threonine-protein phosphatase 2A 55 kDa regulatory subunit B alpha isoform	Protein phosphatase regulatory subunit

PRKAB2	5-AMP-activated protein kinase subunit beta-2	Protein kinase
PRKACA	cAMP-dependent protein kinase catalytic subunit alpha	Protein kinase
PRKACB	cAMP-dependent protein kinase catalytic subunit beta	Protein kinase
PRKAG1	5-AMP-activated protein kinase subunit gamma-1	Protein kinase
PRKAR2A	cAMP-dependent protein kinase type II-alpha regulatory subunit	Protein kinase regulatory subunit
PRKG1	cGMP-dependent protein kinase 1	Protein kinase
PRPS1	Ribose-phosphate pyrophosphokinase 1	Non-protein kinase
PRPS1L1	Ribose-phosphate pyrophosphokinase 3	Non-protein kinase
SLK	STE20-like serine/threonine-protein kinase	Protein kinase
STK24	Serine/threonine-protein kinase 24	Protein kinase
STK38	Serine/threonine-protein kinase 38	Protein kinase
STK38L	Serine/threonine-protein kinase 38-like	Protein kinase
TP53RK	TP53-regulating kinase	Protein kinase
YES1	Tyrosine-protein kinase Yes	Protein kinase

Table 5-3. 135 significantly changed functional kinome interaction partners.

Gene Name	Protein Name	Protein ID	Mean of fold Change	SEM of Fold Change
ACOT9	Acyl-coenzyme A thioesterase 9, mitochondrial	Q9Y305	0.308	0.05
ACSL3	Long-chain-fatty-acid--CoA ligase 3	O95573	0.186	0.04
ACTG1	Actin, cytoplasmic 2;Actin, cytoplasmic 2, N-terminally processed	P63261	0.309	0.08
AHCY	Adenosylhomocysteinase	P23526	0.260	0.02
AHCYL2	Putative adenosylhomocysteinase 3;Adenosylhomocysteinase	Q96HN2	0.336	0.07
ALDH4A1	Delta-1-pyrroline-5-carboxylate dehydrogenase, mitochondrial	P30038	0.184	0.07
ANXA1	Annexin A1;Annexin	P04083	18.769	5.33
ANXA6	Annexin;Annexin A6;Annexin	A6NN80	4.926	1.23
APOBEC2	Probable C->U-editing enzyme APOBEC-2	Q9Y235	20.517	8.05
ARPC3	Actin-related protein 2/3 complex subunit 3	O15145	5.195	1.69
ATP1B1	Sodium/potassium-transporting ATPase subunit beta-1	P05026	4.363	0.90
ATP2B1	Plasma membrane calcium-transporting ATPase 1	P20020	0.419	0.10
ATP5H	ATP synthase subunit d, mitochondrial	O75947	7.243	2.77
C14orf166	UPF0568 protein C14orf166	Q9Y224	55.310	21.12
C1QBP	Complement component 1 Q subcomponent-binding protein, mitochondrial	Q07021	15.448	5.93
C22orf28	tRNA-splicing ligase RtcB homolog	Q9Y3I0	7.119	2.54
CACNB1	Voltage-dependent L-type calcium channel subunit beta-1	Q02641	16.592	6.12
CAP2	Adenylyl cyclase-associated protein 2	P40123	11.697	4.13
CAPRIN1	Caprin-1	Q14444	4.540	1.23
CAPZA1	F-actin-capping protein subunit alpha-1	P52907	0.083	0.01
CBR1	Carbonyl reductase [NADPH] 1	P16152	4.371	0.75
CCDC56	Coiled-coil domain-containing protein 56	Q9Y2R0	17.046	12.06

CLIC4	Chloride intracellular channel protein 4	Q9Y696	4.169	2.40
CLPB	Caseinolytic peptidase B protein homolog	Q9H078	0.458	0.14
CMPK1	UMP-CMP kinase	P30085	6.667	2.32
CYB5R1	NADH-cytochrome b5 reductase 1	Q9UHQ9	0.526	0.07
DARS	Aspartate--tRNA ligase, cytoplasmic	P14868	0.340	0.06
DPM1	Dolichol-phosphate mannosyltransferase	H0Y368	0.096	0.06
DYNC1I2	Cytoplasmic dynein 1 intermediate chain 2	Q13409	2.562	0.48
ECHS1	Enoyl-CoA hydratase, mitochondrial	P30084	7.039	2.18
EEF1A1	Elongation factor 1-alpha 1	P68104	0.624	0.11
EEF1A1P5	Putative elongation factor 1-alpha-like 3	P68104	0.624	0.11
EIF5A	Eukaryotic translation initiation factor 5A-1	I3L504	12.005	4.01
EIF5AL1	Eukaryotic translation initiation factor 5A-1-like	I3L504	12.005	4.01
ERP29	Endoplasmic reticulum resident protein 29	P30040	32.987	12.08
F13A1	Coagulation factor XIII A chain	P00488	0.078	0.04
FAM98A	Protein FAM98A	Q8NCA5	31.981	7.90
FHOD1	FH1/FH2 domain-containing protein 1	Q9Y613	4.336	1.45
FKBP3	Peptidyl-prolyl cis-trans isomerase FKBP3	Q00688	25.973	11.24
FN1	Fibronectin;Anastellin;Ugl-Y1;Ugl-Y2;Ugl-Y3	P02751	14.001	5.37
GLIPR2	Golgi-associated plant pathogenesis-related protein 1	Q9H4G4	0.266	0.14
GLS	Glutaminase kidney isoform, mitochondrial	O94925	0.236	0.08
GSTK1	Glutathione S-transferase kappa 1	Q9Y2Q3	3.789	0.76
GSTM2	Glutathione S-transferase Mu 2	P28161	12.256	3.23
H1F0	Histone H1.0	P07305	14.269	6.09
HMGB1	High mobility group protein B1	P09429	15.483	7.99
HNRNPR	Heterogeneous nuclear ribonucleoprotein R	O43390	6.550	1.27
HRC	Sarcoplasmic reticulum histidine-rich calcium-binding protein	P23327	3.003	0.62
HSD17B10	3-hydroxyacyl-CoA dehydrogenase type-2	Q99714	0.368	0.04

HSPA2	Heat shock-related 70 kDa protein 2	P54652	4.584	1.10
HSPB2	Heat shock protein beta-2	Q16082	5.175	1.85
IDH3G	Isocitrate dehydrogenase [NAD] subunit gamma, mitochondrial	P51553	0.191	0.09
IKBIP	Inhibitor of nuclear factor kappa-B kinase-interacting protein	Q70UQ0	6.037	1.52
ILK	Integrin-linked protein kinase	Q13418	0.449	0.16
ITGA7	Integrin alpha-7	Q13683	0.133	0.07
JPH1	Junctophilin-1	Q9HDC5	8.611	3.08
JSRP1	Junctional sarcoplasmic reticulum protein 1	Q96MG2	8.481	2.41
KIAA0090	Uncharacterized protein KIAA0090	Q8N766	34.524	11.84
LMO7	LIM domain only protein 7	Q8WWI1	0.084	0.04
MAGT1	Magnesium transporter protein 1	Q9H0U3	0.127	0.09
MAP4	Microtubule-associated protein 4	E7EVA0	3.428	0.79
MAPT	Microtubule-associated protein tau	P10636	6.510	1.84
MCU	Calcium uniporter protein, mitochondrial	Q8NE86	2.658	0.53
MTATP6	ATP synthase subunit a	P00846	0.294	0.03
MTCO3	Cytochrome c oxidase subunit 3	P00414	0.253	0.05
MVP	Major vault protein	Q14764	5.133	1.86
MYH1	Myosin-1	P12882	0.209	0.05
NACA	Nascent polypeptide-associated complex subunit alpha	E9PAV3	4.244	1.42
NAP1L4	Nucleosome assembly protein 1-like 4	Q99733	127.136	48.51
NEB	Nebulin	P20929	4.166	1.18
NIPSNAP1	Protein NipSnap homolog 1	Q9BPW8	6.864	2.69
NME1	Nucleoside diphosphate kinase A	Q32Q12	31.955	13.12
NME1-NME2	NME1-NME2 readthrough	J3KPD9	31.955	13.12
NME2	Nucleoside diphosphate kinase B	P22392	31.955	13.12
PA2G4	Proliferation-associated protein 2G4	Q9UQ80	2.757	0.44
PADI2	Protein-arginine deiminase type-2	Q9Y2J8	0.646	0.09
PBXIP1	Pre-B-cell leukemia transcription factor-interacting protein 1	Q96AQ6	2.025	0.43
PDIA4	Protein disulfide-isomerase A4	P13667	2.524	0.44
PDLIM5	PDZ and LIM domain protein 5	Q96HC4	3.139	0.56

PGD	6-phosphogluconate dehydrogenase, decarboxylating	P52209	4.370	1.58
PLOD1	Procollagen-lysine,2-oxoglutarate 5-dioxygenase 1	B4DR87	0.490	0.04
POR	NADPH--cytochrome P450 reductase	P16435	0.359	0.15
PRKAB2	5-AMP-activated protein kinase subunit beta-2	O43741	2.629	0.60
PRKAR2A	cAMP-dependent protein kinase type II-alpha regulatory subunit	P13861	3.597	0.88
PSMA1	Proteasome subunit alpha type-1	P25786	53.646	20.64
PSMC3	26S protease regulatory subunit 6A	P17980	3.605	1.14
PSMD11	26S proteasome non-ATPase regulatory subunit 11	O00231	5.877	2.23
PSMD14	26S proteasome non-ATPase regulatory subunit 14	O00487	6.075	2.15
PSMD2	26S proteasome non-ATPase regulatory subunit 2	Q13200	0.102	0.04
PSMD7	26S proteasome non-ATPase regulatory subunit 7	P51665	17.159	6.72
RCN3	Reticulocalbin-3	Q96D15	4.576	1.50
RPL13A	60S ribosomal protein L13a	P40429	0.243	0.07
RPL15	60S ribosomal protein L15;Ribosomal protein L15	P61313	0.285	0.09
RPL17	60S ribosomal protein L17	P18621	10.436	4.14
RPL29	60S ribosomal protein L29	P47914	5.407	1.94
RPL30	60S ribosomal protein L30	P62888	13.398	5.41
RPL5	60S ribosomal protein L5	P46777	24.588	9.30
RPS12	40S ribosomal protein S12	P25398	8.209	3.33
RPS5	40S ribosomal protein S5	P46782	28.112	10.70
RPS6	40S ribosomal protein S6	P62753	9.061	3.42
SCCPDH	Saccharopine dehydrogenase-like oxidoreductase	Q8NBX0	0.446	0.15
SEC11A	Signal peptidase complex catalytic subunit SEC11A	H0YK83	0.267	0.09
SEC23A	Protein transport protein Sec23A	Q15436	26.210	6.03
SEPT2	Septin-2	Q15019	15.183	6.14
SEPT7	Septin-7	Q16181	6.056	2.12
SFXN3	Sideroflexin-3	Q9BWM7	0.263	0.08
SLC12A2	Solute carrier family 12 member 2	P55011	0.088	0.04
SLC12A4	Solute carrier family 12 member 4	Q9UP95	0.299	0.10
SLC25A13	Calcium-binding mitochondrial carrier protein Aralar2	Q9UJS0	0.076	0.04

SLC25A5	ADP/ATP translocase 2	P05141	0.142	0.07
SPCS2	Signal peptidase complex subunit 2	E9PI68	0.204	0.13
SQRDL	Sulfide:quinone oxidoreductase, mitochondrial	Q9Y6N5	3.341	0.72
ST13	Hsc70-interacting protein	P50502	110.492	43.80
ST13P4	Putative protein FAM10A4	P50502	110.492	43.80
ST13P5	Putative protein FAM10A5	P50502	110.492	43.80
STOML2	Stomatin-like protein 2	Q9UJZ1	3.462	1.03
STT3A	Dolichyl-diphosphooligosaccharide--protein glycosyltransferase subunit STT3A	P46977	0.211	0.07
SUCLG1	Succinyl-CoA ligase [ADP/GDP-forming] subunit alpha, mitochondrial	P53597	0.243	0.07
SYNCRIP	Heterogeneous nuclear ribonucleoprotein Q	O60506	1.731	0.25
TCP1	T-complex protein 1 subunit alpha	P17987	0.026	0.00
TMOD3	Tropomodulin-3	Q9NYL9	0.024	0.01
TNNT3	Troponin T, fast skeletal muscle	P45378	5.713	1.74
TOR1A	Torsin-1A	O14656	0.205	0.08
TP53RK	TP53-regulating kinase	Q96S44	0.374	0.10
TPT1	Translationally-controlled tumor protein	Q5W0H4	33.050	13.45
TRAP1	Heat shock protein 75 kDa, mitochondrial	Q12931	0.639	0.09
TRIM72	Tripartite motif-containing protein 72	Q6ZMU5	5.590	1.93
UBA1	Ubiquitin-like modifier-activating enzyme 1	P22314	1.836	0.32
UGGT1	UDP-glucose:glycoprotein glucosyltransferase 1	Q9NYU2	0.106	0.06
VAPB	Vesicle-associated membrane protein-associated protein B/C	O95292	4.675	1.45
VDAC2	Voltage-dependent anion-selective channel protein 2	P45880	0.604	0.08
VIM	Vimentin	P08670	0.132	0.04
XIRP1	Xin actin-binding repeat-containing protein 1	Q702N8	0.165	0.02
YES1	Tyrosine-protein kinase Yes	J3QRU1	0.268	0.09
ZYX	Zyxin	Q15942	6.145	1.96

CHARTER 6. FUTURE WORK

Protein kinases and their interaction partners have been extensively studied due to the importance that kinases catalyze phosphorylation, which is one of the most critical protein post-translational modifications that mediated numerous molecular functions and biological processes. We successfully profiled the largest functional kinome (54 protein kinases) and kinome interactome (616 proteins) in human skeletal muscle using activity based enrichment probe and quantitative proteomics. The future work of this project would be validate the significantly changed protein kinases and their interaction partners by immunoblotting (i.e., western blots). Multiple protein identification and quantification techniques would robust the results and draw much stronger conclusions. In addition, comparing kinome and kinome interactome in type 2 diabetic patients to those in lean control and obese insulin resistant participants will offers insights into type 2 diabetes specific mechanisms.

REFERENCES

Abdul-Ghani, M. A., & DeFronzo, R. A. (2009). Pathophysiology of prediabetes. *Curr Diab Rep, 9*(3), 193-199. Retrieved from http://www.ncbi.nlm.nih.gov/entrez/query.fcgi?cmd=Retrieve&db=PubMed&dopt=Citation&list_uids=19490820

Acosta, J., Hettinga, J., Fluckiger, R., Krumrei, N., Goldfine, A., Angarita, L., & Halperin, J. (2000). Molecular basis for a link between complement and the vascular complications of diabetes. *Proc Natl Acad Sci U S A, 97*(10), 5450-5455. Retrieved from http://www.ncbi.nlm.nih.gov/pubmed/10805801

Aithal, H. N., Toback, F. G., & Cryst, C. (1980). Enhancement of renal medullary pyruvate kinase activity during cell proliferation induced by potassium depletion. *Am J Physiol, 238*(4), E377-383. Retrieved from http://www.ncbi.nlm.nih.gov/pubmed/7377296

Aldonza, M. B., Hong, J. Y., Bae, S. Y., Song, J., Kim, W. K., Oh, J., . . . Lee, S. K. (2015). Suppression of MAPK Signaling and Reversal of mTOR-Dependent MDR1-Associated Multidrug Resistance by 21alpha-Methylmelianodiol in Lung Cancer Cells. *PLoS One, 10*(6), e0127841. doi:10.1371/journal.pone.0127841

American Diabetes, A. (2012). Standards of medical care in diabetes--2012. *Diabetes Care, 35 Suppl 1*, S11-63. doi:10.2337/dc12-s011

Amin, R. M., Hiroshima, K., Miyagi, Y., Kokubo, T., Hoshi, K., Fujisawa, T., & Nakatani, Y. (2008). Role of the PI3K/Akt, mTOR, and STK11/LKB1 pathways in the tumorigenesis of sclerosing hemangioma of the lung. *Pathol Int, 58*(1), 38-44. doi:10.1111/j.1440-1827.2007.02186.x

Amiri, M., Conserva, F., Panayiotou, C., Karlsson, A., & Solaroli, N. (2013). The human adenylate kinase 9 is a nucleoside mono- and diphosphate kinase. *Int J Biochem Cell Biol, 45*(5), 925-931. doi:10.1016/j.biocel.2013.02.004

Ashburner, M., Ball, C. A., Blake, J. A., Botstein, D., Butler, H., Cherry, J. M., . . . Sherlock, G. (2000). Gene ontology: tool for the unification of biology. The Gene Ontology Consortium. *Nat Genet, 25*(1), 25-29. doi:10.1038/75556

Babchia, N., Calipel, A., Mouriaux, F., Faussat, A. M., & Mascarelli, F. (2010). The PI3K/Akt and mTOR/P70S6K signaling pathways in human uveal melanoma cells: interaction with B-Raf/ERK. *Invest Ophthalmol Vis Sci, 51*(1), 421-429. doi:10.1167/iovs.09-3974

Bae, J. H., & Schlessinger, J. (2010). Asymmetric tyrosine kinase arrangements in activation or autophosphorylation of receptor tyrosine kinases. *Mol Cells, 29*(5), 443-448. doi:10.1007/s10059-010-0080-5

Bandyopadhyay, G. K., Yu, J. G., Ofrecio, J., & Olefsky, J. M. (2005). Increased p85/55/50 expression and decreased phosphotidylinositol 3-kinase activity in insulin-resistant human skeletal muscle. *Diabetes, 54*(8), 2351-2359. Retrieved from http://www.ncbi.nlm.nih.gov/pubmed/16046301

Bandyopadhyay, G. K., Yu, J. G., Ofrecio, J., & Olefsky, J. M. (2006). Increased malonyl-CoA levels in muscle from obese and type 2 diabetic subjects lead to decreased fatty acid oxidation and increased lipogenesis; thiazolidinedione treatment reverses these defects. *Diabetes, 55*(8), 2277-2285. doi:10.2337/db06-0062

Barany, P. (2005). [Iron deficiency in renal anemia is difficult to diagnose. Evidence-based guidelines improve diagnosis and treatment]. *Lakartidningen, 102*(37), 2536-2537. Retrieved from http://www.ncbi.nlm.nih.gov/pubmed/16200898

Bauer, L., Kern, S., Rogacev, K. S., Emrich, I. E., Zawada, A., Fliser, D., . . . Marsche, G. (2017). HDL Cholesterol Efflux Capacity and Cardiovascular Events in Patients With Chronic Kidney Disease. *J Am Coll Cardiol, 69*(2), 246-247. doi:10.1016/j.jacc.2016.10.054

Behr, T. M., Berova, M., Doe, C. P., Ju, H., Angermann, C. E., Boehm, J., & Willette, R. N. (2003). p38 mitogen-activated protein kinase inhibitors for the treatment of chronic cardiovascular disease. *Curr Opin Investig Drugs, 4*(9), 1059-1064. Retrieved from http://www.ncbi.nlm.nih.gov/pubmed/14582449

Belfiore, F., Iannello, S., & Volpicelli, G. (1998). Insulin sensitivity indices calculated from basal and OGTT-induced insulin, glucose, and FFA levels. *Mol Genet Metab, 63*(2), 134-141. doi:10.1006/mgme.1997.2658

Biddinger, S. B., & Kahn, C. R. (2006). From mice to men: insights into the insulin resistance syndromes. *Annu Rev Physiol, 68*, 123-158. doi:10.1146/annurev.physiol.68.040104.124723

Bjornholm, M., & Zierath, J. R. (2005). Insulin signal transduction in human skeletal muscle: identifying the defects in Type II diabetes. *Biochem Soc Trans, 33*(Pt 2), 354-357. doi:10.1042/BST0330354

Bogyo, M., Verhelst, S., Bellingard-Dubouchaud, V., Toba, S., & Greenbaum, D. (2000). Selective targeting of lysosomal cysteine proteases with radiolabeled electrophilic substrate analogs. *Chem Biol, 7*(1), 27-38. Retrieved from http://www.ncbi.nlm.nih.gov/pubmed/10662686

Boon, M. R., Bakker, L. E., Haks, M. C., Quinten, E., Schaart, G., Van Beek, L., . . . Rensen, P. C. (2015). Short-term high-fat diet increases macrophage markers in skeletal muscle accompanied by impaired insulin signalling in healthy male subjects. *Clin Sci (Lond), 128*(2), 143-151. doi:10.1042/CS20140179

Burgering, B. M., & Coffer, P. J. (1995). Protein kinase B (c-Akt) in phosphatidylinositol-3-OH kinase signal transduction. *Nature, 376*(6541), 599-602. doi:10.1038/376599a0

Burnett, G., & Kennedy, E. P. (1954). The enzymatic phosphorylation of proteins. *J Biol Chem, 211*(2), 969-980. Retrieved from http://www.ncbi.nlm.nih.gov/pubmed/13221602

Cao, Y., & Giovannucci, E. (2016). Obesity and Prostate Cancer. *Recent Results Cancer Res, 208*, 137-153. doi:10.1007/978-3-319-42542-9_8

Carling, D., Zammit, V. A., & Hardie, D. G. (1987). A common bicyclic protein kinase cascade inactivates the regulatory enzymes of fatty acid and cholesterol biosynthesis. *FEBS Lett, 223*(2), 217-222. Retrieved from http://www.ncbi.nlm.nih.gov/pubmed/2889619

Caruso, M., Ma, D., Msallaty, Z., Lewis, M., Seyoum, B., Al-janabi, W., . . . Yi, Z. (2014). Increased interaction with insulin receptor substrate 1, a novel abnormality in insulin resistance and type 2 diabetes. *Diabetes, 63*(6), 1933-1947. doi:10.2337/db13-1872

Caruso, M., Ma, D., Msallaty, Z., Lewis, M., Seyoum, B., Al-janabi, W., . . . Yi, Z. (2014). Increased Interaction with Insulin Receptor Substrate-1, a Novel Abnormality in Insulin Resistance and Type 2 Diabetes. *Diabetes, 63*(6), 1933-1947. Retrieved from http://www.ncbi.nlm.nih.gov/pubmed/24584551

Caruso, M., Zhang, X., Ma, D., Yang, Z., Qi, Y., & Yi, Z. (2015). Novel Endogenous, Insulin-Stimulated Akt2 Protein Interaction Partners in L6 Myoblasts. *PLoS One, 10*(10), e0140255. doi:10.1371/journal.pone.0140255

Castellone, M. D., & Laukkanen, M. O. (2017). TGF-beta1, WNT, and SHH signaling in tumor progression and in fibrotic diseases. *Front Biosci (Schol*

Ed), 9, 31-45. Retrieved from http://www.ncbi.nlm.nih.gov/pubmed/27814572

Cazarin, J. M., Andrade, B. M., & Carvalho, D. P. (2014). AMP-activated protein kinase activation leads to lysome-mediated NA(+)/I(-)-symporter protein degradation in rat thyroid cells. *Horm Metab Res, 46*(5), 313-317. doi:10.1055/s-0034-1371803

Cerda, S. R., Mustafi, R., Little, H., Cohen, G., Khare, S., Moore, C., . . . Bissonnette, M. (2006). Protein kinase C delta inhibits Caco-2 cell proliferation by selective changes in cell cycle and cell death regulators. *Oncogene, 25*(22), 3123-3138. doi:10.1038/sj.onc.1209360

Cersosimo, E., MAndarino, L. J., & DeFronzo, R. A. (2011). Pathogenesis of Type 2 Diabetes Mellitus *Endocr Metab Immune Disord Drug Targets, Chapter 6*.

Chen, C. C., Lin, J. T., Cheng, Y. F., Kuo, C. Y., Huang, C. F., Kao, S. H., . . . Chen, H. M. (2014). Amelioration of LPS-induced inflammation response in microglia by AMPK activation. *Biomed Res Int, 2014*, 692061. doi:10.1155/2014/692061

Chen, S., Fisher, R. C., Signs, S., Molina, L. A., Shenoy, A. K., Lopez, M. C., . . . Huang, E. H. (2016). Inhibition of PI3K/Akt/mTOR signaling in PI3KR2-overexpressing colon cancer stem cells reduces tumor growth due to apoptosis. *Oncotarget*. doi:10.18632/oncotarget.9919

Chesney, J., Clark, J., Lanceta, L., Trent, J. O., & Telang, S. (2015). Targeting the sugar metabolism of tumors with a first-in-class 6-phosphofructo-2-kinase (PFKFB4) inhibitor. *Oncotarget, 6*(20), 18001-18011. doi:10.18632/oncotarget.4534

Cheung, C. H. Y., & Juan, H. F. (2017). Quantitative proteomics in lung cancer. *J Biomed Sci, 24*(1), 37. doi:10.1186/s12929-017-0343-y

Chiang, S. H., Bazuine, M., Lumeng, C. N., Geletka, L. M., Mowers, J., White, N. M., . . . Saltiel, A. R. (2009). The protein kinase IKKepsilon regulates energy balance in obese mice. *Cell, 138*(5), 961-975. doi:10.1016/j.cell.2009.06.046

Chihara-Nakashima, M., Hashimoto, E., & Nishizuka, Y. (1977). Intrinsic activity of guanosine 3',5'-monophosphate-dependent protein kinase similar to adenosine 3',5'-monophosphate-dependent protein kinase. II. Phosphorylation of ribosomal proteins. *J Biochem, 81*(6), 1863-1867. Retrieved from http://www.ncbi.nlm.nih.gov/pubmed/197070

Cho, H., Mu, J., Kim, J. K., Thorvaldsen, J. L., Chu, Q., Crenshaw, E. B., 3rd, . . . Birnbaum, M. J. (2001). Insulin resistance and a diabetes mellitus-like syndrome in mice lacking the protein kinase Akt2 (PKB beta). *Science, 292*(5522), 1728-1731. doi:10.1126/science.292.5522.1728

Cho, H., Thorvaldsen, J. L., Chu, Q., Feng, F., & Birnbaum, M. J. (2001). Akt1/PKBalpha is required for normal growth but dispensable for

maintenance of glucose homeostasis in mice. *J Biol Chem, 276*(42), 38349-38352. doi:10.1074/jbc.C100462200

Cohen, P. (1982). The role of protein phosphorylation in neural and hormonal control of cellular activity. *Nature, 296*(5858), 613-620. Retrieved from http://www.ncbi.nlm.nih.gov/pubmed/6280056

Copps, K. D., & White, M. F. (2012). Regulation of insulin sensitivity by serine/threonine phosphorylation of insulin receptor substrate proteins IRS1 and IRS2. *Diabetologia, 55*(10), 2565-2582. doi:10.1007/s00125-012-2644-8

Coughlan, K. A., Valentine, R. J., Ruderman, N. B., & Saha, A. K. (2013). Nutrient Excess in AMPK Downregulation and Insulin Resistance. *J Endocrinol Diabetes Obes, 1*(1), 1008. Retrieved from http://www.ncbi.nlm.nih.gov/pubmed/26120590

Cox, J., & Mann, M. (2008). MaxQuant enables high peptide identification rates, individualized p.p.b.-range mass accuracies and proteome-wide protein quantification. *Nat Biotechnol, 26*(12), 1367-1372. doi:10.1038/nbt.1511

Cox, J., Matic, I., Hilger, M., Nagaraj, N., Selbach, M., Olsen, J. V., & Mann, M. (2009). A practical guide to the MaxQuant computational platform for SILAC-based quantitative proteomics. *Nat Protoc, 4*(5), 698-705. doi:10.1038/nprot.2009.36

Croft, D., O'Kelly, G., Wu, G., Haw, R., Gillespie, M., Matthews, L., . . . Stein, L. (2011). Reactome: a database of reactions, pathways and biological

processes. *Nucleic Acids Res, 39*(Database issue), D691-697. doi:10.1093/nar/gkq1018

Cusi, K., Maezono, K., Osman, A., Pendergrass, M., Patti, M. E., Pratipanawatr, T., . . . Mandarino, L. J. (2000). Insulin resistance differentially affects the PI 3-kinase- and MAP kinase-mediated signaling in human muscle. *J Clin Invest, 105*(3), 311-320. doi:10.1172/JCI7535

Dabernat, S., Secrest, P., Peuchant, E., Moreau-Gaudry, F., Dubus, P., & Sarvetnick, N. (2009). Lack of beta-catenin in early life induces abnormal glucose homeostasis in mice. *Diabetologia, 52*(8), 1608-1617. doi:10.1007/s00125-009-1411-y

Deblon, N., Bourgoin, L., Veyrat-Durebex, C., Peyrou, M., Vinciguerra, M., Caillon, A., . . . Foti, M. (2012). Chronic mTOR inhibition by rapamycin induces muscle insulin resistance despite weight loss in rats. *Br J Pharmacol, 165*(7), 2325-2340. doi:10.1111/j.1476-5381.2011.01716.x

DeFronzo, R. A. (2004). Pathogenesis of type 2 diabetes mellitus. *Med Clin North Am, 88*(4), 787-835, ix. doi:10.1016/j.mcna.2004.04.013

DeFronzo, R. A., & Abdul-Ghani, M. (2011). Assessment and treatment of cardiovascular risk in prediabetes: impaired glucose tolerance and impaired fasting glucose. *Am J Cardiol, 108*(3 Suppl), 3B-24B. doi:S0002-9149(11)01214-8 [pii]

10.1016/j.amjcard.2011.03.013

DeFronzo, R. A., Tobin, J. D., & Andres, R. (1979). Glucose clamp technique: a method for quantifying insulin secretion and resistance. *Am J Physiol, 237*(3), E214-223. Retrieved from http://www.ncbi.nlm.nih.gov/pubmed/382871

Delcommenne, M., Tan, C., Gray, V., Rue, L., Woodgett, J., & Dedhar, S. (1998). Phosphoinositide-3-OH kinase-dependent regulation of glycogen synthase kinase 3 and protein kinase B/AKT by the integrin-linked kinase. *Proc Natl Acad Sci U S A, 95*(19), 11211-11216. Retrieved from http://www.ncbi.nlm.nih.gov/pubmed/9736715

Demagny, H., Araki, T., & De Robertis, E. M. (2014). The tumor suppressor Smad4/DPC4 is regulated by phosphorylations that integrate FGF, Wnt, and TGF-beta signaling. *Cell Rep, 9*(2), 688-700. doi:10.1016/j.celrep.2014.09.020

Diamond-Stanic, M. K., Marchionne, E. M., Teachey, M. K., Durazo, D. E., Kim, J. S., & Henriksen, E. J. (2011). Critical role of the transient activation of p38 MAPK in the etiology of skeletal muscle insulin resistance induced by low-level in vitro oxidant stress. *Biochem Biophys Res Commun, 405*(3), 439-444. doi:10.1016/j.bbrc.2011.01.049

Diamond, M. P., Jacob, R., Connolly-Diamond, M., & DeFronzo, R. A. (1993). Glucose metabolism during the menstrual cycle. Assessment with the euglycemic, hyperinsulinemic clamp. *J Reprod Med, 38*(6), 417-421. Retrieved from http://www.ncbi.nlm.nih.gov/pubmed/8331618

Doherty, M. K., Hammond, D. E., Clague, M. J., Gaskell, S. J., & Beynon, R. J. (2009). Turnover of the human proteome: determination of protein intracellular stability by dynamic SILAC. *J Proteome Res, 8*(1), 104-112. doi:10.1021/pr800641v

Dong, L. X., Sun, L. L., Zhang, X., Pan, L., Lian, L. J., Chen, Z., & Zhong, D. S. (2013). Negative regulation of mTOR activity by LKB1-AMPK signaling in non-small cell lung cancer cells. *Acta Pharmacol Sin, 34*(2), 314-318. doi:10.1038/aps.2012.143

Dormond-Meuwly, A., Roulin, D., Dufour, M., Benoit, M., Demartines, N., & Dormond, O. (2011). The inhibition of MAPK potentiates the anti-angiogenic efficacy of mTOR inhibitors. *Biochem Biophys Res Commun, 407*(4), 714-719. doi:10.1016/j.bbrc.2011.03.086

Duan, X., Kelsen, S. G., Clarkson, A. B., Jr., Ji, R., & Merali, S. (2010). SILAC analysis of oxidative stress-mediated proteins in human pneumocytes: new role for treacle. *Proteomics, 10*(11), 2165-2174. doi:10.1002/pmic.201000020

Dzamko, N., van Denderen, B. J., Hevener, A. L., Jorgensen, S. B., Honeyman, J., Galic, S., . . . Kemp, B. E. (2010). AMPK beta1 deletion reduces appetite, preventing obesity and hepatic insulin resistance. *J Biol Chem, 285*(1), 115-122. doi:10.1074/jbc.M109.056762

Ehyai, S., Dionyssiou, M. G., Gordon, J. W., Williams, D., Siu, K. W., & McDermott, J. C. (2015). A p38 Mitogen-Activated Protein Kinase-

Regulated Myocyte Enhancer Factor 2-beta-Catenin Interaction Enhances Canonical Wnt Signaling. *Mol Cell Biol, 36*(2), 330-346. doi:10.1128/MCB.00832-15

Elghazi, L., Gould, A. P., Weiss, A. J., Barker, D. J., Callaghan, J., Opland, D., . . . Bernal-Mizrachi, E. (2012). Importance of beta-Catenin in glucose and energy homeostasis. *Sci Rep, 2*, 693. doi:10.1038/srep00693

ElMokh, O., Ruffieux-Daidie, D., Roelli, M. A., Stooss, A., Phillips, W. A., Gertsch, J., . . . Charles, R. P. (2017). Combined MEK and Pi3'-kinase inhibition reveals synergy in targeting thyroid cancer in vitro and in vivo. *Oncotarget, 8*(15), 24604-24620. doi:10.18632/oncotarget.15599

Enomoto, A., Kido, N., Ito, M., Morita, A., Matsumoto, Y., Takamatsu, N., . . . Miyagawa, K. (2008). Negative regulation of MEKK1/2 signaling by serine-threonine kinase 38 (STK38). *Oncogene, 27*(13), 1930-1938. doi:10.1038/sj.onc.1210828

Farrar, C., Houser, C. R., & Clarke, S. (2005). Activation of the PI3K/Akt signal transduction pathway and increased levels of insulin receptor in protein repair-deficient mice. *Aging Cell, 4*(1), 1-12. doi:10.1111/j.1474-9728.2004.00136.x

Fink, L. N., Costford, S. R., Lee, Y. S., Jensen, T. E., Bilan, P. J., Oberbach, A., . . . Klip, A. (2014). Pro-inflammatory macrophages increase in skeletal muscle of high fat-fed mice and correlate with metabolic risk markers in humans. *Obesity (Silver Spring), 22*(3), 747-757. doi:10.1002/oby.20615

Fink, L. N., Oberbach, A., Costford, S. R., Chan, K. L., Sams, A., Bluher, M., & Klip, A. (2013). Expression of anti-inflammatory macrophage genes within skeletal muscle correlates with insulin sensitivity in human obesity and type 2 diabetes. *Diabetologia, 56*(7), 1623-1628. doi:10.1007/s00125-013-2897-x

Fontana, J. A., & Lovenberg, W. (1973). Pineal protein kinase: effect of enzymic phosphorylation on actinomycin D binding by, and template activity of, chromatin. *Proc Natl Acad Sci U S A, 70*(3), 755-758. Retrieved from http://www.ncbi.nlm.nih.gov/pubmed/4351803

Forcet, C., & Billaud, M. (2007). Dialogue between LKB1 and AMPK: a hot topic at the cellular pole. *Sci STKE, 2007*(404), pe51. doi:10.1126/stke.4042007pe51

Fujibayashi, K., Yokokawa, H., Gunji, T., Sasabe, N., Okumura, M., Iijima, K., . . . Fukuda, H. (2015). Utility of 75-g Oral Glucose Tolerance Test Results and Hemoglobin A1c Values for Predicting the Incidence of Diabetes Mellitus among Middle-aged Japanese Men -A Large-scale Retrospective Cohort Study Performed at a Single Hospital. *Intern Med, 54*(7), 717-723. doi:10.2169/internalmedicine.54.2839

Gabai, V. L., Mabuchi, K., Mosser, D. D., & Sherman, M. Y. (2002). Hsp72 and stress kinase c-jun N-terminal kinase regulate the bid-dependent pathway in tumor necrosis factor-induced apoptosis. *Mol Cell Biol, 22*(10), 3415-3424. Retrieved from http://www.ncbi.nlm.nih.gov/pubmed/11971973

Galli, C., Piemontese, M., Lumetti, S., Ravanetti, F., Macaluso, G. M., & Passeri, G. (2012). Actin cytoskeleton controls activation of Wnt/beta-catenin signaling in mesenchymal cells on implant surfaces with different topographies. *Acta Biomater, 8*(8), 2963-2968. doi:10.1016/j.actbio.2012.04.043

Gao, Y. F., Zhang, M. N., Wang, T. X., Wu, T. C., Ai, R. D., & Zhang, Z. S. (2016). Hypoglycemic effect of D-chiro-inositol in type 2 diabetes mellitus rats through the PI3K/Akt signaling pathway. *Mol Cell Endocrinol, 433*, 26-34. doi:10.1016/j.mce.2016.05.013

Garamvolgyi, Z., Prohaszka, Z., Rigo, J., Jr., Kecskemeti, A., & Molvarec, A. (2015). Increased circulating heat shock protein 70 (HSPA1A) levels in gestational diabetes mellitus: a pilot study. *Cell Stress Chaperones, 20*(4), 575-581. doi:10.1007/s12192-015-0579-y

Garcia-Jimenez, C., Garcia-Martinez, J. M., Chocarro-Calvo, A., & De la Vieja, A. (2014). A new link between diabetes and cancer: enhanced WNT/beta-catenin signaling by high glucose. *J Mol Endocrinol, 52*(1), R51-66. doi:10.1530/JME-13-0152

Gautam, S., Ishrat, N., Yadav, P., Singh, R., Narender, T., & Srivastava, A. K. (2016). 4-Hydroxyisoleucine attenuates the inflammation-mediated insulin resistance by the activation of AMPK and suppression of SOCS-3 coimmunoprecipitation with both the IR-beta subunit as well as IRS-1. *Mol Cell Biochem, 414*(1-2), 95-104. doi:10.1007/s11010-016-2662-9

Gauthier, M. S., O'Brien, E. L., Bigornia, S., Mott, M., Cacicedo, J. M., Xu, X. J., . . . Ruderman, N. (2011). Decreased AMP-activated protein kinase activity is associated with increased inflammation in visceral adipose tissue and with whole-body insulin resistance in morbidly obese humans. *Biochem Biophys Res Commun, 404*(1), 382-387. doi:10.1016/j.bbrc.2010.11.127

Gehrmann, M., Marienhagen, J., Eichholtz-Wirth, H., Fritz, E., Ellwart, J., Jaattela, M., . . . Multhoff, G. (2005). Dual function of membrane-bound heat shock protein 70 (Hsp70), Bag-4, and Hsp40: protection against radiation-induced effects and target structure for natural killer cells. *Cell Death Differ, 12*(1), 38-51. doi:10.1038/sj.cdd.4401510

Geiger, P. C., Wright, D. C., Han, D. H., & Holloszy, J. O. (2005). Activation of p38 MAP kinase enhances sensitivity of muscle glucose transport to insulin. *Am J Physiol Endocrinol Metab, 288*(4), E782-788. doi:10.1152/ajpendo.00477.2004

Geiger, T., Cox, J., Ostasiewicz, P., Wisniewski, J. R., & Mann, M. (2010). Super-SILAC mix for quantitative proteomics of human tumor tissue. *Nat Methods, 7*(5), 383-385. doi:10.1038/nmeth.1446

Gene Ontology, C. (2015). Gene Ontology Consortium: going forward. *Nucleic Acids Res, 43*(Database issue), D1049-1056. doi:10.1093/nar/gku1179

George, S., Rochford, J. J., Wolfrum, C., Gray, S. L., Schinner, S., Wilson, J. C., . . . Barroso, I. (2004). A family with severe insulin resistance and

diabetes due to a mutation in AKT2. *Science, 304*(5675), 1325-1328. doi:10.1126/science.1096706

Goodwin, P. J., & Chlebowski, R. T. (2016). Obesity and Cancer: Insights for Clinicians. *J Clin Oncol, 34*(35), 4197-4202. doi:10.1200/JCO.2016.70.5327

Green, C. J., Pedersen, M., Pedersen, B. K., & Scheele, C. (2011). Elevated NF-kappaB activation is conserved in human myocytes cultured from obese type 2 diabetic patients and attenuated by AMP-activated protein kinase. *Diabetes, 60*(11), 2810-2819. doi:10.2337/db11-0263

Greenbaum, D., Baruch, A., Hayrapetian, L., Darula, Z., Burlingame, A., Medzihradszky, K. F., & Bogyo, M. (2002). Chemical approaches for functionally probing the proteome. *Mol Cell Proteomics, 1*(1), 60-68. Retrieved from https://www.ncbi.nlm.nih.gov/pubmed/12096141

http://www.mcponline.org/content/1/1/60.full.pdf

Gregorich, Z. R., Chang, Y. H., & Ge, Y. (2014). Proteomics in heart failure: top-down or bottom-up? *Pflugers Arch, 466*(6), 1199-1209. doi:10.1007/s00424-014-1471-9

Guerrero-Zotano, A., Mayer, I. A., & Arteaga, C. L. (2016). PI3K/AKT/mTOR: role in breast cancer progression, drug resistance, and treatment. *Cancer Metastasis Rev, 35*(4), 515-524. doi:10.1007/s10555-016-9637-x

Guidotti, A., Kurosawa, A., Chuang, D. M., & Costa, E. (1975). Protein kinase activation as an early event in the trans-synaptic induction of tyrosine 3-

monooxygenase in adrenal medulla. *Proc Natl Acad Sci U S A, 72*(3), 1152-1156. Retrieved from http://www.ncbi.nlm.nih.gov/pubmed/236557

Han, D., Li, S. J., Zhu, Y. T., Liu, L., & Li, M. X. (2013). LKB1/AMPK/mTOR signaling pathway in non-small-cell lung cancer. *Asian Pac J Cancer Prev, 14*(7), 4033-4039. Retrieved from http://www.ncbi.nlm.nih.gov/pubmed/23991948

Han, J., Liang, H., Tian, D., Du, J., Wang, Q., Xi, P., . . . Li, Y. (2016). mTOR remains unchanged in diet-resistant (DR) rats despite impaired LKB1/AMPK cascade in adipose tissue. *Biochem Biophys Res Commun, 476*(4), 333-339. doi:10.1016/j.bbrc.2016.05.123

Hanks, S. K., & Hunter, T. (1995). Protein kinases 6. The eukaryotic protein kinase superfamily: kinase (catalytic) domain structure and classification. *FASEB J, 9*(8), 576-596. Retrieved from https://www.ncbi.nlm.nih.gov/pubmed/7768349

Hantschel, M., Pfister, K., Jordan, A., Scholz, R., Andreesen, R., Schmitz, G., . . . Multhoff, G. (2000). Hsp70 plasma membrane expression on primary tumor biopsy material and bone marrow of leukemic patients. *Cell Stress Chaperones, 5*(5), 438-442. Retrieved from http://www.ncbi.nlm.nih.gov/pubmed/11189449

Hantschel, O., & Superti-Furga, G. (2004). Regulation of the c-Abl and Bcr-Abl tyrosine kinases. *Nat Rev Mol Cell Biol, 5*(1), 33-44. doi:10.1038/nrm1280

Hardie, D. G. (2005). New roles for the LKB1-->AMPK pathway. *Curr Opin Cell Biol, 17*(2), 167-173. doi:10.1016/j.ceb.2005.01.006

Hatem-Vaquero, M., Griera, M., Garcia-Jerez, A., Luengo, A., Alvarez-Hernandez, J., Rubio-Garcia, J. A., . . . de Frutos, S. (2017). Peripheral insulin resistance in ILK-depleted mice by reduction of GLUT4 expression. *J Endocrinol*. doi:10.1530/JOE-16-0662

Hay, N., & Sonenberg, N. (2004). Upstream and downstream of mTOR. *Genes Dev, 18*(16), 1926-1945. doi:10.1101/gad.1212704

Hein, T. W., Xu, W., Xu, X., & Kuo, L. (2016). Acute and Chronic Hyperglycemia Elicit JIP1/JNK-Mediated Endothelial Vasodilator Dysfunction of Retinal Arterioles. *Invest Ophthalmol Vis Sci, 57*(10), 4333-4340. doi:10.1167/iovs.16-19990

Henstridge, D. C., Bruce, C. R., Pang, C. P., Lancaster, G. I., Allen, T. L., Estevez, E., . . . Febbraio, M. A. (2012). Skeletal muscle-specific overproduction of constitutively activated c-Jun N-terminal kinase (JNK) induces insulin resistance in mice. *Diabetologia, 55*(10), 2769-2778. doi:10.1007/s00125-012-2652-8

Hirosumi, J., Tuncman, G., Chang, L., Gorgun, C. Z., Uysal, K. T., Maeda, K., . . . Hotamisligil, G. S. (2002). A central role for JNK in obesity and insulin resistance. *Nature, 420*(6913), 333-336. doi:10.1038/nature01137

Hotamisligil, G. S. (2006). Inflammation and metabolic disorders. *Nature, 444*(7121), 860-867. doi:10.1038/nature05485

Hou, T., Tieu, B. C., Ray, S., Recinos Iii, A., Cui, R., Tilton, R. G., & Brasier, A. R. (2008). Roles of IL-6-gp130 Signaling in Vascular Inflammation. *Curr Cardiol Rev, 4*(3), 179-192. doi:10.2174/157340308785160570

Houten, S. M., & Wanders, R. J. (2010). A general introduction to the biochemistry of mitochondrial fatty acid beta-oxidation. *J Inherit Metab Dis, 33*(5), 469-477. doi:10.1007/s10545-010-9061-2

Huang da, W., Sherman, B. T., & Lempicki, R. A. (2009). Systematic and integrative analysis of large gene lists using DAVID bioinformatics resources. *Nat Protoc, 4*(1), 44-57. doi:10.1038/nprot.2008.211

Huang, D. W., Sherman, B. T., Tan, Q., Kir, J., Liu, D., Bryant, D., . . . Lempicki, R. A. (2007). DAVID Bioinformatics Resources: expanded annotation database and novel algorithms to better extract biology from large gene lists. *Nucleic Acids Res, 35*(Web Server issue), W169-175. doi:10.1093/nar/gkm415

Husain, S. S., Szabo, I. L., Pai, R., Soreghan, B., Jones, M. K., & Tarnawski, A. S. (2001). MAPK (ERK2) kinase--a key target for NSAIDs-induced inhibition of gastric cancer cell proliferation and growth. *Life Sci, 69*(25-26), 3045-3054. Retrieved from http://www.ncbi.nlm.nih.gov/pubmed/11758830

Insel, P. A., Bourne, H. R., Coffino, P., & Tomkins, G. M. (1975). Cyclic AMP-dependent protein kinase: pivotal role in regulation of enzyme induction

and growth. *Science, 190*(4217), 896-898. Retrieved from http://www.ncbi.nlm.nih.gov/pubmed/171770

Jardim, D. P., Poco, P. C. E., & Campos, A. H. (2017). Dact1, a Wnt-Pathway Inhibitor, Mediates Human Mesangial Cell TGF-beta1-Induced Apoptosis. *J Cell Physiol, 232*(8), 2104-2111. doi:10.1002/jcp.25636

Jimenez-Marin, A., Collado-Romero, M., Ramirez-Boo, M., Arce, C., & Garrido, J. J. (2009). Biological pathway analysis by ArrayUnlock and Ingenuity Pathway Analysis. *BMC Proc, 3 Suppl 4*, S6. doi:10.1186/1753-6561-3-S4-S6

Kahn, B. B., & Flier, J. S. (2000). Obesity and insulin resistance. *J Clin Invest, 106*(4), 473-481. doi:10.1172/JCI10842

Kahn, M. (2015). Wnt Signaling in Stem Cells and Tumor Stem Cells. *Semin Reprod Med, 33*(5), 317-325. doi:10.1055/s-0035-1558404

Kanehisa, M., & Goto, S. (2000). KEGG: kyoto encyclopedia of genes and genomes. *Nucleic Acids Res, 28*(1), 27-30. Retrieved from http://www.ncbi.nlm.nih.gov/pubmed/10592173

Kang, L., Mokshagundam, S., Reuter, B., Lark, D. S., Sneddon, C. C., Hennayake, C., . . . Wasserman, D. H. (2016). Integrin-Linked Kinase in Muscle Is Necessary for the Development of Insulin Resistance in Diet-Induced Obese Mice. *Diabetes, 65*(6), 1590-1600. doi:10.2337/db15-1434

Karczewska-Kupczewska, M., Stefanowicz, M., Matulewicz, N., Nikolajuk, A., & Straczkowski, M. (2016). Wnt Signaling Genes in Adipose Tissue and

Skeletal Muscle of Humans With Different Degrees of Insulin Sensitivity. *J Clin Endocrinol Metab, 101*(8), 3079-3087. doi:10.1210/jc.2016-1594

Khalil, H. (2016). Diabetes microvascular complications-A clinical update. *Diabetes Metab Syndr*. doi:10.1016/j.dsx.2016.12.022

Khan, I. M., Perrard, X. Y., Brunner, G., Lui, H., Sparks, L. M., Smith, S. R., . . . Ballantyne, C. M. (2015). Intermuscular and perimuscular fat expansion in obesity correlates with skeletal muscle T cell and macrophage infiltration and insulin resistance. *Int J Obes (Lond), 39*(11), 1607-1618. doi:10.1038/ijo.2015.104

Kim, A., Nam, Y. J., Shin, Y. K., Lee, M. S., Sohn, D. S., & Lee, C. S. (2017). Rotundarpene inhibits TNF-alpha-induced activation of the Akt, mTOR, and NF-kappaB pathways, and the JNK and p38 associated with production of reactive oxygen species. *Mol Cell Biochem*. doi:10.1007/s11010-017-3041-x

Kim, C., Cheng, C. Y., Saldanha, S. A., & Taylor, S. S. (2007). PKA-I holoenzyme structure reveals a mechanism for cAMP-dependent activation. *Cell, 130*(6), 1032-1043. doi:10.1016/j.cell.2007.07.018

Kinoshita, T., Doi, K., Sugiyama, H., Kinoshita, S., Wada, M., Naruto, S., & Tomonaga, A. (2011). Knowledge-based identification of the ERK2/STAT3 signal pathway as a therapeutic target for type 2 diabetes and drug discovery. *Chem Biol Drug Des, 78*(3), 471-476. doi:10.1111/j.1747-0285.2011.01151.x

Kleinert, M., Sylow, L., Fazakerley, D. J., Krycer, J. R., Thomas, K. C., Oxboll, A. J., . . . Richter, E. A. (2014). Acute mTOR inhibition induces insulin resistance and alters substrate utilization in vivo. *Mol Metab, 3*(6), 630-641. doi:10.1016/j.molmet.2014.06.004

Knox, C., Law, V., Jewison, T., Liu, P., Ly, S., Frolkis, A., . . . Wishart, D. S. (2011). DrugBank 3.0: a comprehensive resource for 'omics' research on drugs. *Nucleic Acids Res, 39*(Database issue), D1035-1041. doi:10.1093/nar/gkq1126

Kornev, A. P., Haste, N. M., Taylor, S. S., & Eyck, L. F. (2006). Surface comparison of active and inactive protein kinases identifies a conserved activation mechanism. *Proc Natl Acad Sci U S A, 103*(47), 17783-17788. doi:10.1073/pnas.0607656103

Kramer, A., Green, J., Pollard, J., Jr., & Tugendreich, S. (2014). Causal analysis approaches in Ingenuity Pathway Analysis. *Bioinformatics, 30*(4), 523-530. doi:10.1093/bioinformatics/btt703

Krook, A., Bjornholm, M., Galuska, D., Jiang, X. J., Fahlman, R., Myers, M. G., Jr., . . . Zierath, J. R. (2000). Characterization of signal transduction and glucose transport in skeletal muscle from type 2 diabetic patients. *Diabetes, 49*(2), 284-292. Retrieved from http://www.ncbi.nlm.nih.gov/pubmed/10868945

Kubota, T., Kubota, N., & Kadowaki, T. (2017). Imbalanced Insulin Actions in Obesity and Type 2 Diabetes: Key Mouse Models of Insulin Signaling Pathway. *Cell Metab, 25*(4), 797-810. doi:10.1016/j.cmet.2017.03.004

Kume, S., Kondo, M., Maeda, S., Nishio, Y., Yanagimachi, T., Fujita, Y., . . . Maegawa, H. (2016). Hypothalamic AMP-Activated Protein Kinase Regulates Biphasic Insulin Secretion from Pancreatic ? Cells during Fasting and in Type 2 Diabetes. *EBioMedicine, 13*, 168-180. doi:10.1016/j.ebiom.2016.10.038

Kuninaka, S., Iida, S. I., Hara, T., Nomura, M., Naoe, H., Morisaki, T., . . . Saya, H. (2007). Serine protease Omi/HtrA2 targets WARTS kinase to control cell proliferation. *Oncogene, 26*(17), 2395-2406. doi:10.1038/sj.onc.1210042

Lackey, D. E., & Olefsky, J. M. (2016). Regulation of metabolism by the innate immune system. *Nat Rev Endocrinol, 12*(1), 15-28. doi:10.1038/nrendo.2015.189

Landau, D., Eshet, R., Troib, A., Gurman, Y., Chen, Y., Rabkin, R., & Segev, Y. (2009). Increased renal Akt/mTOR and MAPK signaling in type I diabetes in the absence of IGF type 1 receptor activation. *Endocrine, 36*(1), 126-134. doi:10.1007/s12020-009-9190-2

Langlais, P., Yi, Z., Finlayson, J., Luo, M., Mapes, R., De Filippis, E., . . . Mandarino, L. J. (2011). Global IRS-1 phosphorylation analysis in insulin

resistance. *Diabetologia, 54*(11), 2878-2889. doi:10.1007/s00125-011-2271-9

Law, V., Knox, C., Djoumbou, Y., Jewison, T., Guo, A. C., Liu, Y., . . . Wishart, D. S. (2014). DrugBank 4.0: shedding new light on drug metabolism. *Nucleic Acids Res, 42*(Database issue), D1091-1097. doi:10.1093/nar/gkt1068

Li, M., Zheng, C., Xu, H., He, W., Ruan, Y., Ma, J., . . . Li, W. (2017). Inhibition of AMPK-related kinase 5 (ARK5) enhances cisplatin cytotoxicity in non-small cell lung cancer cells through regulation of epithelial-mesenchymal transition. *Am J Transl Res, 9*(4), 1708-1719. Retrieved from http://www.ncbi.nlm.nih.gov/pubmed/28469776

Li, W., Qiu, X., Jiang, H., Zhi, Y., Fu, J., & Liu, J. (2015). Ulinastatin inhibits the inflammation of LPS-induced acute lung injury in mice via regulation of AMPK/NF-kappaB pathway. *Int Immunopharmacol, 29*(2), 560-567. doi:10.1016/j.intimp.2015.09.028

Li, X. W., Tuergan, M., & Abulizi, G. (2015). Expression of MAPK1 in cervical cancer and effect of MAPK1 gene silencing on epithelial-mesenchymal transition, invasion and metastasis. *Asian Pac J Trop Med, 8*(11), 937-943. doi:10.1016/j.apjtm.2015.10.004

Liong, S., & Lappas, M. (2015). Activation of AMPK improves inflammation and insulin resistance in adipose tissue and skeletal muscle from pregnant women. *J Physiol Biochem, 71*(4), 703-717. doi:10.1007/s13105-015-0435-7

Lipton, J. O., & Sahin, M. (2014). The neurology of mTOR. *Neuron, 84*(2), 275-291. doi:10.1016/j.neuron.2014.09.034

Liu, H., Yan, Z. Q., Li, B., Yin, S. Y., Sun, Q., Kou, J. J., . . . Liu, S. L. (2014). Reduced expression of SOX7 in ovarian cancer: a novel tumor suppressor through the Wnt/beta-catenin signaling pathway. *J Ovarian Res, 7*, 87. doi:10.1186/s13048-014-0087-1

Liu, W., Chang, J., Liu, M., Yuan, J., Zhang, J., Qin, J., . . . Wang, Y. (2017). Quantitative proteomics profiling reveals activation of mTOR pathway in trastuzumab resistance. *Oncotarget*. doi:10.18632/oncotarget.17415

Liu, X. M., Liu, Y. J., Zhan, J., & He, Q. Q. (2015). Overweight, obesity and risk of all-cause and cardiovascular mortality in patients with type 2 diabetes mellitus: a dose-response meta-analysis of prospective cohort studies. *Eur J Epidemiol, 30*(1), 35-45. doi:10.1007/s10654-014-9973-5

Liu, Y., Patricelli, M. P., & Cravatt, B. F. (1999). Activity-based protein profiling: the serine hydrolases. *Proc Natl Acad Sci U S A, 96*(26), 14694-14699. Retrieved from https://www.ncbi.nlm.nih.gov/pubmed/10611275

https://www.ncbi.nlm.nih.gov/pmc/articles/PMC24710/pdf/pq014694.pdf

Lu, Z., Liu, D., Hornia, A., Devonish, W., Pagano, M., & Foster, D. A. (1998). Activation of protein kinase C triggers its ubiquitination and degradation. *Mol Cell Biol, 18*(2), 839-845. Retrieved from http://www.ncbi.nlm.nih.gov/pubmed/9447980

Lumeng, C. N., & Saltiel, A. R. (2011). Inflammatory links between obesity and metabolic disease. *J Clin Invest, 121*(6), 2111-2117. doi:10.1172/JCI57132

Lustbader, J. W., & Pollak, S. (1991). A method for assessing the reassembly of a multisubunit glycoprotein by western blotting. *Anal Biochem, 192*(1), 39-43. Retrieved from https://www.ncbi.nlm.nih.gov/pubmed/2048731

Ma, H., Deacon, S., & Horiuchi, K. (2008). The challenge of selecting protein kinase assays for lead discovery optimization. *Expert Opin Drug Discov, 3*(6), 607-621. doi:10.1517/17460441.3.6.607

Ma, Y., Wu, D., Zhang, W., Liu, J., Chen, S., & Hua, B. (2015). Investigation of PI3K/PKB/mTOR/S6K1 signaling pathway in relationship of type 2 diabetes and Alzheimer's disease. *Int J Clin Exp Med, 8*(10), 18581-18590. Retrieved from http://www.ncbi.nlm.nih.gov/pubmed/26770471

Mackenzie, R. W., & Elliott, B. T. (2014). Akt/PKB activation and insulin signaling: a novel insulin signaling pathway in the treatment of type 2 diabetes. *Diabetes Metab Syndr Obes, 7*, 55-64. doi:10.2147/DMSO.S48260

Maeda, M., Kato, S., Fukushima, S., Kaneyuki, U., Fujii, T., Kazanietz, M. G., . . . Shigemori, M. (2006). Regulation of vascular smooth muscle proliferation and migration by beta2-chimaerin, a non-protein kinase C phorbol ester receptor. *Int J Mol Med, 17*(4), 559-566. Retrieved from https://www.ncbi.nlm.nih.gov/pubmed/16525710

Makarov, A. (2000). Electrostatic axially harmonic orbital trapping: a high-performance technique of mass analysis. *Anal Chem, 72*(6), 1156-1162. Retrieved from https://www.ncbi.nlm.nih.gov/pubmed/10740853

Manna, P., & Jain, S. K. (2013). L-cysteine and hydrogen sulfide increase PIP3 and AMPK/PPARgamma expression and decrease ROS and vascular inflammation markers in high glucose treated human U937 monocytes. *J Cell Biochem, 114*(10), 2334-2345. doi:10.1002/jcb.24578

Manning, G., Whyte, D. B., Martinez, R., Hunter, T., & Sudarsanam, S. (2002). The protein kinase complement of the human genome. *Science, 298*(5600), 1912-1934. doi:10.1126/science.1075762

March, H. N., & Winton, D. J. (2011). mTOR regulation by JNK: rescuing the starving intestinal cancer cell? *Gastroenterology, 140*(5), 1387-1391. doi:10.1053/j.gastro.2011.03.027

Marin, M. T., Dasari, P. S., Tryggestad, J. B., Aston, C. E., Teague, A. M., & Short, K. R. (2015). Oxidized HDL and LDL in adolescents with type 2 diabetes compared to normal weight and obese peers. *J Diabetes Complications, 29*(5), 679-685. doi:10.1016/j.jdiacomp.2015.03.015

Martini, M., De Santis, M. C., Braccini, L., Gulluni, F., & Hirsch, E. (2014). PI3K/AKT signaling pathway and cancer: an updated review. *Ann Med, 46*(6), 372-383. doi:10.3109/07853890.2014.912836

Mayne, J., Ning, Z., Zhang, X., Starr, A. E., Chen, R., Deeke, S., . . . Figeys, D. (2016). Bottom-Up Proteomics (2013-2015): Keeping up in the Era of

Systems Biology. *Anal Chem, 88*(1), 95-121. doi:10.1021/acs.analchem.5b04230

McCormack, T., Dent, R., & Blagden, M. (2016). Very low LDL-C levels may safely provide additional clinical cardiovascular benefit: the evidence to date. *Int J Clin Pract, 70*(11), 886-897. doi:10.1111/ijcp.12881

McGee, S. L., Howlett, K. F., Starkie, R. L., Cameron-Smith, D., Kemp, B. E., & Hargreaves, M. (2003). Exercise increases nuclear AMPK alpha2 in human skeletal muscle. *Diabetes, 52*(4), 926-928. Retrieved from http://www.ncbi.nlm.nih.gov/pubmed/12663462

McNelis, J. C., & Olefsky, J. M. (2014). Macrophages, immunity, and metabolic disease. *Immunity, 41*(1), 36-48. doi:10.1016/j.immuni.2014.05.010

Mi, H., Huang, X., Muruganujan, A., Tang, H., Mills, C., Kang, D., & Thomas, P. D. (2017). PANTHER version 11: expanded annotation data from Gene Ontology and Reactome pathways, and data analysis tool enhancements. *Nucleic Acids Res, 45*(D1), D183-D189. doi:10.1093/nar/gkw1138

Mi, H., Lazareva-Ulitsky, B., Loo, R., Kejariwal, A., Vandergriff, J., Rabkin, S., . . . Thomas, P. D. (2005). The PANTHER database of protein families, subfamilies, functions and pathways. *Nucleic Acids Res, 33*(Database issue), D284-288. doi:10.1093/nar/gki078

Minde, D. P., Anvarian, Z., Rudiger, S. G., & Maurice, M. M. (2011). Messing up disorder: how do missense mutations in the tumor suppressor protein APC lead to cancer? *Mol Cancer, 10*, 101. doi:10.1186/1476-4598-10-101

Minde, D. P., Radli, M., Forneris, F., Maurice, M. M., & Rudiger, S. G. (2013). Large extent of disorder in Adenomatous Polyposis Coli offers a strategy to guard Wnt signalling against point mutations. *PLoS One, 8*(10), e77257. doi:10.1371/journal.pone.0077257

Mizuguchi, J., Nakabayashi, H., Yoshida, Y., Huang, K. P., Uchida, T., Sasaki, T., . . . Suzuki, K. (1988). Increased degradation of protein kinase C without diminution of mRNA level after treatment of WEHI-231 B lymphoma cells with phorbol esters. *Biochem Biophys Res Commun, 155*(3), 1311-1317. Retrieved from http://www.ncbi.nlm.nih.gov/pubmed/3263124

Monetti, M., Nagaraj, N., Sharma, K., & Mann, M. (2011). Large-scale phosphosite quantification in tissues by a spike-in SILAC method. *Nat Methods, 8*(8), 655-658. doi:10.1038/nmeth.1647

Morino, K., Petersen, K. F., Dufour, S., Befroy, D., Frattini, J., Shatzkes, N., . . . Shulman, G. I. (2005). Reduced mitochondrial density and increased IRS-1 serine phosphorylation in muscle of insulin-resistant offspring of type 2 diabetic parents. *J Clin Invest, 115*(12), 3587-3593. doi:10.1172/JCI25151

Morrow, K. A., Das, S., Meng, E., Menezes, M. E., Bailey, S. K., Metge, B. J., . . . Shevde, L. A. (2016). Loss of tumor suppressor Merlin results in aberrant activation of Wnt/beta-catenin signaling in cancer. *Oncotarget, 7*(14), 17991-18005. doi:10.18632/oncotarget.7494

Moxey, P. W., Gogalniceanu, P., Hinchliffe, R. J., Loftus, I. M., Jones, K. J., Thompson, M. M., & Holt, P. J. (2011). Lower extremity amputations--a review of global variability in incidence. *Diabet Med, 28*(10), 1144-1153. doi:10.1111/j.1464-5491.2011.03279.x

Nagashima, H., Okada, M., Hidai, C., Hosoda, S., Kasanuki, H., & Kawana, M. (1997). The role of cadherin-catenin-cytoskeleton complex in angiogenesis: antisense oligonucleotide of plakoglobin promotes angiogenesis in vitro, and protein kinase C (PKC) enhances angiogenesis through the plakoglobin signaling pathway. *Heart Vessels, Suppl 12*, 110-112. Retrieved from http://www.ncbi.nlm.nih.gov/pubmed/9476558

Nakhjavani, M., Morteza, A., Khajeali, L., Esteghamati, A., Khalilzadeh, O., Asgarani, F., & Outeiro, T. F. (2010). Increased serum HSP70 levels are associated with the duration of diabetes. *Cell Stress Chaperones, 15*(6), 959-964. doi:10.1007/s12192-010-0204-z

Neubert, T. A., & Tempst, P. (2010). Super-SILAC for tumors and tissues. *Nat Methods, 7*(5), 361-362. doi:10.1038/nmeth0510-361

Neuhauser, N., Michalski, A., Cox, J., & Mann, M. (2012). Expert system for computer-assisted annotation of MS/MS spectra. *Mol Cell Proteomics, 11*(11), 1500-1509. doi:10.1074/mcp.M112.020271

Noberini, R., & Bonaldi, T. (2017). A Super-SILAC Strategy for the Accurate and Multiplexed Profiling of Histone Posttranslational Modifications. *Methods Enzymol, 586*, 311-332. doi:10.1016/bs.mie.2016.09.036

Numata, T., Araya, J., Fujii, S., Hara, H., Takasaka, N., Kojima, J., . . . Kuwano, K. (2011). Insulin-dependent phosphatidylinositol 3-kinase/Akt and ERK signaling pathways inhibit TLR3-mediated human bronchial epithelial cell apoptosis. *J Immunol, 187*(1), 510-519. doi:10.4049/jimmunol.1004218

Nunez, C., Bauman, A., Egger, S., Sitas, F., & Nair-Shalliker, V. (2017). Obesity, physical activity and cancer risks: Results from the Cancer, Lifestyle and Evaluation of Risk Study (CLEAR). *Cancer Epidemiol, 47*, 56-63. doi:10.1016/j.canep.2017.01.002

O'Connor, C. M., Gard, D. L., & Lazarides, E. (1981). Phosphorylation of intermediate filament proteins by cAMP-dependent protein kinases. *Cell, 23*(1), 135-143. Retrieved from http://www.ncbi.nlm.nih.gov/pubmed/6260370

Ogata, H., Goto, S., Sato, K., Fujibuchi, W., Bono, H., & Kanehisa, M. (1999). KEGG: Kyoto Encyclopedia of Genes and Genomes. *Nucleic Acids Res, 27*(1), 29-34. Retrieved from http://www.ncbi.nlm.nih.gov/pubmed/9847135

Ohishi, K., Toume, K., Arai, M. A., Koyano, T., Kowithayakorn, T., Mizoguchi, T., . . . Ishibashi, M. (2015). 9-Hydroxycanthin-6-one, a beta-Carboline Alkaloid from Eurycoma longifolia, Is the First Wnt Signal Inhibitor through Activation of Glycogen Synthase Kinase 3beta without Depending on Casein Kinase 1alpha. *J Nat Prod, 78*(5), 1139-1146. doi:10.1021/acs.jnatprod.5b00153

Ohta, M., Fujinami, A., Kobayashi, N., Amano, A., Ishigami, A., Tokuda, H., . . . Obayashi, H. (2015). Two chalcones, 4-hydroxyderricin and xanthoangelol, stimulate GLUT4-dependent glucose uptake through the LKB1/AMP-activated protein kinase signaling pathway in 3T3-L1 adipocytes. *Nutr Res, 35*(7), 618-625. doi:10.1016/j.nutres.2015.05.010

Okerberg, E. S., Hainley, A., Brown, H., Aban, A., Alemayehu, S., Shih, A., . . . Rosenblum, J. S. (2016). Identification of a Tumor Specific, Active-Site Mutation in Casein Kinase 1alpha by Chemical Proteomics. *PLoS One, 11*(3), e0152934. doi:10.1371/journal.pone.0152934

Okerberg, E. S., Wu, J., Zhang, B., Samii, B., Blackford, K., Winn, D. T., . . . Patricelli, M. P. (2005). High-resolution functional proteomics by active-site peptide profiling. *Proc Natl Acad Sci U S A, 102*(14), 4996-5001. doi:10.1073/pnas.0501205102

Okkenhaug, K. (2013). Signaling by the phosphoinositide 3-kinase family in immune cells. *Annu Rev Immunol, 31*, 675-704. doi:10.1146/annurev-immunol-032712-095946

Ortega, F. B., Lavie, C. J., & Blair, S. N. (2016). Obesity and Cardiovascular Disease. *Circ Res, 118*(11), 1752-1770. doi:10.1161/CIRCRESAHA.115.306883

Osborn, O., & Olefsky, J. M. (2012). The cellular and signaling networks linking the immune system and metabolism in disease. *Nat Med, 18*(3), 363-374. doi:10.1038/nm.2627

Otani, H., Erdos, M., & Leonard, W. J. (1993). Tyrosine kinase(s) regulate apoptosis and bcl-2 expression in a growth factor-dependent cell line. *J Biol Chem, 268*(30), 22733-22736. Retrieved from http://www.ncbi.nlm.nih.gov/pubmed/8226783

Oudit, G. Y., Sun, H., Kerfant, B. G., Crackower, M. A., Penninger, J. M., & Backx, P. H. (2004). The role of phosphoinositide-3 kinase and PTEN in cardiovascular physiology and disease. *J Mol Cell Cardiol, 37*(2), 449-471. doi:10.1016/j.yjmcc.2004.05.015

Pagetta, A., Folda, A., Brunati, A. M., & Finotti, P. (2003). Identification and purification from the plasma of Type 1 diabetic subjects of a proteolytically active Grp94Evidence that Grp94 is entirely responsible for plasma proteolytic activity. *Diabetologia, 46*(7), 996-1006. doi:10.1007/s00125-003-1133-5

Papatheodorou, K., Papanas, N., Banach, M., Papazoglou, D., & Edmonds, M. (2016). Complications of Diabetes 2016. *J Diabetes Res, 2016*, 6989453. doi:10.1155/2016/6989453

Patricelli, M. P., Nomanbhoy, T. K., Wu, J., Brown, H., Zhou, D., Zhang, J., . . . Kozarich, J. W. (2011). In situ kinase profiling reveals functionally relevant properties of native kinases. *Chem Biol, 18*(6), 699-710. doi:10.1016/j.chembiol.2011.04.011

Patricelli, M. P., Szardenings, A. K., Liyanage, M., Nomanbhoy, T. K., Wu, M., Weissig, H., . . . Kozarich, J. W. (2007). Functional interrogation of the

kinome using nucleotide acyl phosphates. *Biochemistry, 46*(2), 350-358. doi:10.1021/bi062142x

Patsouris, D., Cao, J. J., Vial, G., Bravard, A., Lefai, E., Durand, A., . . . Rieusset, J. (2014). Insulin resistance is associated with MCP1-mediated macrophage accumulation in skeletal muscle in mice and humans. *PLoS One, 9*(10), e110653. doi:10.1371/journal.pone.0110653

Pelaia, G., Gallelli, L., D'Agostino, B., Vatrella, A., Cuda, G., Fratto, D., . . . Marsico, S. A. (2007). Effects of TGF-beta and glucocorticoids on map kinase phosphorylation, IL-6/IL-11 secretion and cell proliferation in primary cultures of human lung fibroblasts. *J Cell Physiol, 210*(2), 489-497. doi:10.1002/jcp.20884

Phillips, D., Aponte, A. M., Covian, R., & Balaban, R. S. (2011). Intrinsic protein kinase activity in mitochondrial oxidative phosphorylation complexes. *Biochemistry, 50*(13), 2515-2529. doi:10.1021/bi101434x

Pockley, A. G., Henderson, B., & Multhoff, G. (2014). Extracellular cell stress proteins as biomarkers of human disease. *Biochem Soc Trans, 42*(6), 1744-1751. doi:10.1042/BST20140205

Porte, D., Jr., & Schwartz, M. W. (1996). Diabetes complications: why is glucose potentially toxic? *Science, 272*(5262), 699-700. Retrieved from http://www.ncbi.nlm.nih.gov/pubmed/8614830

Pozniak, Y., & Geiger, T. (2014). Design and application of super-SILAC for proteome quantification. *Methods Mol Biol, 1188*, 281-291. doi:10.1007/978-1-4939-1142-4_20

Prada, P. O., & Saad, M. J. (2013). Tyrosine kinase inhibitors as novel drugs for the treatment of diabetes. *Expert Opin Investig Drugs, 22*(6), 751-763. doi:10.1517/13543784.2013.802768

Puigserver, P., Rhee, J., Donovan, J., Walkey, C. J., Yoon, J. C., Oriente, F., . . . Spiegelman, B. M. (2003). Insulin-regulated hepatic gluconeogenesis through FOXO1-PGC-1alpha interaction. *Nature, 423*(6939), 550-555. doi:10.1038/nature01667

Qi, J., Gong, J., Zhao, T., Zhao, J., Lam, P., Ye, J., . . . Li, P. (2008). Downregulation of AMP-activated protein kinase by Cidea-mediated ubiquitination and degradation in brown adipose tissue. *EMBO J, 27*(11), 1537-1548. doi:10.1038/emboj.2008.92

Rask-Madsen, C., & Kahn, C. R. (2012). Tissue-specific insulin signaling, metabolic syndrome, and cardiovascular disease. *Arterioscler Thromb Vasc Biol, 32*(9), 2052-2059. doi:32/9/2052 [pii]

10.1161/ATVBAHA.111.241919

Reno, T. A., Tong, S. W., Wu, J., Fidler, J. M., Nelson, R., Kim, J. Y., & Raz, D. J. (2016). The triptolide derivative MRx102 inhibits Wnt pathway activation and has potent anti-tumor effects in lung cancer. *BMC Cancer, 16*, 439. doi:10.1186/s12885-016-2487-7

Rhee, E. J., Byrne, C. D., & Sung, K. C. (2017). The HDL cholesterol/apolipoprotein A-I ratio: an indicator of cardiovascular disease. *Curr Opin Endocrinol Diabetes Obes, 24*(2), 148-153. doi:10.1097/MED.0000000000000315

Ribeiro-Alves, M. A., & Gordan, P. A. (2014). [Diagnosis of anemia in patients with chronic kidney disease]. *J Bras Nefrol, 36*(1 Suppl 1), 9-12. Retrieved from http://www.ncbi.nlm.nih.gov/pubmed/24770596

Richards, A. L., Hebert, A. S., Ulbrich, A., Bailey, D. J., Coughlin, E. E., Westphall, M. S., & Coon, J. J. (2015). One-hour proteome analysis in yeast. *Nat Protoc, 10*(5), 701-714. doi:10.1038/nprot.2015.040

Rider, M. H. (2006). The ubiquitin-associated domain of AMPK-related protein kinases allows LKB1-induced phosphorylation and activation. *Biochem J, 394*(Pt 3), e7-9. doi:10.1042/BJ20060184

Rippe, J. M., & Angelopoulos, T. J. (2016). Sugars, obesity, and cardiovascular disease: results from recent randomized control trials. *Eur J Nutr, 55*(Suppl 2), 45-53. doi:10.1007/s00394-016-1257-2

Rose, A. J., Kiens, B., & Richter, E. A. (2006). Ca2+-calmodulin-dependent protein kinase expression and signalling in skeletal muscle during exercise. *J Physiol, 574*(Pt 3), 889-903. doi:10.1113/jphysiol.2006.111757

Rubio, T., Vernia, S., & Sanz, P. (2013). Sumoylation of AMPKbeta2 subunit enhances AMP-activated protein kinase activity. *Mol Biol Cell, 24*(11), 1801-1811, S1801-1804. doi:10.1091/mbc.E12-11-0806

Russo, G. L., Russo, M., & Ungaro, P. (2013). AMP-activated protein kinase: a target for old drugs against diabetes and cancer. *Biochem Pharmacol, 86*(3), 339-350. doi:10.1016/j.bcp.2013.05.023

Sabio, G., Kennedy, N. J., Cavanagh-Kyros, J., Jung, D. Y., Ko, H. J., Ong, H., . . . Davis, R. J. (2010). Role of muscle c-Jun NH2-terminal kinase 1 in obesity-induced insulin resistance. *Mol Cell Biol, 30*(1), 106-115. doi:10.1128/MCB.01162-09

Sacco, F., Silvestri, A., Posca, D., Pirro, S., Gherardini, P. F., Castagnoli, L., . . . Cesareni, G. (2016). Deep Proteomics of Breast Cancer Cells Reveals that Metformin Rewires Signaling Networks Away from a Pro-growth State. *Cell Syst, 2*(3), 159-171. doi:10.1016/j.cels.2016.02.005

Saghatelian, A., Jessani, N., Joseph, A., Humphrey, M., & Cravatt, B. F. (2004). Activity-based probes for the proteomic profiling of metalloproteases. *Proc Natl Acad Sci U S A, 101*(27), 10000-10005. doi:10.1073/pnas.0402784101

Sakiyama, S., Usuki, T., Sakai, H., & Sakane, F. (2014). Regulation of diacylglycerol kinase delta2 expression in C2C12 skeletal muscle cells by free fatty acids. *Lipids, 49*(7), 633-640. doi:10.1007/s11745-014-3912-9

Salt, I., Celler, J. W., Hawley, S. A., Prescott, A., Woods, A., Carling, D., & Hardie, D. G. (1998). AMP-activated protein kinase: greater AMP dependence, and preferential nuclear localization, of complexes

containing the alpha2 isoform. *Biochem J, 334 (Pt 1)*, 177-187. Retrieved from http://www.ncbi.nlm.nih.gov/pubmed/9693118

Sanchez, A., Tripathy, D., Yin, X., Desobry, K., Martinez, J., Riley, J., . . . Grammas, P. (2012). p38 MAPK: a mediator of hypoxia-induced cerebrovascular inflammation. *J Alzheimers Dis, 32*(3), 587-597. doi:10.3233/JAD-2012-120829

Sanguinetti, S. M., Brites, F. D., Fasulo, V., Verona, J., Elbert, A., Wikinski, R. L., & Schreier, L. E. (2001). HDL oxidability and its protective effect against LDL oxidation in Type 2 diabetic patients. *Diabetes Nutr Metab, 14*(1), 27-36. Retrieved from http://www.ncbi.nlm.nih.gov/pubmed/11345163

Sano, H., Kane, S., Sano, E., Miinea, C. P., Asara, J. M., Lane, W. S., . . . Lienhard, G. E. (2003). Insulin-stimulated phosphorylation of a Rab GTPase-activating protein regulates GLUT4 translocation. *J Biol Chem, 278*(17), 14599-14602. doi:10.1074/jbc.C300063200

Sarbassov, D. D., Guertin, D. A., Ali, S. M., & Sabatini, D. M. (2005). Phosphorylation and regulation of Akt/PKB by the rictor-mTOR complex. *Science, 307*(5712), 1098-1101. doi:10.1126/science.1106148

Sawada, K., Yamashita, Y., Zhang, T., Nakagawa, K., & Ashida, H. (2014). Glabridin induces glucose uptake via the AMP-activated protein kinase pathway in muscle cells. *Mol Cell Endocrinol, 393*(1-2), 99-108. doi:10.1016/j.mce.2014.06.009

Schwanhausser, B., Gossen, M., Dittmar, G., & Selbach, M. (2009). Global analysis of cellular protein translation by pulsed SILAC. *Proteomics, 9*(1), 205-209. doi:10.1002/pmic.200800275

Scott, J. W., Hawley, S. A., Green, K. A., Anis, M., Stewart, G., Scullion, G. A., . . . Hardie, D. G. (2004). CBS domains form energy-sensing modules whose binding of adenosine ligands is disrupted by disease mutations. *J Clin Invest, 113*(2), 274-284. doi:10.1172/JCI19874

Senn, J. J. (2006). Toll-like receptor-2 is essential for the development of palmitate-induced insulin resistance in myotubes. *J Biol Chem, 281*(37), 26865-26875. doi:10.1074/jbc.M513304200

Seyfried, N. T., Gozal, Y. M., Dammer, E. B., Xia, Q., Duong, D. M., Cheng, D., . . . Peng, J. (2010). Multiplex SILAC analysis of a cellular TDP-43 proteinopathy model reveals protein inclusions associated with SUMOylation and diverse polyubiquitin chains. *Mol Cell Proteomics, 9*(4), 705-718. doi:10.1074/mcp.M800390-MCP200

Shanware, N. P., Bray, K., Eng, C. H., Wang, F., Follettie, M., Myers, J., . . . Abraham, R. T. (2014). Glutamine deprivation stimulates mTOR-JNK-dependent chemokine secretion. *Nat Commun, 5*, 4900. doi:10.1038/ncomms5900

Shaw, R. J., Bardeesy, N., Manning, B. D., Lopez, L., Kosmatka, M., DePinho, R. A., & Cantley, L. C. (2004). The LKB1 tumor suppressor negatively

regulates mTOR signaling. *Cancer Cell, 6*(1), 91-99. doi:10.1016/j.ccr.2004.06.007

Sidarala, V., & Kowluru, A. (2016). The Regulatory Roles of Mitogen-activated Protein Kinase (MAPK) Pathways in Health and Diabetes: Lessons Learned from the Pancreatic beta-cell. *Recent Pat Endocr Metab Immune Drug Discov*. Retrieved from http://www.ncbi.nlm.nih.gov/pubmed/27779078

Smith, B. K., Mukai, K., Lally, J. S., Maher, A. C., Gurd, B. J., Heigenhauser, G. J., . . . Holloway, G. P. (2013). AMP-activated protein kinase is required for exercise-induced peroxisome proliferator-activated receptor co-activator 1 translocation to subsarcolemmal mitochondria in skeletal muscle. *J Physiol, 591*(6), 1551-1561. doi:10.1113/jphysiol.2012.245944

Smith, G. I., Yoshino, J., Stromsdorfer, K. L., Klein, S. J., Magkos, F., Reeds, D. N., . . . Mittendorfer, B. (2015). Protein Ingestion Induces Muscle Insulin Resistance Independent of Leucine-Mediated mTOR Activation. *Diabetes, 64*(5), 1555-1563. doi:10.2337/db14-1279

Smith, S. F. (1989). A simple method for western blotting very thin SDS-polyacrylamide gels. *Biotechniques, 7*(10), 1060-1064. Retrieved from https://www.ncbi.nlm.nih.gov/pubmed/2629836

Soltani, A., Argani, H., Rahimipour, H., Soleimani, F., Rahimi, F., & Kazerouni, F. (2016). Oxidized LDL: As a risk factor for cardiovascular disease in renal

transplantation. *J Bras Nefrol, 38*(2), 147-152. doi:10.5935/0101-2800.20160023

Somwar, R., Kim, D. Y., Sweeney, G., Huang, C., Niu, W., Lador, C., . . . Klip, A. (2001). GLUT4 translocation precedes the stimulation of glucose uptake by insulin in muscle cells: potential activation of GLUT4 via p38 mitogen-activated protein kinase. *Biochem J, 359*(Pt 3), 639-649. Retrieved from http://www.ncbi.nlm.nih.gov/pubmed/11672439

https://www.ncbi.nlm.nih.gov/pmc/articles/PMC1222186/pdf/11672439.pdf

Spiga, R., Marini, M. A., Mancuso, E., Di Fatta, C., Fuoco, A., Perticone, F., . . . Sesti, G. (2017). Uric Acid Is Associated With Inflammatory Biomarkers and Induces Inflammation Via Activating the NF-kappaB Signaling Pathway in HepG2 Cells. *Arterioscler Thromb Vasc Biol, 37*(6), 1241-1249. doi:10.1161/ATVBAHA.117.309128

Sriwijitkamol, A., Coletta, D. K., Wajcberg, E., Balbontin, G. B., Reyna, S. M., Barrientes, J., . . . Musi, N. (2007). Effect of acute exercise on AMPK signaling in skeletal muscle of subjects with type 2 diabetes: a time-course and dose-response study. *Diabetes, 56*(3), 836-848. doi:10.2337/db06-1119

Sriwijitkamol, A., Ivy, J. L., Christ-Roberts, C., DeFronzo, R. A., Mandarino, L. J., & Musi, N. (2006). LKB1-AMPK signaling in muscle from obese insulin-resistant Zucker rats and effects of training. *Am J Physiol Endocrinol Metab, 290*(5), E925-932. doi:10.1152/ajpendo.00429.2005

Sutherland, C., Leighton, I. A., & Cohen, P. (1993). Inactivation of glycogen synthase kinase-3 beta by phosphorylation: new kinase connections in insulin and growth-factor signalling. *Biochem J, 296 (Pt 1)*, 15-19. Retrieved from http://www.ncbi.nlm.nih.gov/pubmed/8250835

Sweeney, G., Somwar, R., Ramlal, T., Volchuk, A., Ueyama, A., & Klip, A. (1999). An inhibitor of p38 mitogen-activated protein kinase prevents insulin-stimulated glucose transport but not glucose transporter translocation in 3T3-L1 adipocytes and L6 myotubes. *J Biol Chem, 274*(15), 10071-10078. Retrieved from http://www.ncbi.nlm.nih.gov/pubmed/10187787

Tai, H., Wang, X., Zhou, J., Han, X., Fang, T., Gong, H., . . . Xiao, H. (2017). Protein kinase Cbeta activates fat mass and obesity-associated protein by influencing its ubiquitin/proteasome degradation. *FASEB J*. doi:10.1096/fj.201601159RR

Tam, C. S., Covington, J. D., Bajpeyi, S., Tchoukalova, Y., Burk, D., Johannsen, D. L., . . . Ravussin, E. (2014). Weight gain reveals dramatic increases in skeletal muscle extracellular matrix remodeling. *J Clin Endocrinol Metab, 99*(5), 1749-1757. doi:10.1210/jc.2013-4381

Tang, H., & Thomas, P. D. (2016). PANTHER-PSEP: predicting disease-causing genetic variants using position-specific evolutionary preservation. *Bioinformatics, 32*(14), 2230-2232. doi:10.1093/bioinformatics/btw222

Taniguchi, C. M., Emanuelli, B., & Kahn, C. R. (2006). Critical nodes in signalling pathways: insights into insulin action. *Nat Rev Mol Cell Biol, 7*(2), 85-96. doi:10.1038/nrm1837

Thomas, S. M., & Brugge, J. S. (1997). Cellular functions regulated by Src family kinases. *Annu Rev Cell Dev Biol, 13*, 513-609. doi:10.1146/annurev.cellbio.13.1.513

Torimoto, Y., & Kogo, Y. (2006). [Diagnosis and treatment of anemia. 1. Iron-deficiency anemia]. *Nihon Naika Gakkai Zasshi, 95*(10), 2005-2009. Retrieved from http://www.ncbi.nlm.nih.gov/pubmed/17100255

Treiber, D. K., & Shah, N. P. (2013). Ins and outs of kinase DFG motifs. *Chem Biol, 20*(6), 745-746. doi:10.1016/j.chembiol.2013.06.001

Tsolis, K. C., & Economou, A. (2017). Quantitative Proteomics of the E. coli Membranome. *Methods Enzymol, 586*, 15-36. doi:10.1016/bs.mie.2016.09.026

Tsuchiya, A., Kanno, T., & Nishizaki, T. (2014). PI3 kinase directly phosphorylates Akt1/2 at Ser473/474 in the insulin signal transduction pathway. *J Endocrinol, 220*(1), 49-59. doi:10.1530/JOE-13-0172

Tunduguru, R., Chiu, T. T., Ramalingam, L., Elmendorf, J. S., Klip, A., & Thurmond, D. C. (2014). Signaling of the p21-activated kinase (PAK1) coordinates insulin-stimulated actin remodeling and glucose uptake in skeletal muscle cells. *Biochem Pharmacol, 92*(2), 380-388. doi:10.1016/j.bcp.2014.08.033

Uehara, T., Kage-Nakadai, E., Yoshina, S., Imae, R., & Mitani, S. (2015). The Tumor Suppressor BCL7B Functions in the Wnt Signaling Pathway. *PLoS Genet, 11*(1), e1004921. doi:10.1371/journal.pgen.1004921

Varma, V., Yao-Borengasser, A., Rasouli, N., Nolen, G. T., Phanavanh, B., Starks, T., . . . Peterson, C. A. (2009). Muscle inflammatory response and insulin resistance: synergistic interaction between macrophages and fatty acids leads to impaired insulin action. *Am J Physiol Endocrinol Metab, 296*(6), E1300-1310. doi:10.1152/ajpendo.90885.2008

Vijayan, R. S., He, P., Modi, V., Duong-Ly, K. C., Ma, H., Peterson, J. R., . . . Levy, R. M. (2015). Conformational analysis of the DFG-out kinase motif and biochemical profiling of structurally validated type II inhibitors. *J Med Chem, 58*(1), 466-479. doi:10.1021/jm501603h

Vijayvargia, R., Mann, K., Weiss, H. R., Pownall, H. J., & Ruan, H. (2010). JNK deficiency enhances fatty acid utilization and diverts glucose from oxidation to glycogen storage in cultured myotubes. *Obesity (Silver Spring), 18*(9), 1701-1709. doi:10.1038/oby.2009.501

Visconti, R., Gadina, M., Chiariello, M., Chen, E. H., Stancato, L. F., Gutkind, J. S., & O'Shea, J. J. (2000). Importance of the MKK6/p38 pathway for interleukin-12-induced STAT4 serine phosphorylation and transcriptional activity. *Blood, 96*(5), 1844-1852. Retrieved from http://www.ncbi.nlm.nih.gov/pubmed/10961885

von Ahsen, O., & Bomer, U. (2005). High-throughput screening for kinase inhibitors. *Chembiochem, 6*(3), 481-490. doi:10.1002/cbic.200400211

Walsh, J. S., & Vilaca, T. (2017). Obesity, Type 2 Diabetes and Bone in Adults. *Calcif Tissue Int, 100*(5), 528-535. doi:10.1007/s00223-016-0229-0

Ward, N. E., & O'Brian, C. A. (1992). The intrinsic ATPase activity of protein kinase C is catalyzed at the active site of the enzyme. *Biochemistry, 31*(25), 5905-5911. Retrieved from http://www.ncbi.nlm.nih.gov/pubmed/1535219

Warden, S. M., Richardson, C., O'Donnell, J., Jr., Stapleton, D., Kemp, B. E., & Witters, L. A. (2001). Post-translational modifications of the beta-1 subunit of AMP-activated protein kinase affect enzyme activity and cellular localization. *Biochem J, 354*(Pt 2), 275-283. Retrieved from http://www.ncbi.nlm.nih.gov/pubmed/11171104

Wepf, A., Glatter, T., Schmidt, A., Aebersold, R., & Gstaiger, M. (2009). Quantitative interaction proteomics using mass spectrometry. *Nat Methods, 6*(3), 203-205. doi:10.1038/nmeth.1302

Whelan, S. A., Dias, W. B., Thiruneelakantapillai, L., Lane, M. D., & Hart, G. W. (2010). Regulation of insulin receptor substrate 1 (IRS-1)/AKT kinase-mediated insulin signaling by O-Linked beta-N-acetylglucosamine in 3T3-L1 adipocytes. *J Biol Chem, 285*(8), 5204-5211. doi:10.1074/jbc.M109.077818

Wieten, L., van der Zee, R., Spiering, R., Wagenaar-Hilbers, J., van Kooten, P., Broere, F., & van Eden, W. (2010). A novel heat-shock protein coinducer boosts stress protein Hsp70 to activate T cell regulation of inflammation in autoimmune arthritis. *Arthritis Rheum, 62*(4), 1026-1035. doi:10.1002/art.27344

Wishart, D. S., Knox, C., Guo, A. C., Cheng, D., Shrivastava, S., Tzur, D., . . . Hassanali, M. (2008). DrugBank: a knowledgebase for drugs, drug actions and drug targets. *Nucleic Acids Res, 36*(Database issue), D901-906. doi:10.1093/nar/gkm958

Wishart, D. S., Knox, C., Guo, A. C., Shrivastava, S., Hassanali, M., Stothard, P., . . . Woolsey, J. (2006). DrugBank: a comprehensive resource for in silico drug discovery and exploration. *Nucleic Acids Res, 34*(Database issue), D668-672. doi:10.1093/nar/gkj067

Wixon, J., & Kell, D. (2000). The Kyoto encyclopedia of genes and genomes--KEGG. *Yeast, 17*(1), 48-55. doi:10.1002/(SICI)1097-0061(200004)17:1<48::AID-YEA2>3.0.CO;2-H

Wu, H., & Ballantyne, C. M. (2017). Skeletal muscle inflammation and insulin resistance in obesity. *J Clin Invest, 127*(1), 43-54. doi:10.1172/JCI88880

Xiao, B., Heath, R., Saiu, P., Leiper, F. C., Leone, P., Jing, C., . . . Gamblin, S. J. (2007). Structural basis for AMP binding to mammalian AMP-activated protein kinase. *Nature, 449*(7161), 496-500. doi:10.1038/nature06161

Yamada, E., Lee, T. W., Pessin, J. E., & Bastie, C. C. (2010). Targeted therapies of the LKB1/AMPK pathway for the treatment of insulin resistance. *Future Med Chem, 2*(12), 1785-1796. doi:10.4155/fmc.10.264

Yao, Z., Zhou, G., Wang, X. S., Brown, A., Diener, K., Gan, H., & Tan, T. H. (1999). A novel human STE20-related protein kinase, HGK, that specifically activates the c-Jun N-terminal kinase signaling pathway. *J Biol Chem, 274*(4), 2118-2125. Retrieved from http://www.ncbi.nlm.nih.gov/pubmed/9890973

Yi, Z., Langlais, P., De Filippis, E. A., Luo, M., Flynn, C. R., Schroeder, S., . . . Mandarino, L. J. (2007). Global assessment of regulation of phosphorylation of insulin receptor substrate-1 by insulin in vivo in human muscle. *Diabetes, 56*(6), 1508-1516. doi:10.2337/db06-1355

Yin, X., Xu, Z., Zhang, Z., Li, L., Pan, Q., Zheng, F., & Li, H. (2017). Association of PI3K/AKT/mTOR pathway genetic variants with type 2 diabetes mellitus in Chinese. *Diabetes Res Clin Pract, 128*, 127-135. doi:10.1016/j.diabres.2017.04.002

Yissachar, N., Salem, H., Tennenbaum, T., & Motro, B. (2006). Nek7 kinase is enriched at the centrosome, and is required for proper spindle assembly and mitotic progression. *FEBS Lett, 580*(27), 6489-6495. doi:10.1016/j.febslet.2006.10.069

Yu, C., Chen, Y., Cline, G. W., Zhang, D., Zong, H., Wang, Y., . . . Shulman, G. I. (2002). Mechanism by which fatty acids inhibit insulin activation of insulin

receptor substrate-1 (IRS-1)-associated phosphatidylinositol 3-kinase activity in muscle. *J Biol Chem, 277*(52), 50230-50236. doi:10.1074/jbc.M200958200

Yuan, M., Konstantopoulos, N., Lee, J., Hansen, L., Li, Z. W., Karin, M., & Shoelson, S. E. (2001). Reversal of obesity- and diet-induced insulin resistance with salicylates or targeted disruption of Ikkbeta. *Science, 293*(5535), 1673-1677. doi:10.1126/science.1061620

Zbinden-Foncea, H., Raymackers, J. M., Deldicque, L., Renard, P., & Francaux, M. (2012). TLR2 and TLR4 activate p38 MAPK and JNK during endurance exercise in skeletal muscle. *Med Sci Sports Exerc, 44*(8), 1463-1472. doi:10.1249/MSS.0b013e31824e0d5d

Zhang, H., Bajraszewski, N., Wu, E., Wang, H., Moseman, A. P., Dabora, S. L., . . . Kwiatkowski, D. J. (2007). PDGFRs are critical for PI3K/Akt activation and negatively regulated by mTOR. *J Clin Invest, 117*(3), 730-738. doi:10.1172/JCI28984

Zhang, T., Berrocal, J. G., Frizzell, K. M., Gamble, M. J., DuMond, M. E., Krishnakumar, R., . . . Kraus, W. L. (2009). Enzymes in the NAD+ salvage pathway regulate SIRT1 activity at target gene promoters. *J Biol Chem, 284*(30), 20408-20417. doi:10.1074/jbc.M109.016469

Zhang, W., Shen, C., Li, C., Yang, G., Liu, H., Chen, X., . . . Zhao, S. (2016). miR-577 inhibits glioblastoma tumor growth via the Wnt signaling pathway. *Mol Carcinog, 55*(5), 575-585. doi:10.1002/mc.22304

Zhang, X., Damacharla, D., Ma, D., Qi, Y., Tagett, R., Draghici, S., . . . Yi, Z. (2016). Quantitative proteomics reveals novel protein interaction partners of PP2A catalytic subunit in pancreatic beta-cells. *Mol Cell Endocrinol, 424*, 1-11. doi:10.1016/j.mce.2016.01.008

Zhang, X., Ma, D., Caruso, M., Lewis, M., Qi, Y., & Yi, Z. (2014). Quantitative Phosphoproteomics Reveals Novel Phosphorylation Events in Insulin Signaling Regulated by Protein Phosphatase 1 Regulatory Subunit 12A. *J Proteomics*. doi:10.1016/j.jprot.2014.06.010

Zhang, Y., Kwok-Shing Ng, P., Kucherlapati, M., Chen, F., Liu, Y., Tsang, Y. H., . . . Creighton, C. J. (2017). A Pan-Cancer Proteogenomic Atlas of PI3K/AKT/mTOR Pathway Alterations. *Cancer Cell, 31*(6), 820-832 e823. doi:10.1016/j.ccell.2017.04.013

Zhong, J., Gavrilescu, L. C., Molnar, A., Murray, L., Garafalo, S., Kehrl, J. H., . . . Kyriakis, J. M. (2009). GCK is essential to systemic inflammation and pattern recognition receptor signaling to JNK and p38. *Proc Natl Acad Sci U S A, 106*(11), 4372-4377. doi:10.1073/pnas.0812642106

Zhou, Y., Wei, L., Zhang, H., Dai, Q., Li, Z., Yu, B., . . . Lu, N. (2015). FV-429 Induced Apoptosis Through ROS-Mediated ERK2 Nuclear Translocation and p53 Activation in Gastric Cancer Cells. *J Cell Biochem, 116*(8), 1624-1637. doi:10.1002/jcb.25118

Zierath, J. R., Krook, A., & Wallberg-Henriksson, H. (2000). Insulin action and insulin resistance in human skeletal muscle. *Diabetologia, 43*(7), 821-835. doi:10.1007/s001250051457

ABSTRACT

HUMAN KINOME IN SKELETAL MUSCLE INSULIN RESISTANCE

by

YUE QI

August 2017

Advisor: Dr. Zhengping Yi

Major: Pharmaceutical Sciences

Degree: Doctor of Philosophy

Protein kinases play fundamental roles in regulation of biological processes and functions, such as insulin signaling and glucose metabolism. Dysregulation of protein kinases may cause impaired cell signaling and human diseases, such as metabolic syndrome and type 2 diabetes (T2D). Skeletal muscle is the main site responsible for insulin-stimulated glucose disposal, and insulin resistance in skeletal muscle is one of the key features of the pathogenesis of T2D. Therefore, malfunction of protein kinases and their interaction proteins may contribute to the molecular mechanism of insulin resistance in human skeletal muscle. However, no large scale profiling study has been reported to investigate the abnormal active kinases and their interaction partners that might cause skeletal muscle insulin resistance. Here, we present a high throughput platform coupling activity-based ATP probes and quantitative proteomics to globally profile functional kinome and its interactome in human skeletal muscle in 8 lean healthy and 8 obese insulin

resistant participants. We identified 54 active protein kinases in human skeletal muscle, which is the largest catalog of experimental determined active kinases to date. Twenty-two out of the 54 active kinases displayed a significant change in insulin resistant obese subjects, including the protein kinases regulate JNK signaling, p38 MAPK signaling, Wnt signaling, AMPK signaling, ERK1/2 signaling and mTOR signaling. In addition, we identified 616 functional kinome interaction partners in human skeletal muscle, which is the largest human kinome interactome to date. Among the 616 interaction partners, 385 has a fold change > 1.5 or <0.67. Out of these 385 kinome interaction partners, 135 displayed significantly difference between lean heathy and insulin resistant obese subjects. The kinome interactome participate in various cell signaling pathways (i.e. diabetes pathway, mTOR pathway, insulin signaling pathway, etc.) and biofunctions (i.e. protein synthesis and degradation, cytoskeleton dynamics, and apoptosis). In summary, we generated the 1st global picture of functional kinome and kinome interactome in skeletal muscle in lean heathy individuals, and how it differs in obese insulin resistant participants. These results provide novel insights into molecular mechanism of skeletal muscle insulin resistance, and may facilitate identifying new targets for treating metabolic diseases.

AUTOBIOGRAPHICAL STATEMENT

EDUCATION

09/2012-08/2017 Ph.D Pharmaceutical Sciences, Wayne State University

09/2009-07/2012 M.S Pharmaceutical Sciences, Tianjin Medical University

09/2005-07/2009 B.S Pharmacy Degree, Tianjin Medical University

PUBLICATIONS

1. Xiangmin Zhang, Divyasri Damacharla, Danjun Ma, **Yue Qi**, Rebecca Tagett, Sorin Draghici, Anjaneyulu Kowluru, Zhengping Yi. Quantitative proteomics reveals novel protein interaction partners of PP2A catalytic subunit in pancreatic β-cells. Mol Cell Endocrinol. 2016 Mar 15;424.1-11.
2. Michael Caruso, Xiangmin Zhang, Danjun Ma, Zhao Yang, **Yue Qi**, Zhengping Yi. Novel Endogenous, Insulin-Stimulated Akt2 Protein Interaction Partners in L6 Myoblasts. PLoS One. 2015 Oct 14;10(10).
3. Xiangmin Zhang, Danjun Ma, Michael Caruso, Monique Lewis, **Yue Qi**, & Zhengping Yi. Quantitative Phosphoproteomics Reveals Novel Phosphorylation Events in Insulin Signaling Regulated by Protein Phosphatase 1 Regulatory Subunit 12A, Journal of Proteomics, 2014, 109, 23 September, 63–75.
4. Yu Jing, **Yue Qi**, Luo Gang, Zhou Jing. Extraction and Analysis of the Essential Oil in Pogostemon cablin by Enzymatic Hydrolysis and Inhibitory Activity Against Hela Cell Proliferation. Journal of Chinese Medicinal Materials. 2012 May, 35(5).
5. **Yue Qi**, Qin,N.,& Duan, HQ. (Z)-3α-(1,3-Dioxoisoindolin-2-yl)-17(20)-pregnene. Acta Cryst. 2011, E67, o2065.
6. **Yue Qi**, Tang, C.,& Duan, HQ. Pharmacokinetic study on flavones from Potentilla chinensis in rats in vivo. J Drug Evaluation Research.2010,3,187-190.